FEMTOSECOND LASER MASS SPECTROMETRY (FLMS)

Derek John Smith
Department of Physics and Astronomy

UNIVERSITY
of
GLASGOW

Glasgow G12 8QQ
Scotland

Presented as a thesis for the degree of *Doctor of Philosophy* in the University of Glasgow

ProQuest LLC.
789 East Eisenhower Parkway
P.O. Box 1346
Ann Arbor, MI 48106 – 1346

Written and Produced by

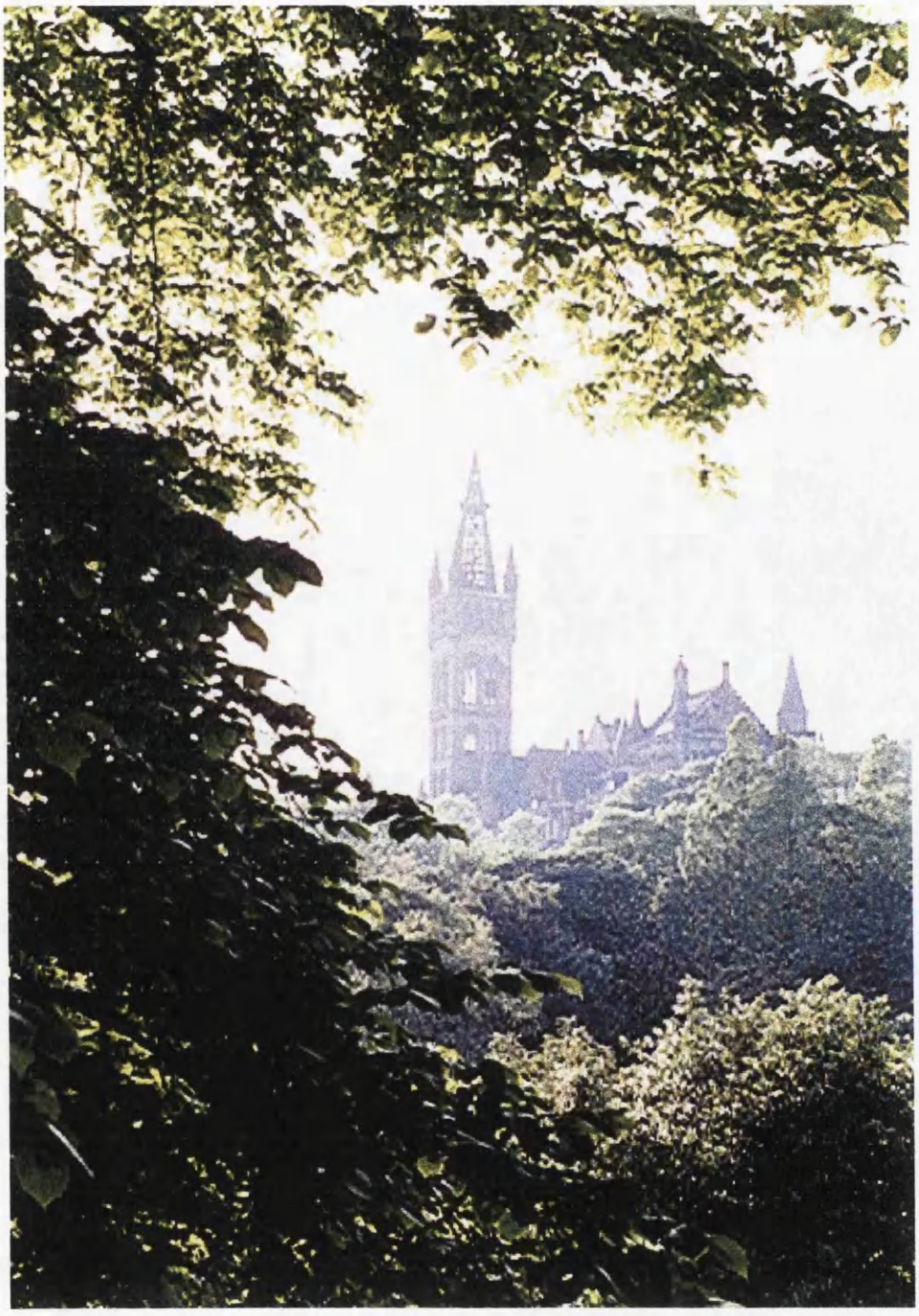

The University Tower viewed from Kelvingrove Park

D.J.S. 1998

To Mum

- for your unfailing support

"We must not cease from exploration. And the end of all our exploring will be to arrive at the place where we began and to know it for the first time."

T.S. Elliot

ACKNOWLEDGEMENTS

In addition to the thesis dedication, I would like to express thanks to a number of people:

★ my supervisor and friend Dr. Kenneth W. D. Ledingham for his consistent availability, enthusiasm and integrity. His leadership will remain with me long after the completion of this thesis.

☆ my second supervisor Dr. Ravi P. Singhal for his help whenever needed.

★ my remaining colleagues in Glasgow and beyond for playing as part of the team. This includes the Laser Ionisation Studies group members and associates: Mr. Thomas McCanny for his excellent technical and experimental assistance, Dr. Hamdi S. Kilic for experimental and theoretical aid, Mr Paul Graham for useful discussions and finally the support staff at Rutherford Appleton Laboratory, Dr. P.F. Taday, Dr. A.J. Langley and Mr. I. Mohammed.

☆ Miss MacIntyre for secretarial assistance.

★ the funding body E.P.S.R.C.

★ my Dad for his help whenever called upon and his uplifting proactive paradigm.

☆ my brothers George and Paul, and my sister Louise, who are all cherished.

★ all my friends but especially Thomas "Dan-the-Man", Alec, Tamir, Martin, Kirsten and Debbie.

☆ Dr. Denis Waitley and Dr. Stephen Covey who've shown me how to live from inside-out, and to try again.

PUBLICATIONS AND PRESENTATIONS

PAPERS

1) ***Time-of-Flight Mass Spectrometry of Aromatic Molecules Subjected to High Intensity Laser Beams***

D.J. Smith, K.W.D. Ledingham, R.P. Singhal, H.S. Kilic, T. McCanny, A.J. Langley, P.F. Taday and C. Kosmidis.

Rapid Commun. Mass Spectrom. **12**, 813 (1998).

2) ***Multiply Charged Ionisation from Aromatic Molecules Following Irradiation in Intense Laser Fields***

K.W.D. Ledingham, **D.J. Smith**, R.P. Singhal, H.S. Kilic, T. McCanny, A.J. Langley, P.F. Taday and C. Kosmidis.

Submitted to *J. Phys. Chem.*

3) ***Environmental Applications of Femtosecond Laser Mass Spectrometry***

D.J. Smith, K.W.D. Ledingham, R.P. Singhal, T. McCanny, P. Graham, A.J. Langley, P.F. Taday and C. Kosmidis.

To be published.

4) ***Ionization and Dissociation of Benzaldehyde Using Short Intense Laser Pulses***

D.J. Smith, K.W.D. Ledingham, H.S. Kilic, T. McCanny, W.X. Peng, R.P. Singhal, A.J. Langley, P.F. Taday and C. Kosmidis.

J. Phys. Chem. A **102**, 2519 (1998).

5) ***The Behavior of Polyatomic Molecules in Intense Infrared Laser Beams***

K.W.D. Ledingham, R.P. Singhal, **D.J. Smith**, T. McCanny, P. Graham, H.S. Kilic, W.X. Peng, S. Wang, A.J. Langley, P.F. Taday and C. Kosmidis.

J. Phys. Chem A **102**, 3002 (1998).

6) ***Comment on "On the Ionisation and Dissociation of NO_2 by Short Intense Laser Pulses"***

R.P. Singhal, H.S. Kilic, K.W.D. Ledingham, T. McCanny, W.X. Peng, **D.J. Smith**, C. Kosmidis, A.J. Langley and P.F. Taday.

Accepted for publication in *Chem. Phys. Lett.*

7) ***Dissociative Ionization and Angular Distributions of CS_2 and its Ions***

P. Graham, K.W.D. Ledingham, R.P. Singhal, **D.J. Smith**, S. Wang, T. McCanny, H.S. Kilic, A.J. Langley, P.F. Taday and C. Kosmidis.

To be published in *AIP Conference Proceedings* 9th RIS '98.
UMIST Manchester.

8) ***Multiphoton Ionization and Dissociation of Nitromethane using Femtosecond Laser Pulses at 375 and 750 nm***

H.S. Kilic, K.W.D. Ledingham, C. Kosmidis, T. McCanny, R.P. Singhal, S. Wang, **D.J. Smith**, A.J. Langley and W. Shaikh.

J. Phys. Chem A **101**, 817 (1997).

9) ***Femtosecond Laser Mass Spectrometry as an Ultra-Sensitive Analytical Technique***

K.W. D. Ledingham, R.P. Singhal, H.S. Kilic, T. McCanny, **D.J. Smith**, W.X. Peng, C. Kosmidis, A.J. Langley and P.F. Taday.

Rutherford Appleton Laboratory Annual Report, 154 (1996 - 1997).

10) ***The Photo-Dissociative Pathways of Nitromethane Using Femtosecond Laser Pulses at 375 nm***

H.S. Kilic, K.W.D. Ledingham, **D.J. Smith**, S. Wang, C. Kosmidis, T. McCanny, R.P. Singhal, A.J. Langley and W. Shaikh.

AIP Conference Proceedings 8th RIS '96, **388**, 395 (1996).

11) ***The Potential of Femtosecond Laser Mass Spectrometry***

K.W.D. Ledingham, R.P. Singhal, H.S. Kilic, T. McCanny, **D.J. Smith**, S. Wang, C. Kosmidis, A.J. Langley and W. Shaikh.

Rutherford Appleton Laboratory Annual Report, 165 (1995 - 1996).

12) ***Multiphoton Processes in Organic Molecules Using VUV Laser Photons***

K.W.D. Ledingham, R.P. Singhal, H.S. Kilic, S. Wang, T. McCanny, **D.J. Smith**, E. Turcu and R. Allott.

Rutherford Appleton Laboratory Annual Report, 167 (1995 - 1996).

POSTERS

1) ***The Ionization and Photofragmentation of CS_2 using Intense Laser Beams***

P. Graham, K.W.D. Ledingham, R.P. Singhal, **D.J. Smith**, S. Wang, T. McCanny, A.J. Langley and P.F. Taday.

9th International Symposium on Resonance Ionization Spectroscopy (RIS 98), 21st - 25th June, 1998, UMIST, Manchester.

2) ***Advances in Femtosecond Laser Mass Spectrometry utilising time-of-flight techniques***

D.J. Smith, K.W.D. Ledingham, H.S. Kilic, T. McCanny, R.P. Singhal, W.X. Peng, A.J. Langley, P.Taday and C. Kosmidis.

14th International Mass Spectrometry Conference (IMSC), 25th - 29th August, 1997. Tampere Conference Centre, Tampere, Finland.

3) ***Ultra Fast Laser Mass Spectrometry***

T. McCanny, K.W.D. Ledingham, **D.J. Smith**, C. Kosmidis, H.S. Kilic, R.P. Singhal, W.X. Peng, S. Wang, A.J. Langley and P. Taday.

The Institute of Physics Annual Congress, 24th - 27th March, 1997. The University of Leeds.

4) ***The Potential of Femtosecond Laser Mass Spectrometry for Gas Phase Samples***

D.J. Smith, K.W.D. Ledingham, H.S. Kilic, T. McCanny, R.P. Singhal, S. Wang, C. Kosmidis, A.J. Langley and W. Shaikh.

Highlights of British Research and R&D by Young Physicists and Scientists, 2 7th September, 1996. The Royal Society, London.

5) ***The Potential for Femtosecond Laser Mass Spectrometry***

H.S. Kilic, K.W.D. Ledingham, **D.J. Smith**, S. Wang, T. McCanny, R.P. Singhal, C. Kosmidis, A.J. Langley and W. Shaikh.

22nd Annual Meeting of British Mass Spectrometry (BMSS), 8th - 11th September, 1996.

6) ***Dissociation Pathways of Nitromethane***

H.S. Kilic, K.W.D. Ledingham, **D.J. Smith**, S. Wang, T. McCanny, R.P. Singhal, C. Kosmidis, A.J. Langley and W. Shaikh.

8th International Symposium on Resonance Ionization Spectroscopy (RIS 96), 30th June - 5th July, 1996. State College, Pennsyvania USA.

ORALS

1) ***Femtosecond Laser Mass Spectrometry (FLMS)***

D.J. Smith

Final Year PhD Workshop, 27th May 1998. The University of Glasgow.

2) ***Ionisation and Dissociation of Molecules using Short Intense Laser Pulses***

D.J. Smith

2nd EPSRC Laser Spectroscopy Summer School, 7th - 13th September, 1997. The University of East Anglia, Norwich.

3) ***Femtosecond Multiphoton Processes***

D.J. Smith

6th Annual Northern Universities' Meeting on Chemical Physics, July 4th 1996. The University of Northumbria at Newcastle.

4) ***The Potential for Femtosecond Laser Mass Spectrometry (FLMS)***

D.J. Smith

Graduate Workshop, Ultrafast Spectroscopy, 26th - 27th March, 1996. The University of Manchester.

ABSTRACT

This thesis applies and develops the new experimental technique known as femtosecond laser mass spectrometry (FLMS) to the molecules benzene, deuterated benzene, toluene, naphthalene, benzaldehyde, 1,3-butadiene and carbon disulphide. The procedure couples ultrashort intense pulsed lasers to time-of-flight mass spectrometry (TOF). Similar characteristics are found in the molecular dynamics of all species studied, effectively rendering FLMS as a general technique. FLMS, which combines trace-sensitivity with on-line analysis, has the capability to investigate molecular detection and dynamics, specifically in the exploration of ionisation and/or dissociation pathways with their associated transitional lifetimes, and the mechanisms of such activity.

Due to the high ionisation efficiency of FLMS, dominant parent ions and minimal associated fragmentation are observed in the mass spectra, particularly using infrared (IR) compared to ultraviolet (UV) wavelengths. Such molecular fingerprints are advantageous in terms of identification. Moreover, the results have indicated that there is a potential for sensitive uniform analysis. Additionally IR FLMS reveals multiply charged molecular ions with doubly charged parents becoming the second most intense ion present in the mass spectra. Such atomic-like behaviour of medium mass polyatomic molecules is remarkable.

The above results are largely in contrast to conventional nanosecond laser studies, with characteristic dissociation and corresponding loss of parent signatures, analytical non-uniformity and non-production of multiply charged species. In such respects FLMS is replacing its nanosecond forerunner.

Interpretation of the results is addressed in terms of multiphoton (MPI) and tunnelling (TI) ionisation. At high laser intensities upwards of $\sim 10^{14}$ W cm^{-2}, the electric fields are no longer small compared to the binding molecular potential felt by valence electrons and new physical effects are expected. TI is thought to significantly contribute to the ionisation rate, particularly using IR wavelengths, with ionisation following the evolution of the laser pulse profile.

SUMMARY

The primary objective of the work carried out in this thesis is to explore and develop the potential of a new laser based analytical technique known as femtosecond laser mass spectrometry (FLMS). FLMS, which couples an ultrafast pulsed laser beam with time-of-flight mass spectrometry (TOF), has been utilised in an investigation into a series of polyatomic molecules. Particular emphasis has been placed on the ultra-sensitive detection and identification of molecules. However, the potential is also demonstrated for more fundamental molecular studies.

Chapter 1 provides a concise introduction. The motivation behind the work is addressed with specific aims being identified. The second chapter deals with the required theoretical knowledge and includes fundamental principles of laser-matter interaction as well as a look at multiphoton and tunnelling ionisation models. Following on, the experimental apparatus is discussed in chapter 3 which incorporates a detailed description and the procedures for use.

The next four chapters are the results section of the thesis. Specifically, chapter 4 investigates the molecule benzaldehyde which is used as a starting point for the exploration and development of FLMS. Building on this, chapters 5 and 6 look at the related aromatic molecules benzene with its deuterated counterpart, toluene and naphthalene. Ahead of general conclusions and future planning in the eighth chapter, chapter 7 expands the study to other polyatomic molecules including 1,3-butadiene and carbon disulphide. The results reveal several similar characteristics in molecular detection and dynamics, which demonstrates the generality of the method. These are outlined below.

FLMS is seen to be an excellent tool for trace-sensitive detection due to its high ionisation efficiency and ability to produce dominant parent ion signatures with little or no fragmentation - particularly in the infrared wavelength region compared to ultraviolet wavelengths. This parent dominance is in considerable contrast to similar nanosecond pulse width studies, and as a result is leading to FLMS largely replacing its nanosecond forerunner in such respects. Implications of the above findings are

thought to be considerable. Moreover, molecular detection without the use of standards is investigated for benzene, toluene and naphthalene. Similar detection efficiencies are found for the three molecules. The major conclusion follows that universal molecular detection is a possibility.

FLMS can also be used to establish transitional-state lifetimes in molecules. This can include ionisation and/or dissociation intermediate states. A specific example of this is seen for benzaldehyde in chapter 4, in which upper and lower lifetime limits are postulated on a particular fast dissociation channel.

An interesting new result is found. At infrared wavelengths, the appearance of double ionised parent ions have been observed for all of the molecules studied. Furthermore, triple ionised species have been identified in most of the molecules. This occurs with little or no fragmentation. This atomic-like behaviour of molecules using IR FLMS is unprecedented and is considered in detail.

Throughout chapters 4 - 7, the mechanisms of ionisation are considered. The conclusion is stated that multiphoton ionisation can largely explain the results using FLMS at laser intensities less than ~ 10^{14} W cm^{-2}, after which tunnelling becomes increasingly prevalent. A sequential ionisation process is considered to describe the findings in which the ionisation matches the evolution of the intensity profile of the laser pulse. The production of multiply ionised species is incorporated in this discussion, particularly in the sixth chapter. Below ~ 10^{16} W cm^{-2}, coulomb explosions are not thought to explain the results for the medium mass molecules studied here.

The results in this thesis demonstrate that the control of chemical dynamics is becoming increasingly possible with FLMS. Experimental and particularly laser parameters, such as intensity, pulse-width and wavelength, are chosen which reflect the goals of the experiment whether they be of an analytical nature, an investigation into molecular structure or multiply ionised phenomenon.

AUTHOR'S CONTRIBUTION

The experimentation has been a team effort between the Glasgow group and the Rutherford Appleton Laboratory (RAL) staff. Specifically, RAL staff were responsible for the running of the laser system with the author (DJS) involved whenever possible. This lead to DJS having a working understanding of the femtosecond apparatus. The Glasgow group were solely responsible for directing and aligning the laser beam into the time-of flight mass spectrometer (TOF). The TOF was assembled and operated exclusively by the Glasgow group. DJS became fully competent in the operation of the TOF in active experimentation. This also included usage and control of surrounding components such as the digital oscilloscope and laser pulse alignment and diagnostic equipment on the optics bench - mirrors, beam splitters, filters, frequency doublers, energy meters, infrared cameras etc. DJS was partly responsible, in conjunction with the Glasgow group technician, for the preparation of the experimental apparatus, obtaining the desired molecular samples and liasing with the staff at RAL prior to the experimental runs. The work on the aromatics benzene, toluene, naphthalene and benzaldehyde was exclusively planned and arranged by DJS with the experimentation carried out with DJS as the team leader. For the remaining molecules investigated in this thesis, DJS was a frontrunner in the practical and preparatory work.

The background research, data analysis, interpretation and conclusions, and the presentation contained in this thesis is completely the work of the author with useful guidance and support from Dr. K.W.D. Ledingham. The one exception to this is the 'cross-section' analysis in chapter 4 which was mainly the work of Dr. R.P. Singhal.

CONTENTS

FRONTISPIECE		i
UNIVERSITY PHOTOGRAPH		iii
THESIS DEDICATION		iv
ACKNOWLEDGEMENTS		v
PUBLICATIONS AND PRESENTATIONS		vi
ABSTRACT		x
SUMMARY		xi
AUTHOR'S CONTRIBUTION		xiii
CONTENTS		xiv
LIST OF FIGURES AND TABLES		xv
CHAPTER 1	INTRODUCTION	1
CHAPTER 2	THEORETICAL	9
CHAPTER 3	EXPERIMENTAL	35
CHAPTER 4	IONISATION AND DISSOCIATION OF BENZALDEHYDE	62
CHAPTER 5	FLMS OF BENZENE, TOLUENE AND NAPHTHALENE	84
CHAPTER 6	FURTHER EXPLORATION OF FLMS APPLIED TO AROMATIC MOLECULES	105
CHAPTER 7	AN EXTENSION OF FLMS BEYOND AROMATIC MOLECULES	139
CHAPTER 8	CHARACTERISTIC BEHAVIOUR OF POLYATOMIC MOLECULES IN INTENSE LASER BEAMS - CONCLUSIONS AND FUTURE WORK	144
REFERENCES		154

LIST OF FIGURES AND TABLES

Figure 1a	A Model Two-Level Energy System	3
Figure 1b	Interaction of Photons with a Two Level Energy System	3
Figure 2a	Three and Four-Level Laser Systems for Population Inversion	11
Figure 2b	An Illustration of Spatial Coherence Between Two Waves	12
Figure 2c	A Illustration of Temporal Coherence for a Wave	12
Figure 2d	Resonant and Non-Resonant Two-Photon Atomic Ionisation	14
Figure 2e	Classification of RIS Schemes for Atomic Ionisation	15
Figure 2f	A simple illustration of electronic, vibrational and rotational energy levels in a typical diatomic molecule undergoing anharmonic oscillations	17
Figure 2g	Several different ionisation schemes for molecules involving resonant and non-resonant processes	18
Figure 2h	An Illustration of Molecular Dissociation Processes	21
Figure 2i	Examples of ladder - switching and ladder climbing mechanisms for a diatomic molecule AB	23
Figure 2j	A Simple Two-Level System for Rate Equations	25
Figure 2k	Tunnel and Over the Barrier Ionisation for an Atom	30
Figure 2l	Tunnel and Over the Barrier Ionisation for a Diatomic Molecule	31
Figure 3a	Time-of-flight mass spectrometer (TOF) in-situ at Rutherford Appleton Laboratory (RAL) with the laser system and bench optics	36
Figure 3b	Experimental Schematic	37
Figure 3c.i	Schematic of the Original Laser System	38
Figure 3c.ii	Schematic of the Refurbished Laser System	38
Figure 3d	Absorption and Emission Properties of Titanium doped Sapphire	40
Figure 3e	Schematic of an Optically Pumped Four Level Laser System	40
Figure 3f	Stimulated Emission in a Ti:Al_2O_3 Rod	41

Figure 3g	The Laser Pulse Evolution in the Original Femtosecond System	42
Figure 3h	A Pulse with a Frequency Chirp (stretched)	42
Figure 3i	Diffraction of a Light Beam by a Grating	43
Figure 3j	The Laser Pulse Evolution in the Refurbished Femtosecond System	46
Figure 3k	The Ion Detection and Data Acquisition System essentially comprising of a Linear TOF, Electron Multiplier and Digital Oscilloscope	48
Figure 3l	Two Peaks Just Resolved	49
Figure 3m	Laser Focal Spot Alignment and Ion Optics within the TOF	51
Figure 3n	A Schematic of the Electron Multiplier	54
Figure 3o	A typical TOF mass spectrum recorded using FLMS	55
Figure 3p	Single Pulse Autocorrelator	56
Figure 3q	Single shot autocorrelation of an amplified laser pulse	57
Figure 3r	Bench-top optical components used for laser direction and measurement	58
Table 3.i	Calculations of Laser Intensity at the Beam Spot for varying conditions	61
Figure 4a	The Benzaldehyde Molecule	63
Figure 4b	The UV Absorption Spectrum of Benzaldehyde	64
Figure 4c	Some Benzaldehyde Fragmentation Pathways	64
Figure 4d	Absorption Spectrum Acquisition	67
Figure 4e	Benzaldehyde Mass Specta at 750/375 nm and 90 fs	69
Figure 4f	Benzaldehyde Mass Spectra at 355nm and 25 ps	70
Figure 4g	Laser Intensity Dependence at 90 fs and 750/375 nm	71
Figure 4h	Benzaldehyde Mass Spectrum with insets of multiply charged regions	74
Figure 4i	The Summed Laser Intensity Dependence at 90 fs and 750/375 nm	76
Figure 4j	Parent and Hydrogen Loss Ion Peaks for Varying Pulse Widths	79
Figure 4k	$C_7H_6O^+$ / $C_7H_5O^+$ as a Function of Pulse Width at 750/375 nm	80

Figure 5a	Some Aromatic Molecules	85
Figure 5b	Benzene Mass Spectra at 750/375 nm and 50/90 fs respectively: Relative Ion Yield vs mass-to-charge ratio (m/z)	91
Figure 5c	Toluene Mass Spectra at 750/375 nm and 50/90 fs respectively: Relative Ion Yield vs mass-to-charge ratio (m/z)	92
Figure 5d	Naphthalene Mass Spectra at 750/375 nm and 50/90 fs respectively: Relative Ion Yield vs mass-to-charge ratio (m/z)	93
Figure 5e	Laser Intensity Dependences for 750/375 nm at 50/90 fs respectively: Relative Ion Yield vs Laser Intensity	97
Figure 5f	The Laser Intensity Dependence for benzene (5f.i), toluene (5f.ii) and naphthalene (5f.iii) parent molecular ions at 750/375 nm and 50/90 fs respectively: Relative Ion Yield vs Laser Intensity	99
Figure 5g	Benzene Mass Spectra at 750/375 nm for Various Pulse Widths Relative Ion Yield vs mass-to-charge ratio (m/z)	101
Figure 6a	The Summation of an Atomic Potential and a dc Laser Field Potential	108
Figure 6b	High Intensity Toluene Mass Spectrum with inset at double ionisation region	118
Figure 6c	High Intensity Benzene Mass Spectrum with insets at multiply ionised regions	120
Figure 6d	High Intensity Deuterated Benzene Mass Spectrum with insets at multiply ionised regions	121
Table 6.i	Benzene and Deuterated Benzene Peak Identification	122
Figure 6e	Benzene and Deuterated Benzene Laser Intensity Dependences for Single and Multiply Ionised Masses at 790 nm and 50 fs	128
Figure 6f	Single-to-Multiple Parent Ratio Dependences at 790 nm and 50 fs	129
Figure 6g	A Higher Intensity Toluene Mass Spectrum with insets at multiply ionised regions	136
Figure 6h	High Intensity Mass Spectra Sections: Multiple Ionised Carbon Comparison for Different Laser Intensities	137

Figure 7a	Carbon Disulphide Mass Spectrum with insets of multiply ionised regions	142
Figure 7b	1,3-butadiene Mass Spectrum with insets of multiply ionised regions	143
Figure 8a	Multi - Molecular Mass Spectra for various polyatomic molecules recorded using infrared FLMS: Ion Yields vs mass-to-charge ratios (m/z)	153

CHAPTER 1

INTRODUCTION

§1.0	**Introduction**	2
§1.0.1	*Quantum Optics - Absorption and Emission*	2
§1.0.2	*Lasers and Analysis*	6
§1.0.3	*Aims and Motivation*	7
§1.0.4	*Thesis Layout*	7

§1.0 Introduction

The first chapter of this thesis provides an introduction to the author's field of study. This report consists of experimentation into, and interpretation of, light interacting with matter. Therefore it is appropriate to discuss as a starting point some background theory and related concepts for a simple semi-classical two-level energy system and its interaction with incident radiation. The usefulness of lasers in analytical studies is then addressed and the motivations behind the work undertaken set out.

§1.0.1 Quantum Optics - Absorption and Emission

Laser (light amplification by stimulated emission of radiation) processes involve the fundamental atomic nature of matter, which is made up of atoms, molecules or ions. Such particles have discrete or quantized energy levels which is intimately related to the wave-particle duality that exists in nature. Light behaves with this duality. In a particle sense, a photon carries the discrete energy associated with the wave with a quantum energy associated with a frequency ν being given by $h\nu$, where h is Planck's constant (6.6×10^{-34} Js). Emission of such quanta are involved in the amplification of light in a laser. Therefore the term quantum optics is often used to describe the branch of science involving lasers.

Optical photons come from the emission from atoms in excited states. Such atoms can be excited by a number of different mechanisms e.g. a gas discharge lamp in which electrons in the electrical discharge collide with atoms, or photons from an external source. These microscopic processes, in which atoms can be excited and de-excited were first studied by Einstein in 1917. This interaction of light with matter is best explained by considering a two-level energy system with the assumption that it is in thermal equilibrium - see figure 1a.

Following from the Boltzmann distribution law, a comparison of the numbers of atoms can be made at two different energy levels with N_1 particles at energy E_1 and N_2 particles at energy E_2, with $E_2 > E_1$.

$$\frac{N_2}{N_1} = \exp\left[-\frac{(E_2 - E_1)}{kT}\right] \qquad \textit{eqn 1.0.1a}$$

for temperature T and Boltzmann constant k. This relationship tells us that no matter how high the temperature or how small the energy difference, the number of atoms in the higher energy state cannot exceed the number in the lower state.

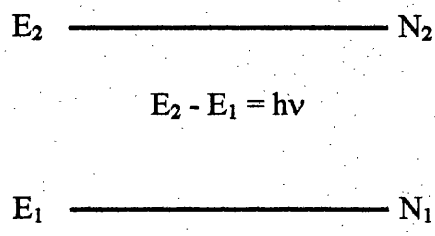

Figure 1a A Model Two-Level Energy System

Photons can interact with an energy level system in different ways as shown in figure 1b.

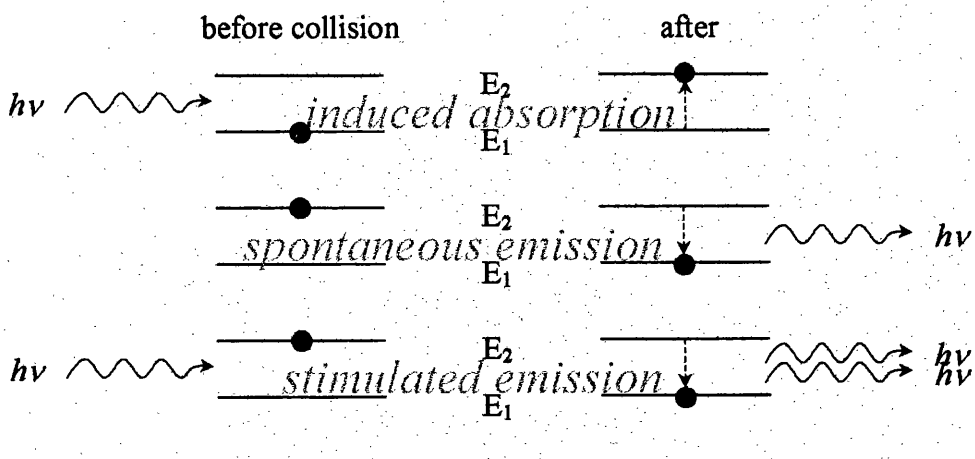

Figure 1b Interaction of Photons with a Two Level Energy System

(i) upon *absorption* of a photon of suitable frequency, the excited atom can be raised from a lower to higher energy level; (ii) the atom can then return to the lower level *spontaneously* by emitting a photon of equal frequency to the incident photon; (iii) the atom in the excited upper state is *stimulated* by another photon to return to its lower energy state with the emission of a photon. In the second case, the emitted photon is out of coherence with the incident photon, while in the third case the stimulating and

stimulated photons are coherent, that is they have the same phase relative to one another.

Einstein defined coefficients for the three processes illustrated in figure 1b. He postulated that the induced absorption transition rate dN_{12}/dt, was proportional to the number of atoms with electrons in the lower energy state N_1, and the density of radiation energy incident on these atoms ρ, with energy equal to the energy difference between the two states. This is illustrated in equation *1.0.1b.*

$$\frac{dN_{12}}{dt} \alpha N_1 \rho \qquad \textit{eqn 1.0.1b}$$

Therefore:

$$\frac{dN_{12}}{dt} = B_{12} \rho N_1 \qquad \textit{eqn 1.0.1c}$$

where B_{12} is the Einstein coefficient for induced absorption.

In a similar manner the spontaneous emission transition rates were postulated as being proportional to the number of atoms with electrons in the upper state, quite independent of incident radiation density ρ:

$$\frac{dN_{21}}{dt} = A_{21} N_2 \qquad \textit{eqn 1.0.1d}$$

where A_{21} is the Einstein coefficient for spontaneous emission. The transition lifetime for the upper state is simply given by taking the reciprocal of A_{21}.

Following on, the transition rate for stimulated emission was postulated as:

$$\frac{dN_{21}}{dt} = B_{21} \rho N_2 \qquad \textit{eqn 1.0.1 e}$$

where B_{21} is the Einstein coefficient for stimulated emission.

Einstein then showed that for thermal equilibrium, the coefficients of absorption and stimulated emission are equal:

$$B_{12} = B_{21} \qquad \textit{eqn 1.0.1f}$$

and that the relationship between the coefficient of spontaneous emission and stimulated emission is given by:

$$A_{21} = \frac{8\pi(E_2 - E_1)^3}{h^2 c^3} B_{21} \qquad \textit{eqn 1.0.1g}$$

where E_2 - E_1 is the energy difference between two states, h is Planck's constant and c the speed of light. Equations *1.0.1f* and *1.0.1g* are known as the Einstein relations. Svelto [1989] provides a particularly thorough explanation of such derivations.

It is useful to think of the above energy system as a damped driven quantum oscillator with the damping being supplied by spontaneous emission and the driving force provided by the incident laser field. If this incident laser field has a low intensity, then spontaneous emission is more important than stimulated processes - the system behaves like an over-damped oscillator. This is comparable to a classical oscillator which will vibrate at its own natural frequency if possible. On the other hand for sufficiently intense incident radiation, stimulated processes will become more important than spontaneous ones because the incident photon flux is so high that other photons stimulate emission before spontaneous decay can occur. Stimulated emission outruns spontaneous emission and the system behaves like an under-damped oscillator. Again a comparison to classical oscillator can be made in which the oscillator will settle down to an imposed harmonic motion at the external driving perturbation frequency.

The rate at which transitions are induced between two energy levels is known as the Rabi frequency. As well as in the population of excited levels, Rabi oscillations also show up as a modulation of the quantum dipole moment. For an atom, when the

atomic dipole moment oscillates at an external driving frequency it radiates a field at that frequency. The atomic dipole may have an additional time dependence which shows up as extra frequencies above and below the driving frequency - known as dynamic Stark splitting.

§1.0.2 Lasers and Analysis

With the development of lasers, the principles of which are described above and in chapter 2, section 2.1, a great many avenues of experimentation and application have arisen. The high optical flux associated with lasers lends itself particularly well to the investigation of atomic and molecular species. Indeed, one of the most exciting laser applications in the past two decades has been to mass spectrometry. This has seen the development of trace-sensitive analytical techniques such as resonance ionisation mass spectrometry (RIMS) and resonance enhanced multiphoton ionisation (REMPI), which are described in the next chapter. As well as in analytical studies, such techniques have been used to great effect in fundamental investigations of atomic and molecular structure. Generally, this experimentation has seen the utilisation of pulsed lasers in the nanosecond region coupled to time-of-flight mass spectrometers (TOF). Species excited by the laser beam are then ionised and/or fragmented followed by detection. Analysis of the resulting mass spectra can yield considerable information about the target species.

With the ongoing development and introduction of commercially available intense short-pulse width lasers, the nanosecond methods are being superseded to some degree. Femtosecond laser mass spectrometry (FLMS) developed by the Glasgow group in recent years [Smith *et al*, 1998a, 1998b; Ledingham *et al*, 1998a, 1998b, 1997, 1996/7, 1995/6, 1995a, 1995b; Kilic *et al*, 1997; Kosmidis *et al*, 1997; Singhal *et al*, 1998, 1996] and along with similar techniques using ultrafast lasers [e.g. He *et al*, 1997a; Willey *et al*, 1997; Weickhardt *et al*, 1997, DeWitt *et al*, 1997, Levis *et al*, 1996; Schutze *et al*, 1996, Purnell *et al*, 1994], has been shown to have considerable potential in many fields of application. These centre around chemical detection and include analytical work on gas phase species as well as solid state surface analysis. The present thesis aims to exploit and develop the analytical capabilities of such experimentation.

§1.0.3 Aims and Motivation

Ultra-sensitive detection and fundamental studies of atoms and molecules is of great importance in analytical and theoretical science. This is particularly true in the investigation of strategic and environmentally sensitive molecules such as explosives and atmospheric pollutants, but also in the trace detection of semi-conductor components, biological molecules and drugs of abuse. If a system can be developed to reliably detect and identify such a wide range substances, then the implications will be enormous.

With the above in mind, the initial aim of the study was to develop a practical method for chemical detection and identification using FLMS. The generality, or otherwise, of the technique was also to be investigated.

To this end, the well known aromatic group of molecules were chosen for research. The importance of the analytical detection of benzene and its derivatives is apparent when one considers that they are utilised and/or are by-products in many manufacturing processes. Studying such medium mass molecules was seen as an evolutionary choice as the vast majority of the ultrafast studies to date have focused on atoms and small-mass molecules. From this foothold, it was then hoped that the methods developed and utilised could be further extended to other molecules, and perhaps even multi-component samples.

The above goals, although specific, were encompassed in a wider vision. This was because the subjection of the molecules included in the present study to femtosecond lasers was a new course of experimentation, and as such would likely yield results of an original nature. In fact, this is found to be the case.

§1.0.4 Thesis Layout

Subsequent to chapter 1, the second and third chapters respectively describe necessary theoretical and experimental concepts for the results, analysis and conclusions presented in chapters 4 to 7. Chapter 8 provides global conclusions and speculates on future studies.

Throughout the thesis certain discussions relating to experimental, theoretical and analytical concepts are considered on more than one occasion. As such it is hoped that the various chapters of the thesis will inter-relate in an optimum progressive manner.

CHAPTER 2

THEORETICAL

§2.0	**Introduction**	10
§2.1	**General Laser Principles**	10
§2.2	**Atoms and Molecules in Laser Fields**	12
§2.2.1	*The Ionisation Process*	13
§2.3	**Multiphoton Ionisation (MPI)**	13
§2.3.1	*Development of Resonance Ionisation Spectroscopy (RIS)*	14
§2.3.2	*Development of Resonance Enhanced Multiphoton Ionisation (REMPI)*	16
§2.3.3	*Processes Competing with Multiphoton Ionisation*	19
	Molecular Dissociation	20
	Luminescence	21
	Intersystem Crossing and Internal Conversion	22
	Isomerisation	22
§2.3.4	*Ionisation and Dissociation Pathways*	22
§2.3.5	*Rate Equation Modelling in Multiphoton Processes*	24
§2.4	**Tunnel Ionisation (TI)**	30
§2.5	**Coulomb Explosions**	34

§2.0 Introduction

This chapter provides necessary theoretical information. It is presented as a concise summary. Firstly, general principles of laser action are discussed, after which the response of atoms and molecules subjected to laser fields is addressed.

§2.1 General Laser Principles

A brief outline of the principles of lasers is provided in this section which builds on the discussion on quantum optics located in the previous chapter, section *1.0.1.* There are many excellent laser textbooks [e.g. Davis, 1996; Svelto, 1989] which can be referred to for further reading. Detailed discussions of the particular lasers used in this study can be found in chapter 3, section 3.1.

As noted in chapter 1, it is not possible to create a population inversion by optical pumping in a two-level system due to the Boltzmann factor. In intense radiation of appropriate energy, the numbers of atoms in the upper excited state will increase, although the tendency towards thermal equilibrium prevents the number in the higher state quite equalling the number in the lower. In other words, mere intense radiation cannot cause more stimulated emission than absorption. Therefore some other mechanism must be employed to cause a population inversion with more atoms in the higher state and resulting in stimulated emission exceeding absorption.

The solution is found by employing more than two atomic states. As an example, figure 2a shows three and four-level laser systems. In the first case, the atoms are excited by some means (optical, collisional) from the ground state 0 to a highly excited state 2. From Boltzmann, $N_2 < N_0$. However, if a fast decay channel exists from state 2-to-1, then a population inversion can be set up between states 1 and 0. Stimulated emission begins from spontaneously decaying photons with a subsequent avalanche of emissions of very similar direction, monochromaticity and coherence, and high intensity. The situation is similar for the four-level laser. The population inversion is between levels 2 and 1 upon

rapid decay from the highly excited state 3. Four-level lasers are more common than three-level systems because it is in general easier to produce a population inversion with the former. This is because a three-level system requires a minimum of half of the atoms in the ground state to be excited into state 1, whereas a population inversion between levels 2 and 1 in a four-level system requires less intense pumping since state 1 is initially empty and decays very quickly upon population.

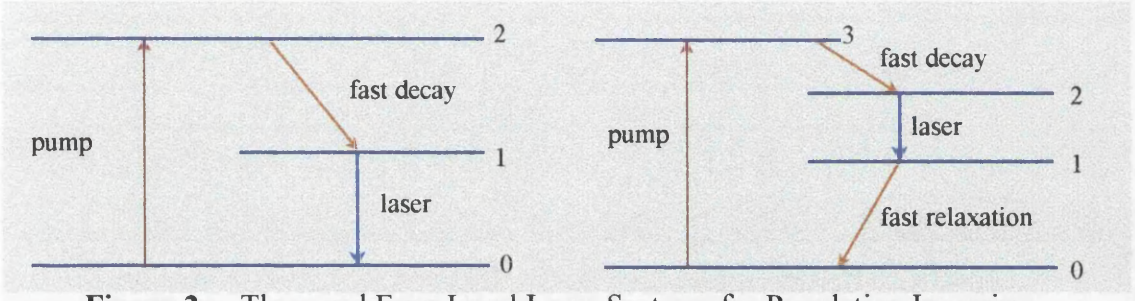

Figure 2a Three and Four-Level Laser Systems for Population Inversion

The direction of the laser beam is very non-divergent because the active lasing medium is contained within a cylindrical resonant cavity. To amplify this stimulated emission, mirrors are generally used within the laser cavity to reflect the light beam back into the active medium. Any radiation not in the direction of this reflection axis will be lost and therefore not amplified. Therefore after the beam has emerged from the cavity the only divergence comes from diffraction. The beam divergence is measured as the angle between the two outer edges of the beam where the beam edge is defined as the location in the beam where the intensity decreases to 1/e of that at the centre. A typical divergence for a small laser may be ~ 10^{-4} rad.

Lasers are highly monochromatic with a narrow range of frequencies in the beam (bandwidth $\Delta\nu$) although there are some sources of frequency broadening. For example, in a solid active medium, strains and slight inhomogeneities may distort energy levels of the emitting ions. In a gas, Doppler broadening may occur in which the atoms' different velocities can lead to shifts in frequency emission. Careful selection of cavity geometry can lead to restrictions in the modes of operation of the laser beam, which can result in an

extremely monochromatic light source. A good laser may have a bandwidth of as little as ~ 0.001 nm.

A coherent light source has a connection between the amplitude and phase at one point and time and the amplitude and phase at another point in time. A light source is said to be spatially coherent if two electric wave vectors at any two fixed points in space have a phase difference which is time independent. Figure 2b illustrates this. At time t_1 the phase difference between two electric vectors E_1 and E_2 is zero for positions x_1 and x_2. At a time t_2 later, for the same two fixed points in space, the phase difference between the electric vectors, now E_3 and E_4, is still zero.

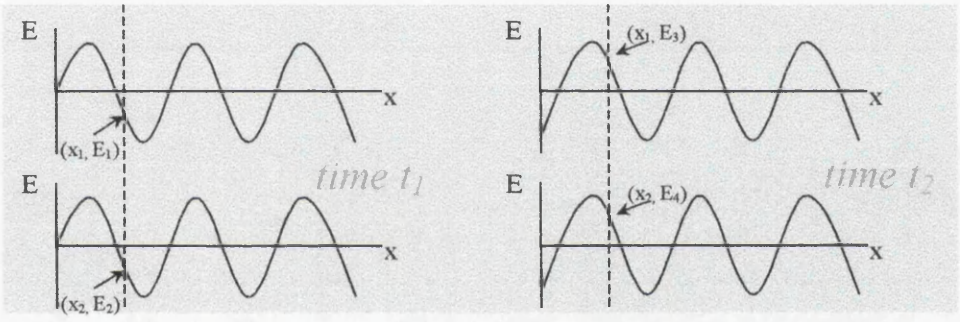

Figure 2b An Illustration of Spatial Coherence Between Two Waves

Temporal coherence results when the phase difference ϕ measured for two points in time (t_1-t_2 = τ) at one point in space does not change for any given two points in time of equal separation (t_3-t_4 = τ) - see figure 2c.

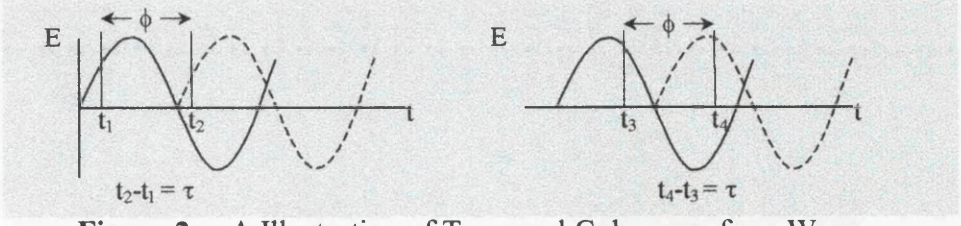

Figure 2c A Illustration of Temporal Coherence for a Wave

§2.2 Atoms and Molecules in Laser Fields

The remaining sections of this chapter concentrate on atomic and molecular behaviour when subjected to laser fields. When an atom or molecule is bathed in a laser pulse, its

response is dependent on associated laser beam parameters such as wavelength, pulse width and intensity, as well as its own properties. The effect of laser characteristics on atoms and molecules is considered in a discussion on multiphoton and tunnelling processes and associated concepts relevant to this thesis. The emphasis is placed on molecules reflecting the thesis content.

§2.2.1 The Ionisation Process

When a neutral substance X, is ionised by a light source, an electron is freed from the neutral parent species leaving a positive parent ion X^+. This photo-ionisation process is shown in equation *2.2.1a.* with $nh\nu$ representing n photons of a suitable frequency.

$$X + nh\nu \rightarrow X^+ + e^- \qquad \textit{eqn 2.2.1a}$$

The resulting positive ion is known as a radical and often has an unstable configuration. The energy required to remove an electron from a ground state neutral substance and therefore create an ion is known as the ionisation potential. Many photons may be required to achieve this.

§2.3 Multiphoton Ionisation (MPI)

When weak radiation interacts with atoms or molecules, only one or two photons are absorbed or emitted. However, it has long been known that an atom or molecule can undergo a coherent (i.e. simultaneous) multiphoton transition provided a sufficiently intense radiation field is available, as was predicted by Goppert-Mayer in her 1931 thesis. In these circumstances many photons may be absorbed simultaneously. With the invention and development of lasers over the last forty years or so, and particularly in the last twenty years with the availability of intense, tuneable and pulsed lasers, multiphoton excitation experiments have become widespread and diverse with the possibility of a great number of photons being involved in the transitions. The first intense optical experiments of this nature were performed in the early 1960s using the then new ruby

laser to excite transitions in $CaF_2:Eu^{2+}$ crystals. Since then, the advancement has been significant.

§2.3.1 Development of Resonance Ionisation Spectroscopy (RIS)

The development of a technique known as resonance ionisation spectroscopy (RIS) has been fundamental in laying the foundations for laser based analytical and fundamental methods. RIS evolved primarily in the 1970s with development into the 1980s [Fassett *et al*, 1988; Letokhov, 1988, 1987; Hurst *et al*, 1988, 1979; Bekov *et al*, 1983; Antonov *et al*, 1981; Johnson, 1980]. The idea was originally proposed as an isotopic separation technique, but the widespread applicability for atomic detection soon became evident.

The principles of RIS are straight forward. Different atoms have unique sets of well defined excited states which can be reached from the ground state via absorption of one or more photons of suitable frequency. If the excited atom quickly absorbs a sufficient number of quanta without decaying back to the ground state, then ionisation can be achieved. The process can either be resonant (RIS) or non-resonant as figure 2d shows.

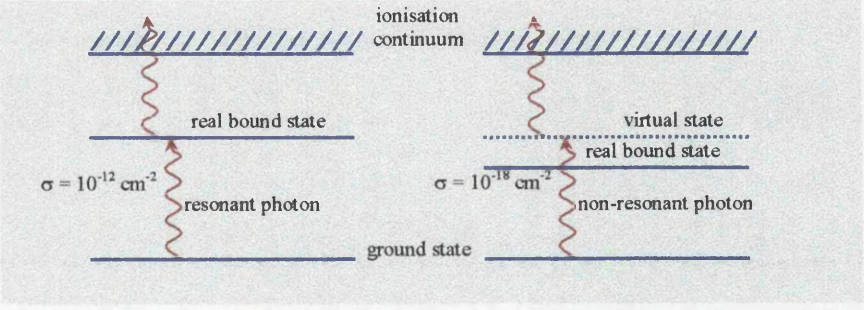

Figure 2d Resonant and Non-Resonant Two-Photon Ionisation

The intermediate states shown in the figure are short lived - ~ upwards of tens of nanoseconds for real states, and as short as tens of femtoseconds for virtual states [Zare, 1984]. This is reflected in the cross-sections for absorption indicated in the figure with σ increasing dramatically if real bound states are involved. RIS is therefore an elemental selective process.

Additionally for sufficiently high laser fluxes, dependent on the atom under study and the experimental conditions, saturation of the process is possible with all the atoms in the interaction volume of the laser beam being ionised. This maximises the sensitivity of the process and points towards single atom detection [Ledingham, 1987; Singhal and Ledingham, 1987; Hurst *et al*, 1979].

With the exception of helium and neon, which have large ionisation potentials and large energy differences between the ground and lowest lying excited state, Hurst *et al* [1979] proposed five basic ionisation schemes for the atoms of the periodic table according to the relative energy positions from the ground state to the intermediate energy states and the ionisation continuum. These are shown in figure 2e. It is evident that many elements can be ionised with a single laser which has a frequency doubling capacity. If this laser is also tuneable, then atoms of nearly every element can be detected.

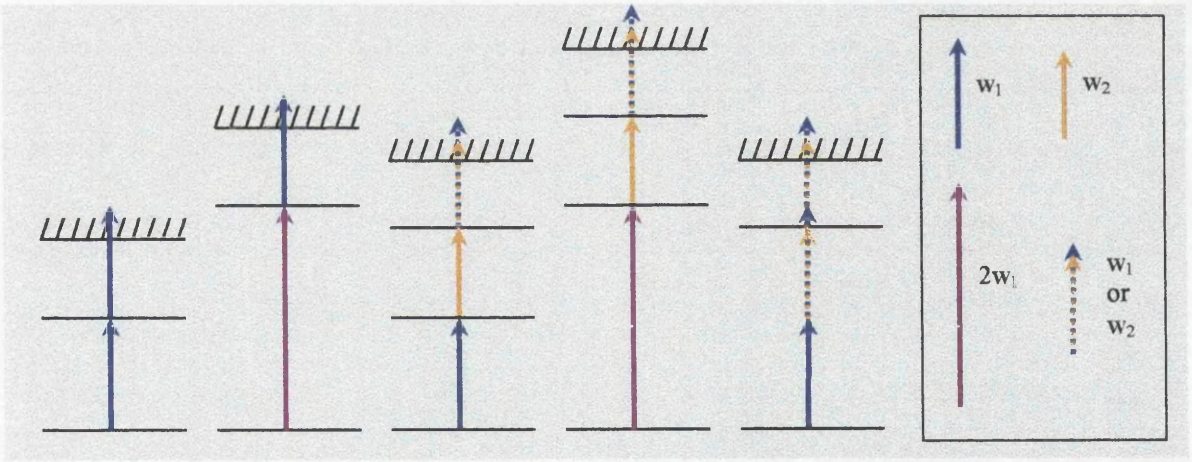

Figure 2e Classification of RIS Schemes for Atomic Ionisation proposed by Hurst *et al*

When researchers first developed RIS, they detected and counted the free electrons created in the ionisation process. With the development of new methods and technologies in the 1980s, a sensitive analytical technique known as resonance ionisation mass spectroscopy (RIMS) [Hurst *et al*, 1988; Letokhov, 1986; Fassett *et al*, 1985; Bekov *et al*, 1983] evolved from RIS, in which the positive ions were detected by extracting and accelerating them through an electric field in a mass spectrometer. This allowed quantitative identification according to the ions' mass-to-charge ratios.

§2.3.2 Development of Resonance Enhanced Multiphoton Ionisation (REMPI)

The same techniques were soon applied to molecules with pioneering work done by Johnson *et al* [1980, 1976a, 1976b, 1975], Dalby and his co-workers [Petty *et al*, 1975] and Zandee *et al* [1979] on small to medium mass species such as iodine, nitric oxide and benzene. It quickly became obvious that the potential for ultra-sensitive analytical molecular studies was considerable [Lubman, 1988a, 1988b] with ionisation efficiencies approaching unity. The multiphoton-molecular interactions were given the name resonance enhanced multiphoton ionisation (REMPI) and non-resonant multiphoton ionisation (NRMPI), depending on the nature of the absorption event. Boesl *et al* [1994] provides a good review of such processes. These techniques generally employed tuneable lasers in the ultraviolet (UV) wavelength regime, with nanosecond pulse widths at beam intensities around 10^7-10^9 W cm^{-2}.

The energy levels of atoms are associated with the kinetic energy of electron motion relative to the nucleus and with the potential energy of interaction of the electrons with the nucleus and each other. Molecular excitation spectra are much more complicated than atomic spectra because of the motions of the nuclei of the atoms with respect to one another, resulting in molecules being able to absorb energy in a vibrational or rotational sense as well as electronically. These characteristic ro-vibrational energy levels can smear out the electronic levels making resonant detection more difficult to attain than with atoms.

It is instructive to consider molecular energy levels in detail [Barnwell, 1983] in order to gain a fuller understand of the REMPI and NRMPI processes. Figure 2f is a schematic of some allowed molecular energy states for a diatomic molecule. Each electronic level (separated by a few eV) contains vibrational levels (separated by ~ 0.1 eV) and rotational sub-levels (separated by ~ 0.01 eV).

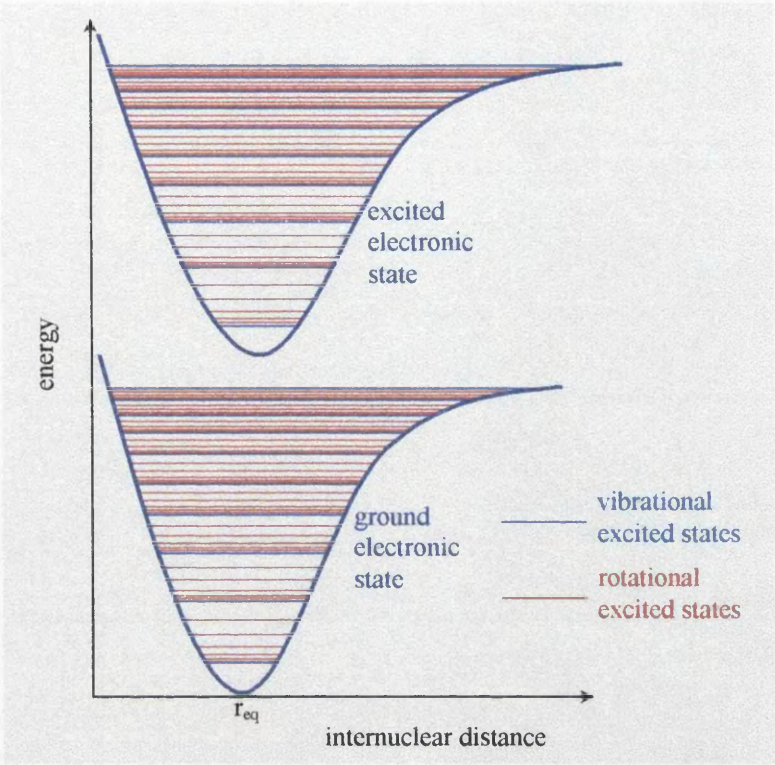

Figure 2f A simple illustration of electronic, vibrational and rotational energy levels in a typical diatomic molecule undergoing anharmonic oscillations

The energy curves in figure 2f are a function of the internuclear separation and are called Morse potentials. A stable or equilibrium state exists at the minimum of the potential energy curves. This arises when the forces are balanced between strong nuclear repulsion and attraction from the interaction of nuclei with binding electrons. If the overall attractive forces are insufficient to counteract the nuclear repulsive tendencies, there exists no potential energy minimum and the molecule doesn't exist.

In the case of polyatomic molecules, one may expect the energy spectra to be more complicated than for diatomic species. A molecule with three or more atoms has additional modes of vibratory motion, each with its own set of energy levels and sub-rotational levels. The resulting energy level scheme is usually quite complex and can be made more complex by transition line broadening effects such as Doppler, radiative, and collisional line broadening. Jet cooling [Zandee *et al*, 1979] into a vacuum can alleviate the broad-band absorption to some extent by effectively quenching the internal ro-

vibrational states. This cooling is carried out by seeding the molecules into a light carrier gas (e.g. He or Ne) at high pressure and expanding into a vacuum through a narrow orifice. For the polyatomic case, the diatomic internuclear separation shown in figure 2f must be replaced by some generalised co-ordinate which may be dependent on particular bond strength, angle and separation. Some basic molecular photo-ionisation schemes are shown in figure 2g [Ledingham, 1995c] and are explained below.

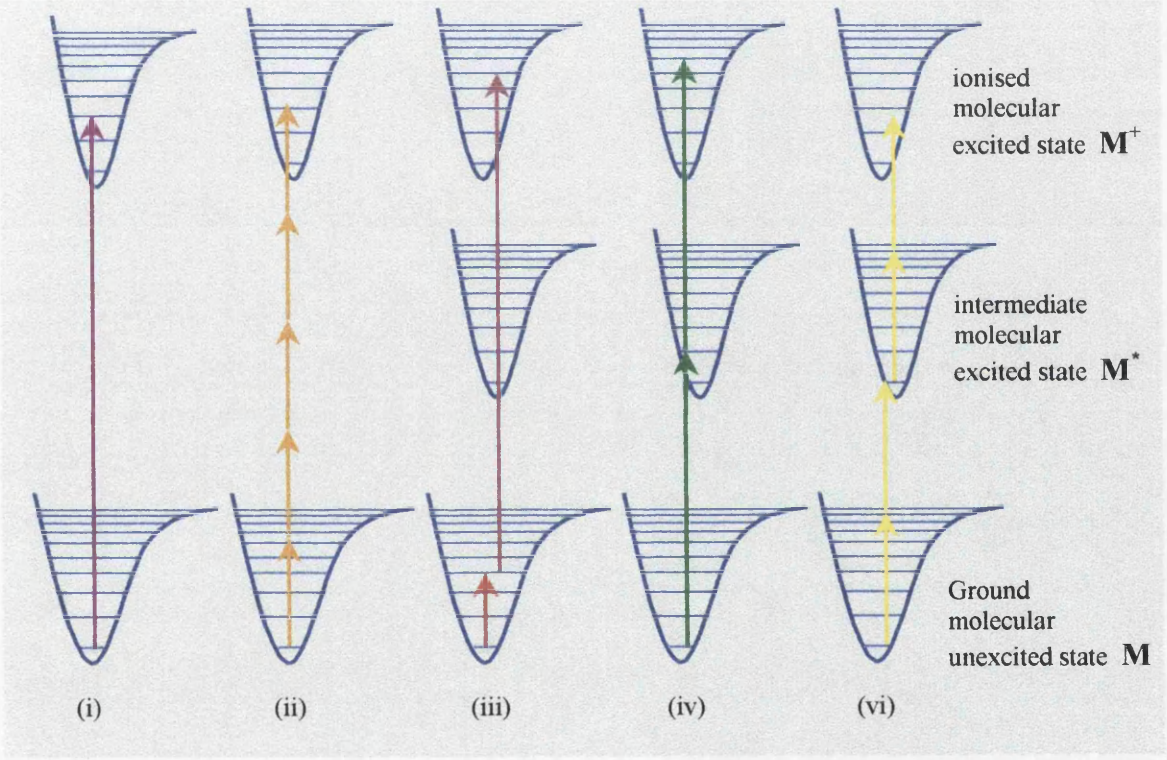

Figure 2g Several different ionisation schemes for molecules involving resonant and non-resonant processes

Note that for ease of viewing, the rotational levels (red lines in figure 2f) are not included in the figure. Because transitions between energy levels are very rapid in a molecule, the internuclear distances essentially remain constant during such transitions, which is depicted by a vertical line starting and finishing on the initial and final energetic levels respectively. A key to the figure is given below.

(i) single photon ionisation

(ii) non-resonant multiphoton ionisation (NRMPI) (e.g. 5 photons)

(iii) resonant two-photon ionisation via ground state ro-vibrational levels

(iv) resonant two-photon ionisation via excited state ro-vibrational levels

(v) resonance enhanced multiphoton ionisation (REMPI) (e.g. 2+2 process)

RIMS and REMPI are more sensitive than their non-resonant equivalents due to the greatly increased probability of photon absorption in the resonant case. If an excited intermediate state of the target compound is in resonance with the irradiating laser wavelength, the multiphoton yield is increased by many orders of magnitude. Additionally, because resonant steps are characteristic of the species under investigation, analysis can be more successful with species selective ionisation, with the potential for a sought analyte being preferentially ionised out of a complex mixture by tuning the laser wavelength to a characteristic transition [Boesl, 1991].

On the other hand, sensitivity and ionic yields may be partially sacrificed using NRMPI for more general investigations into a series of species. The inherent non-specific nature of NRMPI may make it a more broad-based, but less selective experimental technique than REMPI. As well as decreasing ionic yields, which can be partially compensated for by increasing the laser beam intensity (e.g. strong focussing), another disadvantage with a general NRMPI process is the fact that differing ionisation potentials of various molecules can lead to a non-uniformity in detection probabilities. In other words, quantification difficulties. However, NRMPI remains more successful than REMPI for widespread studies.

§2.3.3 Processes Competing with Multiphoton Ionisation

The ionisation efficiency of the above processes can be much reduced if decay or relaxation mechanisms in an excited state of the neutral species become prevalent over ionisation. In terms of molecular analysis this is undesirable because it can lead to small or non-existent parent ion production, and therefore ambiguous detection and identification. Such decay mechanisms can inherently limit the effectiveness of REMPI

and NRMPI, and are now considered. These include dissociation, luminescence, intersystem crossing and internal conversion [Sears *et al*, 1987].

Molecular Dissociation

Molecular photo-dissociation is the break up of a molecule as a result of photon absorption. It can be considered as a decay or loss mechanism in the context of a competition between dissociation to fragments and ionisation to the parent species. Equations *2.3.3a* and *2.3.3b* illustrate example pathways for this conflict in a three atom molecule, ABC.

$$ABC + n\text{h}\nu \rightarrow ABC^{*} \rightarrow ABC^{+} \qquad \textit{eqn 2.3.3a}$$

$$ABC + m\text{h}\nu \rightarrow ABC^{*} \rightarrow AB^{+} + C \qquad \textit{eqn 2.3.3b}$$

The above two processes are known as ladder-climbing and ladder-switching respectively [Gedanken *et al*, 1982] with the products being available for further photon absorption, ionisation and/or fragmentation. Further attention is given to this in section *2.3.4*.

Fragmentation can occur as direct-dissociation or pre-dissociation. These are illustrated in figure 2h. As in figure 2g, rotational levels are omitted for clarity. Simply note that each vibrational level has a myriad of associated rotational sub-levels which can be involved in the ionisation/dissociation processes. Direct dissociation occurs when a molecule is excited by photons of suitable frequency from a ground vibrational state to the vibrational continuum of either the ground or excited electronic states, where all levels are unbound (red arrows). A subsequent break-up of the molecule occurs. This usually requires multiphoton absorption processes. Alternatively, the molecule can be excited to an unbound excited state below the vibrational continuum, which results in fragmentation (orange arrow). This is in contrast to bound ground state to bound excited state ionisation transitions shown in figure 2g. However, in some cases a transition between two bound vibrational levels in different electronic states may still result in

dissociation of the molecule. The molecule in the excited vibrational state in the excited electronic state oscillates and will spend most of its time in the minimum of the potential well in the vibrational level. However, the oscillation may allow a radiationless transition to occur from the bound vibrational level to an unbound neighbouring state. This results in dissociation, so-called pre-dissociation, and is enhanced if the electronic potential curve is nearby.

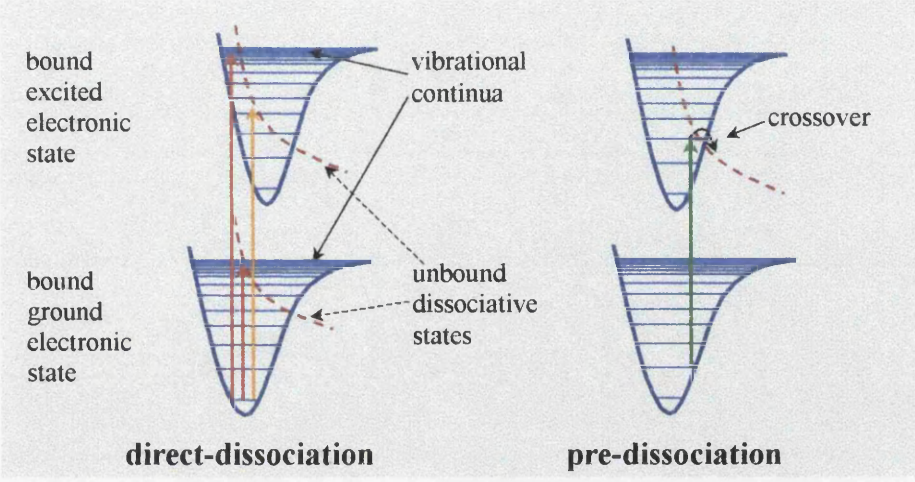

Figure 2h An Illustration of Molecular Dissociation Processes

Luminescence

Luminescence occurs in two ways, fluorescence and phosphorescence. A molecule can absorb photons between a transition from a singlet electronic ground state (S_0) to a singlet electronic excited state (S_1). In the S_1 state the molecule may undergo radiationless relaxation (phonon emission) down through the vibrational levels until the lowest level is reached within S_1. Fluorescence occurs when the molecule further relaxes to a vibrational level in the S_0 state with the emission of a photon. This occurs on a timescale of $\sim 10^{-9}$ seconds.

On the other hand, radiationless transitions may occur from an S_1 state to a triplet state T_1, which may then continue relaxing until the system reaches the lowest vibrational level in the state. A radiation transition from this level in the T_1 state to a vibrational level in the ground state S_0 state can occur and is known as phosphorescence. The time scale for

this radiation from metastable states to occur can be upwards of several seconds since triplet-singlet transitions have smaller probabilities of decay than singlet-singlet transitions.

Intersystem Crossing and Internal Conversion

Intersystem crossing occurs when a radiationless transition takes place between states which have different multiplicity (S→T or T→S). Internal conversion is the term used to describe a radiationless transition between similar states (S→S, T→T). Such transitions can be caused by inter-molecular collisions.

Isomerisation

Compounds with the same molecular formula but different chemical arrangements or structures are called isomers. Isomerisation can occur during the laser-molecular interaction and is usually caused when the molecule relaxes in the sense of intersystem crossing. In the sense of ionisation of the original parent species, isomerisation can be considered as a competing mechanism.

§2.3.4 Ionisation and Dissociation Pathways

Multiphoton absorption in molecules can lead to fragmentation by two distinct mechanisms, ladder-climbing and ladder-switching [Kilic *et al*, 1997; Yang *et al*, 1985; Schlag *et al*, 1983; Gedanken *et al*, 1982; Antonov *et al*, 1981].

These are illustrated in figure 2i for a model diatomic molecule AB. Note that the energy levels indicated by dashed lines may be real or virtual states corresponding to resonant or non-resonant absorption. Also note that the pathways indicated are only illustrative examples. In practice a myriad of additional and further channels would likely be available for ionisation and/or dissociation. The situation is more complex for polyatomic molecules with an inter-related network of possible pathways available.

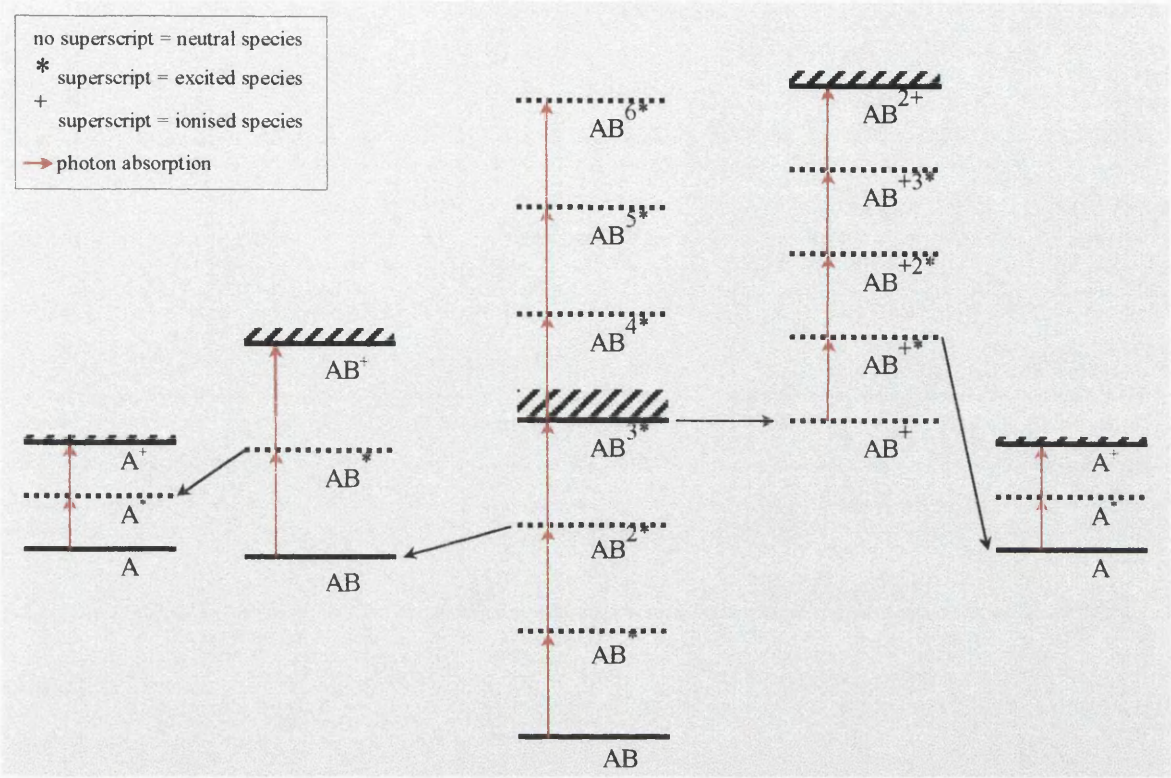

Figure 2i Examples of ladder-switching and ladder climbing mechanisms for a diatomic molecule AB

The left-hand-side of figure 2i demonstrates ladder-switching. The molecule in an excited state below the ionisation level fragments to form neutral moieties. These fragments may absorb further photons within the laser pulse to ionise and/or dissociate. If the intermediate excited states have lifetimes shorter than the laser pulse width, then dissociation followed by ionisation (DI) is favoured.

Efficient multiphoton absorption of photons can suppress fragmentation channels in the sense that rapid up-pumping to the molecular ion continuum can bypass predissociative states. This usually requires laser pulse widths shorter than intermediate state lifetimes. This is known as ladder-climbing. Dissociation can then occur from a myriad of states within the ionisation continuum: ionisation-dissociation (ID) - see right hand side of figure 2i.

It is also important to note that the molecule can be pumped via a series of autoionisation levels to highly excited states of the molecular ion, as shown in the central portion of figure 2i. From these states, ionisation and/or dissociation can occur.

ID and DI will continue until the final products are obtained. Processes may be a mixture of both ladder-switching and ladder-climbing. In fact, DI often competes with ID, the latter becoming more dominant as the laser pulse duration decreases [Yang *et al*, 1985]. Additionally the laser intensity is influential on the molecular dynamics with a large influx of photons supporting up-pumping through a myriad of dissociative states. Also, wavelength choice can also determine the molecular dynamics.

Short pulse width, intense lasers are therefore well suited for analytical purposes in which the suppression of the fragment formation and other relaxation processes previously discussed is of importance. FLMS employs such lasers, and therefore overcomes some of the inherent shortcomings of nanosecond REMPI. The large bandwidths of femtosecond lasers makes for a broad-based non-resonant process, with the high beam intensities compensating for the lack of tuning in terms of ionic yield, in contrast to NRMPI.

§2.3.5 Rate Equation Modelling in Multiphoton Processes

This section briefly considers cross-sections for multiphoton ionisation and associated rate-equations [Singhal *et al*, 1989] which have been developed to fit experimental data. An example of such a fit is given for benzaldehyde in chapter 4, section *4.2.4.*

A two-photon perturbative absorption process is considered for simplicity. The overall rate of ionisation R_2 will depend on the square of the laser intensity I (each absorption is proportional to the intensity) according to:

$$R_2 = \sigma_2 I^2 \qquad \textit{eqn 2.3.5a}$$

where the proportionality constant σ_2 (in units of cm^4s) is a generalised cross-section incorporating the competing processes between ionisation and relaxation as discussed previously. The units of I are number of photons per cm^{-2} per s^{-1}.

This can be extended to a general N photon absorption given by:

$$R_N = \sigma_N I^N \qquad \textit{eqn 2.3.5b}$$

with σ_N in units of $cm^{2N}s^{N-1}$.

An important point worth noting at this stage is the order of the multiphoton process. Taking the natural logarithm of equation *2.3.5b* yields:

$$ln\, R_N = N ln I + ln \sigma_N \qquad \textit{eqn 2.3.5c}$$

Therefore the number of photons N, absorbed to produce an ion, the order of the multiphoton process, is given by the gradient of a plot of the logarithm of the ionic yield against the logarithm of the laser intensity. A more detailed discussion on rate equations and how they can predict ionic yields given suitable cross-sections is now considered. For a more in depth study, reference should be made to Singhal *et al* [1989].

Let a laser of pulse width T with a top-hat intensity profile be interacting with a two-level atomic or molecular system such that the ionisation process proceeds via an intermediate real or virtual state - see figure 2j.

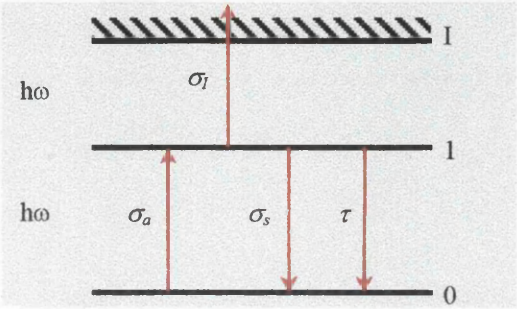

Figure 2j A Simple Two-Level System for Rate Equations

σ_a is the stimulated absorption cross section.

σ_s is the stimulated emission cross section.

τ is the mean lifetime for spontaneous emission from state 1→0.

σ_I is the ionisation cross section from state 1→I.

Let the levels be populated with N_0, N_1 and N_I particles. Let Φ be the incident photon flux i.e. no. of photons/unit area/unit time. Assume that σ_a equals σ_s in an equilibrium state. Then the rate equations describing the time development of the level populations 0, 1 and I are [Ledingham, 1995c]:

$$\frac{dN_0}{dt} = -N_0\sigma_a\Phi + \frac{N_1}{\tau} + N_1\sigma_a\Phi \qquad \textit{eqn 2.3.5d}$$

$$\frac{dN_1}{dt} = N_0\sigma_a\Phi - \frac{N_1}{\tau} - N_1\sigma_a\Phi - N_1\sigma_I\Phi \qquad \textit{eqn 2.3.5e}$$

$$\frac{dN_I}{dt} = N_1\sigma_I\Phi \qquad \textit{eqn 2.3.5f}$$

N_0 and N_1 must first of all be found if the ionic yield N_I is to be calculated...

Add *2.3.5d* and *2.3.5e*, and differentiate *2.3.5e* with respect to time to give:

$$\frac{dN_0}{dt} = -\frac{dN_1}{dt} - N_1\sigma_I\Phi \qquad \textit{eqn 2.3.5g}$$

$$\frac{d^2N_1}{dt^2} = \sigma_a\Phi\frac{dN_0}{dt} - \frac{1}{\tau}\frac{dN_1}{dt} - \sigma_a\Phi\frac{dN_1}{dt} - \sigma_I\Phi\frac{dN_1}{dt} \qquad \textit{eqn 2.3.5h}$$

Upon substitution of *2.3.5g* into *2.3.5h* we get:

$$\frac{d^2N_1}{dt^2} + 2b\frac{dN_1}{dt} + \omega^2 N_1 = 0 \qquad \textit{eqn 2.3.5i}$$

where:

$$2b = (2\sigma_a + \sigma_I)\Phi + \frac{1}{\tau} \quad \text{and} \quad \omega^2 = \sigma_a \sigma_I \Phi^2 \qquad \textit{eqns 2.3.5j/k}$$

Letting:

$$N_1 = e^{-\lambda t} \qquad \textit{eqn 2.3.5l}$$

eqn *2.3.5i* becomes:

$$\lambda^2 e^{-\lambda t} - 2b\lambda e^{-\lambda t} + \omega^2 e^{-\lambda t} = 0 \qquad \textit{eqn 2.3.5m}$$

with:

$$\lambda = \frac{2b \pm (4b^2 - 4\omega^2)^{1/2}}{2} \qquad \lambda_1 = b - (b^2 - \omega^2)^{1/2} \qquad \lambda_2 = b + (b^2 - \omega^2)^{1/2} \qquad \textit{eqns 2.3.5n/o/p}$$

Therefore:

$$N_1 = Ae^{-\lambda_2 t} + Be^{-\lambda_1 t} \qquad \textit{eqn 2.3.5q}$$

Now $A = -B$ since $N_1 = 0$ at $t = 0$. Therefore:

$$N_1 = A[\exp(-\lambda_1 t) - \exp(-\lambda_2 t)] \qquad \textit{eqn 2.3.5r}$$

Substitute *2.3.5r* into *2.3.5e* and note that the initial number of ground state (level 0) particles at $t = 0$ equals N_0 and N_1 equals zero. This yields:

$$N_0 = \frac{A(\lambda_2 - \lambda_1)}{\sigma_a \Phi} \qquad \text{or} \qquad A = \frac{N_0 \sigma_a \Phi}{(\lambda_2 - \lambda_1)} \qquad \textit{eqns 2.3.5 s/t}$$

Substituting eqn *2.3.5t* into *2.3.5r*

$$N_1 = \frac{N_0 \sigma_a \Phi}{\lambda_2 - \lambda_1}\left[\exp(-\lambda_1 t) - \exp(-\lambda_2 t)\right] \qquad \textit{eqn 2.3.5u}$$

Therefore *2.3.5f* can be written as:

$$\frac{dN_I}{dt} = \frac{N_0 \sigma_I \sigma_a \Phi^2}{\lambda_2 - \lambda_1}\left[\exp(-\lambda_1 t) - \exp(-\lambda_2 t)\right] \qquad \textit{eqn 2.3.5v}$$

Solving the above equation by integrating over the length of the laser pulse T, with respect to time, gives:

$$N_I = \frac{N_0 \sigma_I \sigma_a \Phi^2}{\lambda_2 - \lambda_1}\left[\frac{1}{\lambda_2}\left(\exp\{-\lambda_2 T\} - 1\right) - \frac{1}{\lambda_1}\left(\exp\{-\lambda_1 T\} - 1\right)\right] \qquad \textit{eqn 2.3.5w}$$

which is an expression for the ionic yield. This expression, for known cross sections, allows a theoretical plot of ionic yield against laser flux.

This situation also encompasses a saturation condition in which all the particles in the ground state are ionised. Usually σ_a (= σ_s in the present case) is much greater than σ_I. Then from eqns *2.3.5j/k/p* it is evident that $b^2 >> w^2$ and:

$$2b \approx 2\sigma_a \Phi + \frac{1}{\tau} \approx \lambda_2 \qquad \textit{eqn 2.3.5x}$$

Also $\lambda_2 >> \lambda_1$ and eqn *2.3.5u* simplifies to:

$$N_1 = \frac{N_0 \sigma_a \Phi}{\lambda_2}\left[\exp(-\lambda_1 t)\right] \qquad \textit{eqn 2.3.5y}$$

Assuming that $\sigma_a\Phi >> 1/\tau$ then the above equation becomes:

$$N_1 = \frac{N_0}{2}\exp(-\lambda_1 t) \qquad \textit{eqn 2.3.5z}$$

Now again applying the above assumption that $b^2>>w^2$ and $\sigma_a\Phi >> 1/\tau$, λ_1 given by *2.3.5o* simplifies to:

$$\lambda_1 = \frac{1}{2}\sigma_I\Phi \qquad \textit{eqn 2.3.5A}$$

From eqn *2.3.5f* an integration over the length of the laser pulse T yields N_I as done previously to arrive at eqn *2.3.5w*.

$$N_I = \sigma_I\Phi\int_0^T \frac{N_0}{2}\exp(-\lambda_1 t)dt \qquad \textit{eqn 2.3.5B}$$

$$N_I = \sigma_I\Phi\frac{N_0}{2}\left[\frac{1}{\lambda_1} - \frac{1}{\lambda_1}\exp(-\lambda_1 T)\right] \qquad \textit{eqn 2.3.5C}$$

Therefore recalling λ_1 from eqn *2.3.5A*, then it is clear that $N_I = N_0$ for $\lambda_1 T >> 1$. In terms of λ_1 this is $\sigma_I\phi >> 1$. The two equations highlighted in bold are the saturation conditions in which all the particles in the ground state are ionised and $N_0 = N_I$ i.e.

$$\sigma_a\Phi >> \frac{1}{\tau} \qquad \sigma_I\Phi >> 1 \qquad \textit{eqns 2.3.5 D/E}$$

The treatment is much more complex when considering a many level system and a 'real' laser beam that may have an non-flat temporal and intensity profile [Singhal *et al*, 1989]. An example of fitting rate equations to experimental data is performed by Dr. R.P. Singhal for benzaldehyde in chapter 4, section *4.2.4.*

§2.4 Tunnel Ionisation (TI)

As laser intensities increase, the physics can become more and more non-perturbative and tunnel ionisation (TI) can begin to compete with perturbative multiphoton processes. In TI, the bound state atomic/molecular structure has no effect on the ionisation yield. Beam intensities upwards of ~ 10^{14} W cm^{-2} in the ultrafast pulse width regime, have associated electric fields (~ 10^{9} V cm^{-1}) which are comparable to the coulomb electric fields which bind electrons in atoms or molecules. A summation of the atomic or molecular potential and the instantaneous field of the laser can lead to a situation in which the valence electron(s) can very quickly escape by tunnelling through the suppressed coulomb barrier. Figure 2k shows the resultant electric potential (V) as a function of displacement (x) for an atom which is highly perturbed by an external field. The electrons shown are escaping either by tunnelling (field ionisation) through a potential barrier, or if the external field is sufficiently intense, by a process known as over the barrier ionisation (OTBI) [Augst *et al*, 1991] which can be described in purely classical terms.

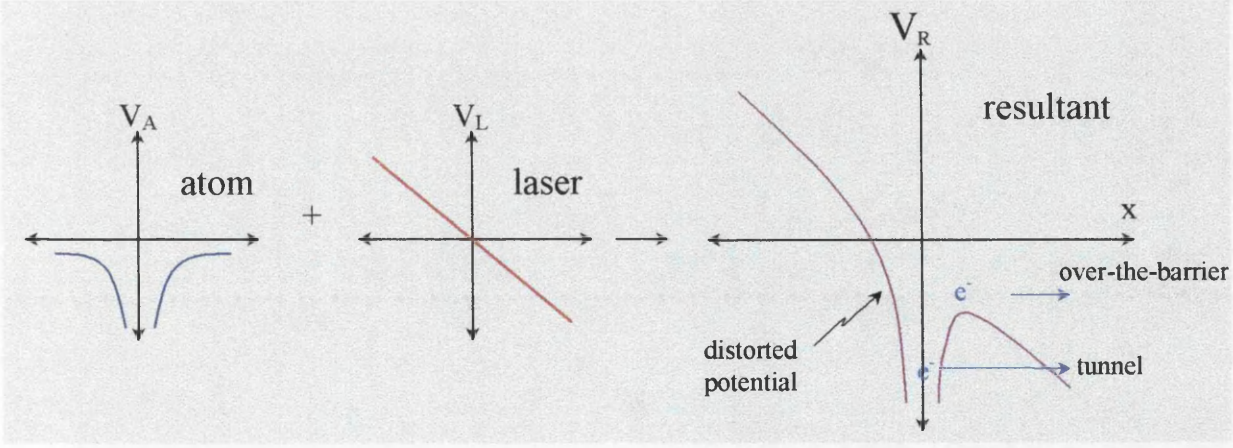

Figure 2k Tunnel and Over the Barrier Ionisation for an Atom

The situation is more complex for a molecule due to it's inherently more complex potential make-up. However, the principles are similar. Figure 2l shows a simple picture of the field ionisation and OTBI for a diatomic molecule [Constant *et al*, 1996; Codling *et al*, 1993].

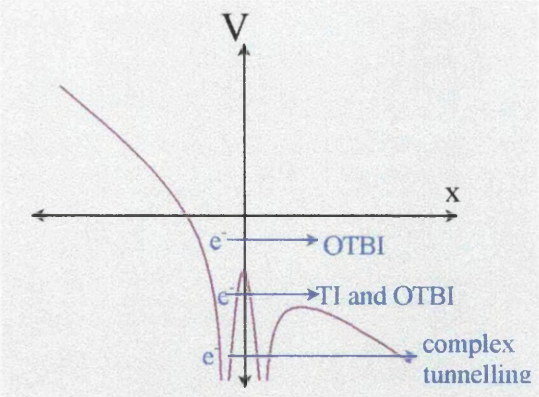

Figure 2l Tunnel and Over the Barrier Ionisation for a Diatomic Molecule

OTBI can be simply described in one dimension as a classical superposition of the coulomb potential felt by an electron and a quasi-static laser field. The resulting potential may be written as:

$$V(x) = -\frac{Ze^2}{4\pi\varepsilon_0 x} - e\Sigma x \qquad \textit{eqn 2.4a}$$

for charge Z and external field Σ, along an x-axis. This potential has a relative maximum located at x_{max} and is found by setting $dV/dx = 0$. Equating $V(x)_{\max}$ to the ionisation potential E_i of an atom or ion allows a calculation of the critical electric field which is necessary for the electron to escape without tunnelling. This turns out as:

$$\Sigma_{crit} \sim \frac{E_i^2}{Z} \qquad \textit{eqn 2.4b}$$

The corresponding threshold laser intensity I_{th} defined as the intensity at which the potential barrier is reduced to the ionisation potential of the atom and therefore permitting this free electron escape is then given by [Augst *et al*, 1991, 1989; Gibson *et al*, 1990]:

$$I_{th} \sim \frac{E_i^4}{Z^2} \qquad \textit{eqn 2.4c}$$

when noting that:

$$I = \frac{1}{2} c\varepsilon_0 \Sigma^2 \qquad \textit{eqn 2.4d}$$

for speed of light c and permittivity of free space ε_0 [Protopapas *et al*, 1997]. This can be expressed more definitely as [Augst *et al*, 1991]:

$$I_{th}(Wcm^{-2}) = 4\times10^{9}\frac{E_i^4(eV)}{Z^2} \qquad \textit{eqn 2.4e}$$

The situation is obviously more complex in three-dimensions and for molecules with more complex potential patterns [DeWitt *et al*, 1998a, 1998b]. For example, a barrier may only be suppressed in one direction, and electron shielding may occur.

One of the first publications on ionisation in the field of a strong electromagnetic wave was by L.V. Keldysh [1965]. In his pioneering paper, Keldysh noted that the ionisation potential of an atom can be effectively lowered under the influence of a large external electric field perturbation. The electrons could effectively escape the pull of the atomic potential in a tunnelling mechanism. Their tunnelling time is determined essentially by the mean free time of the electron passing through a barrier of width l:

$$l = \frac{E_i}{e\Sigma} \qquad \textit{eqn 2.4f}$$

where E_i is the ionisation potential, e the electronic charge and Σ the electric field strength. The average kinetic energy of such an electron in the laser field can be used to gain an expression for the mean electron velocity V:

$$V = \left[\frac{2E_i}{m}\right]^{1/2} \qquad \textit{eqn 2.4g}$$

for electronic mass m. Note that this time-averaged kinetic energy which the electron experiences in the laser field is called the quiver energy or pondermotive potential [Protopapas *et al*, 1997; Kyrala, 1993]. Combining equations *2.4f* and *2.4g* then gives the tunnelling time and frequency:

$$t = \frac{l}{V} = \frac{(E_i m)^{1/2}}{\sqrt{2}e\Sigma} \qquad \textit{eqn 2.4h}$$

$$v = \frac{1}{t} = \frac{\sqrt{2}e\Sigma}{(E_i m)^{1/2}} \qquad \textit{eqn 2.4i}$$

Therefore the tunnel effect is largely dependent on the instantaneous value of the field intensity Σ and the ionisation potential E_i. Tunnelling can occur if the mean tunnelling time given by equation *2.4h* is less than half the period of the laser [DeWitt *et al*, 1998a] because this allows the coulombic barrier felt by the electron to be distorted for a sufficient time to allow the electron to pass through. From this the Keldysh parameter γ can be defined:

$$\gamma = \frac{2t}{t_0} = \frac{2v_0}{v} = \frac{l}{l_0} = v_0 \frac{(2E_i m)^{1/2}}{e\Sigma} \qquad \textit{eqn 2.4j}$$

where t_0 is the period of the laser, v_0 is the laser frequency and l_0 the mean distance which an electron travels during one half-period of the laser at mean velocity V. This can be written as:

$$\gamma = \left[\frac{E_i}{1.87 \times 10^{-19} I\lambda^2} \right]^{1/2} \qquad \textit{eqn 2.4k}$$

with E_i in units of eV, I in units of W cm^{-2} and λ in units of nm, which is the form used in this thesis.

The criterion for tunnelling as indicated above therefore means that values of $\gamma << 1$ correspond to tunnelling. For $\gamma >> 1$ tunnelling will not occur and the ionisation will proceed via a multiphoton pathway. It follows that high wavelengths (low frequencies) coupled to high beam intensities will be suited to tunnelling - provided that the intensity is not so high that OTBI results instead of tunnelling. A multiphoton process is more

suited to lower wavelengths and lesser beam intensities, again if the field is low enough as to avoid OTBI. In the intermediate Keldysh parameter range i.e. $\gamma \sim 1$ a contribution to the ionisation rate can be from both mechanisms. A more pragmatic criterion for tunnelling has recently been postulated as $\gamma < 0.5$ [Ilkov *et al*, 1992].

As stated earlier, the situation is more complex for molecules. In deriving the Keldysh parameter for atoms, the actual shape of the potential surface was not considered. The potentials were taken as zero-range in nature. This is a good approximation for atoms, and a reasonable approximation for molecules - it is employed in this thesis. However, it is worth noting that potential surfaces of molecules can be very different to the zero-range simplification. Extended molecular orbitals are not too well described in this manner, particularly for polyatomic molecules as reported by DeWitt *et al* [1998a] in a very recent publication.

§2.5 Coulomb Explosions

Associated with high intensity short pulse lasers is a phenomenon known as coulomb explosions in molecules [e.g. Codling *et al*, 1994, 1993]. Once a molecule has been ionised beyond the first charged state, the components constituting the transient parent molecular ion are subject to a considerable coulomb repulsion. This can result in the molecule flying apart with the fragments having considerable kinetic energy. The phenomenon is known as a coulomb explosion. The dynamics of the process are complex with considerable interplay between excitation, dissociation and ionisation. The appearance of stable multiply charged atomic and daughter ions from the parent ion is thought to be evidence of coulomb explosion activity. On the other hand, the appearance of stable multiply charged parent ions is suggestive of a lack of this mechanism because any multiply charged molecular ions will have a transient existence in a coulomb explosion event.

CHAPTER 3

EXPERIMENTAL

§3.0	**Introduction**	37
§3.1	**The Laser Systems**	37
§3.1.1	*The Original Laser System*	39
§3.1.2	*The Refurbished Laser System*	46
§3.2	**Ion Detection and Data Acquisition**	47
§3.2.1	*The Linear Time-of-Flight Mass Spectrometer (TOF)*	49
	The Inlet System	50
	High-Vacuum Environment	51
	Laser Beam Alignment, Ion Optics and the Drift Region	51
§3.2.2	*The Electron Multiplier and Digital Oscilloscope*	53
§3.2.3	*A Typical Time-of-Flight Mass Spectrum*	55
§3.3	**Laser Diagnostics**	55
§3.3.1	*Autocorrelation Measurement of the Laser Pulse Width*	56
§3.3.2	*Bench Optics and Measurement of the Pulse Energy*	57
§3.3.3	*Determining the Laser Intensity at the Focused Spot*	59

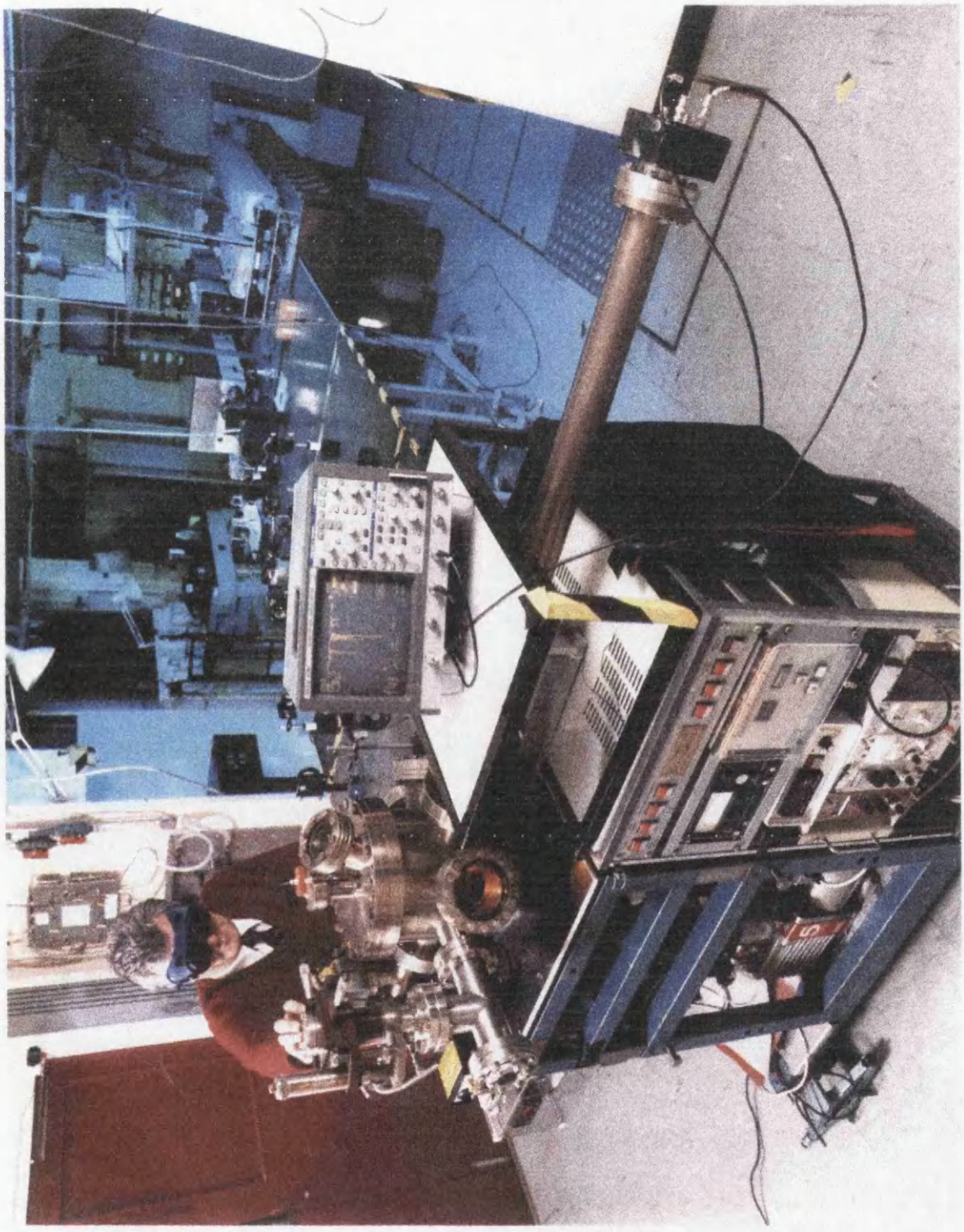

Figure 3a Time-of-flight mass spectrometer (TOF) in-situ at Rutherford Appleton Laboratory (RAL) with the laser system and bench optics

§3.0 Introduction

This chapter provides precise details of the experimental apparatus and procedures used in this study of femtosecond laser mass spectrometry (FLMS). Mass spectrometry is utilised for molecular analysis. The set-up is schematically illustrated in figure 3b.

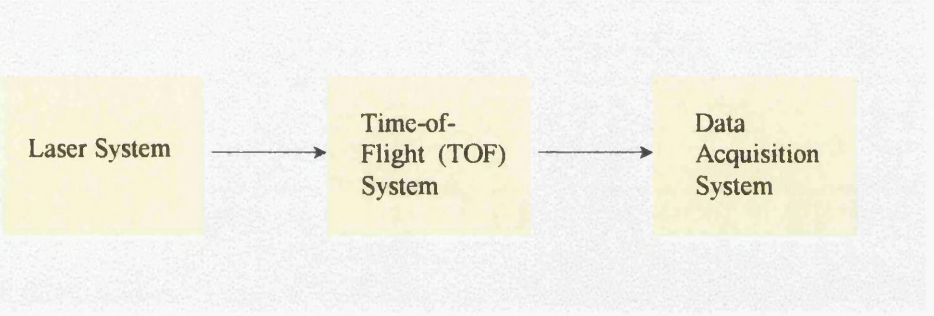

Figure 3b Experimental Schematic

The FLMS arrangement employs a short-pulsed laser system coupled to a linear time-of-flight mass spectrometer (TOF) within which a vapour sample is ionised. The resultant ions are then accelerated by an electrostatic field before traversing a zero-field drift region towards detection and data storage according to their flight times and relative abundance. Figure 3a shows the TOF in-situ with the laser system and bench optics in the background.

This chapter is split into three main sections. Firstly, the laser systems are described. Secondly, ion detection and data acquisition are considered. Finally, relevant laser diagnostics are discussed.

§3.1 The Laser Systems

Ultrafast laser systems are becoming "turnkey" devices, capable of producing peak output powers of the order of a megawatt in a pulse duration of a few femtoseconds. Amplification systems can increase this factor by as much as 10^6 times. This can lead to high order focused intensities of the order of 10^{20} W cm^{-2}, which, as Backus *et al* [1998] noted, is greater than the entire solar flux incident on the earth focused onto a pinhead!

The general principles of lasers has been outlined in the second chapter, section 2.1. Here the treatment is more specific. The laser system used for the present study is located at the Rutherford Appleton Laboratory (R.A.L.) in Oxfordshire. An extensive refurbishment was done during the experimental period. Therefore this section consists of two main parts, pre and post refurbishment. Schematics of the arrangements are shown in figure 3c [Langley *et al*, 1994; Taday *et al*, 1998].

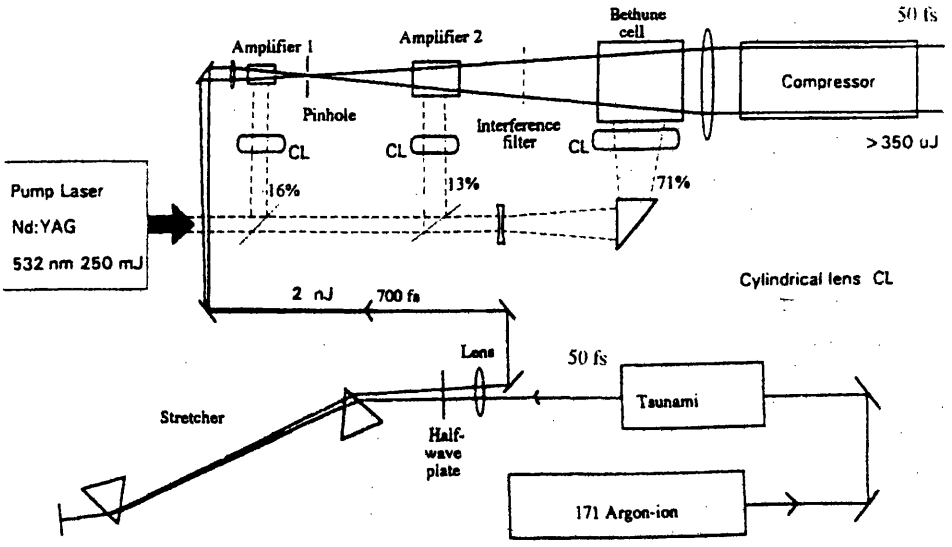

Figure 3c.i Schematic of the Original Laser System

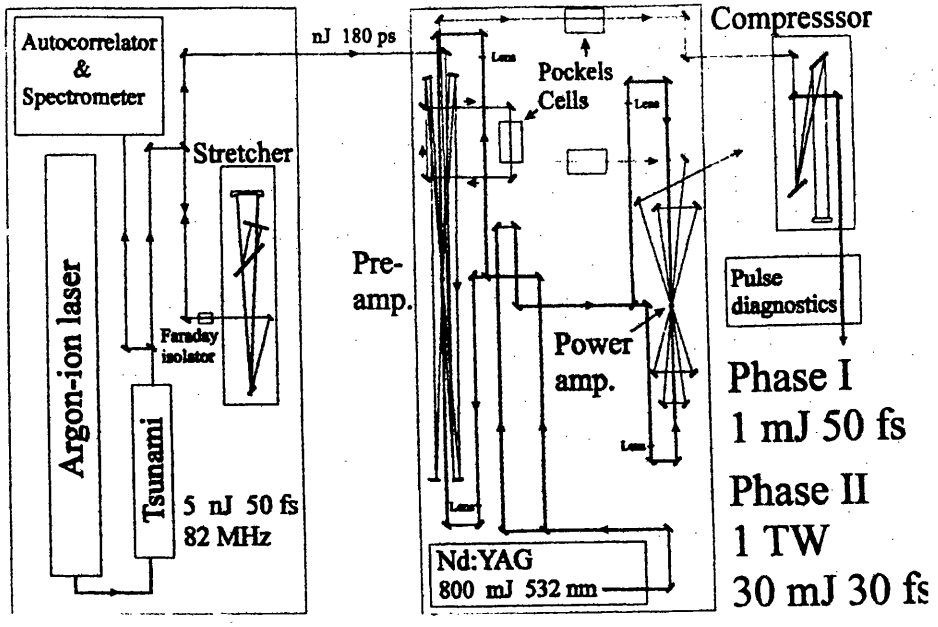

Figure 3c.ii Schematic of the Refurbished Laser System

§3.1.1 The Original Laser System

This section describes the laser system [Langley *et al*, 1994] before the refurbishment took place and is related to the results in chapters 4, 5 and part of 7 and 8. The system was a high-brightness femtosecond laser utilising titanium-sapphire (Ti:S) technology and amplification in dyes. The arrangement is shown in figure 3c.i shown on the previous page.

The short pulse source comprised a mode-locked titanium-saphire ($Ti:Al_2O_3$) oscillator (Spectra-Physics Tsunami) pumped by 7 W from a continuous wave (cw) all-lines argon-ion laser (Spectra-Physics 171). The system produced a train of pulses tuneable from 50 to 300 fs and 730 to beyond 800 nm with a gaussian beam profile.

The principles of an argon-ion laser are briefly described [Svelto, 1989]. The Ar^+ ground state at ~ 16 eV is obtained by removing one electron from the outer shell. A further excited state is then obtained by promoting one of the remaining electrons in the Ar^+ ion to a higher excited state around 35 eV. High current densities are required to create the population inversion such that the system can lase from the above said excited state at ~ 35 eV to a state at ~ 32 eV. This decay occurs on a time scale of ~ 10^{-8} s, with further decay to the ground Ar^+ level in a time ~ 10 times shorter, and therefore satisfying the condition for cw laser action. The argon-ion laser can oscillate on many lines in the UV wavelength region due to the presence of many lasing sub-levels. In practice the laser was operated around 500 nm.

As previously mentioned, the argon-ion laser is used as an optical pump for the solid-state ti-sapphire oscillator. Figure 3d shows the absorption and emission spectroscopic properties of the $Ti:Al_2O_3$ material [Davis, 1996]. The Ar-ion laser wavelength was suitably in the middle and most intense part of the absorption spectrum of the ti-sapphire crystal. The Ti:S laser is a four level lasing system based on the schematic illustration shown in figure 3e. Ground state particles are optically excited into an absorption band (4) followed by a rapid non-radiative transfer into the upper laser level (3) such that a population inversion will result between levels 3 and 2 and laser action can be obtained. Then a fast drain transition (2-to-1) occurs.

Section 2.1 in chapter 2 should be referred to for a fundamental look at laser transitions.

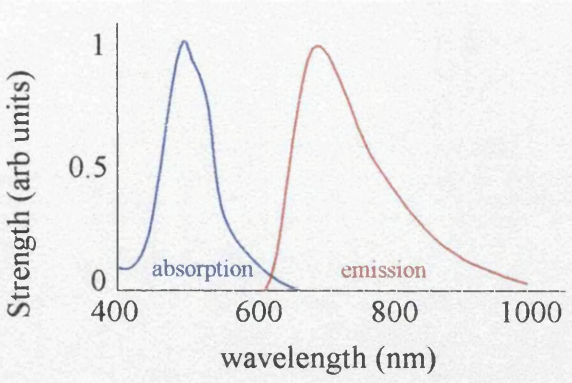

Figure 3d Absorption and Emission Properties of Titanium doped Sapphire

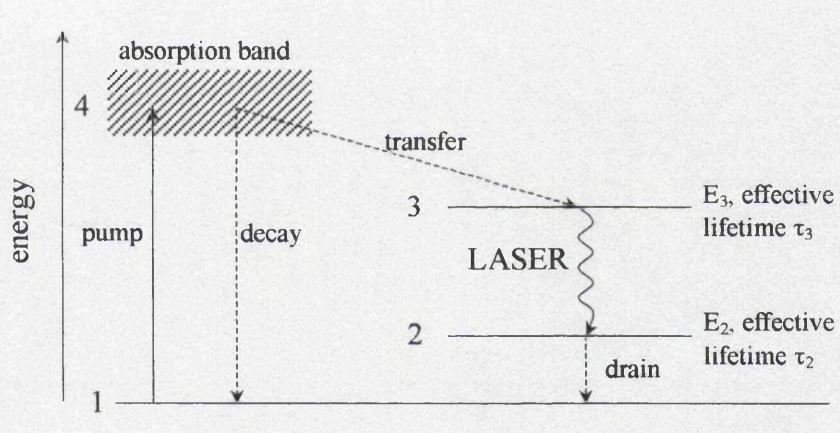

Figure 3e Schematic of an Optically Pumped Four Level Laser System

The gain medium, Ti:Al_2O_3, was a thin rod of a few centimetres in length. It provided an attractive gain medium for laser operation in the near infrared spectral region with a large gain bandwidth required to facilitate ultrashort pulse generation, very high thermal conductivity and a high energy storage density. Photons spontaneously emitted after excitation by the pump source had a finite chance of encountering further excited Ti ions and stimulating them to decay, emitting more photons but in the same direction. Photons spontaneously emitted into the side directions were just lost. This resulted in an avalanche of stimulated emission producing an amplified beam of light down the axis of the laser rod. Figure 3f [Knight, 1989] illustrates this. Cavity mirrors were used to reflect the light beam back into the active medium for amplification.

The Tsumami was optimised for a wavelength of 750 nm at a pulse width of 50 fs and energy ~ 2nJ with a wavelength bandwidth (FWHM) around 20 nm. The polarisation of the emergent beam was vertical and the pulse-to-pulse stability was consistent to less than 5 %. Such a laser was ideal as a front-end source for a high-power, ultrafast amplifier system.

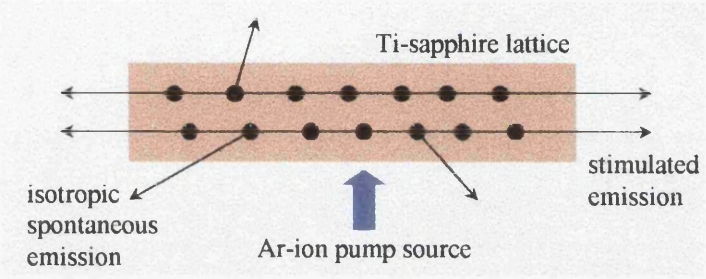

Figure 3f Stimulated Emission in a Ti:Al_2O_3 Rod

The generation of such intense short pulses [Backus *et al*, 1998] has been achieved by many groups, generally using a mode-locking technique [e.g. Zhou *et al*, 1994; Barty *et al*, 1994; Spence *et al*, 1991; Kmetec *et al*, 1991]. In the present case, the mode-locking is performed using a fast saturable absorber on the pulse intensity, placed in the laser cavity, such that preferential absorption occurs in the lower intensity parts of the laser pulse i.e the leading and trailing pulse edges. The absorber is the host material, sapphire, in the Ti:S crystal. High intensity parts are so intense that they saturate the absorber which allows most of the intense light through. This results in a high gain for the high intensity pulse part and a low gain for the low intensity pulse part. The high intensity part is transmitted by an output mirror on each cavity pass, resulting in a mode-locked pulse train of ultrafast pulse widths separated by 2L/c where L is the length of the laser cavity and c, the speed of light.

The evolution of the laser pulse through the system is summarised in figure 3g. The generation and manipulation of ultrafast intense pulses has been the subject of considerable attention in very recent years [Backus *et al*, 1998; Davis *et al*, 1996; Barty *et al*, 1996, 1994; Singhal *et al*, 1995; Perry *et al*, 1994; Rudd *et al*, 1993; Mataloni *et al*, 1991; Spence *et al*, 1991; Knox, 1988; Maine *et al*, 1988; Rolland *et al*, 1986; Strickland *et al*, 1985; Shank *et al*, 1982; Fork *et al*, 1982]. If amplification is required, the initial pulse must first be stretched to reduce its intensity, primarily to avoid damage to the optical components, while maintaining the frequency spectrum of

the initial pulse. Stretching also limits non-linear distortion to the spatial and temporal profile of the beam. It can then be recompressed to its initial size after amplification. This was achieved using a sophisticated technique known as chirped pulse amplification (CPA) followed by optical pulse compression (OPC). Previous to application and development to lasers, CPA was used in radar applications [Strickland *et al*, 1985].

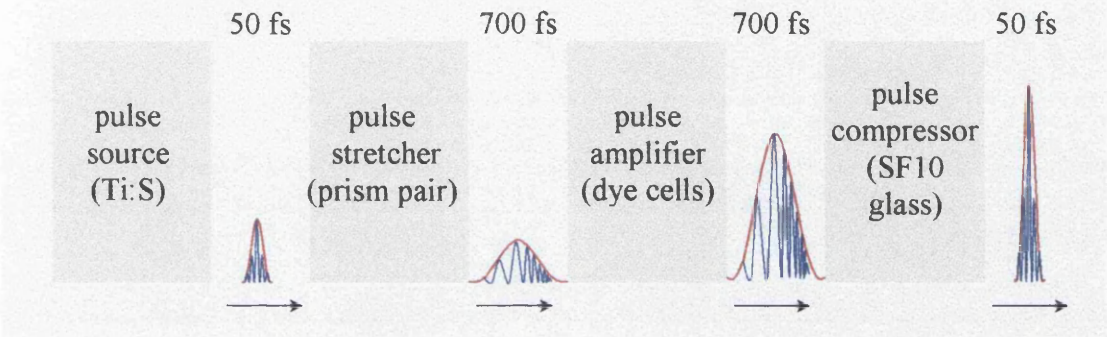

Figure 3g The Laser Pulse Evolution in the Original Femtosecond System

A common method of pulse length manipulation uses two diffraction gratings [Davis, 1996; Hutchinson, 1989] which can form the basis of optimally matched stretching/compressing and allow large, reversible stretch factors. Depending on the geometry of the gratings with respect to each other and the laser beam, the pulse can either be stretched or compressed. The higher frequencies contained within the spectrum of the pulse are diffracted through smaller angles at the gratings. So for example, if the higher frequencies follow a longer path than the lower frequencies, then the pulse is stretched with the lower frequencies leading the higher frequencies. This is shown in figure 3h with t_1 occurring earlier than t_2.

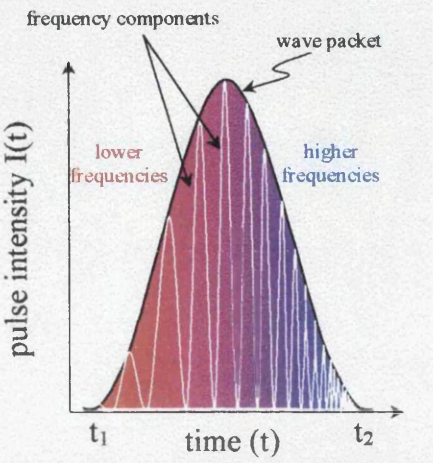

Figure 3h A Pulse with a Frequency Chirp (stretched)

The frequency coded pulse can be restored to its original form by appropriate phase delays between the frequency components, such that the red-shifted leading edge of the pulse is delayed by a suitable amount relative to the blue-shifted trailing edge. Examples of simple diffraction grating geometry for CPA and OPC are shown in figure 3i.

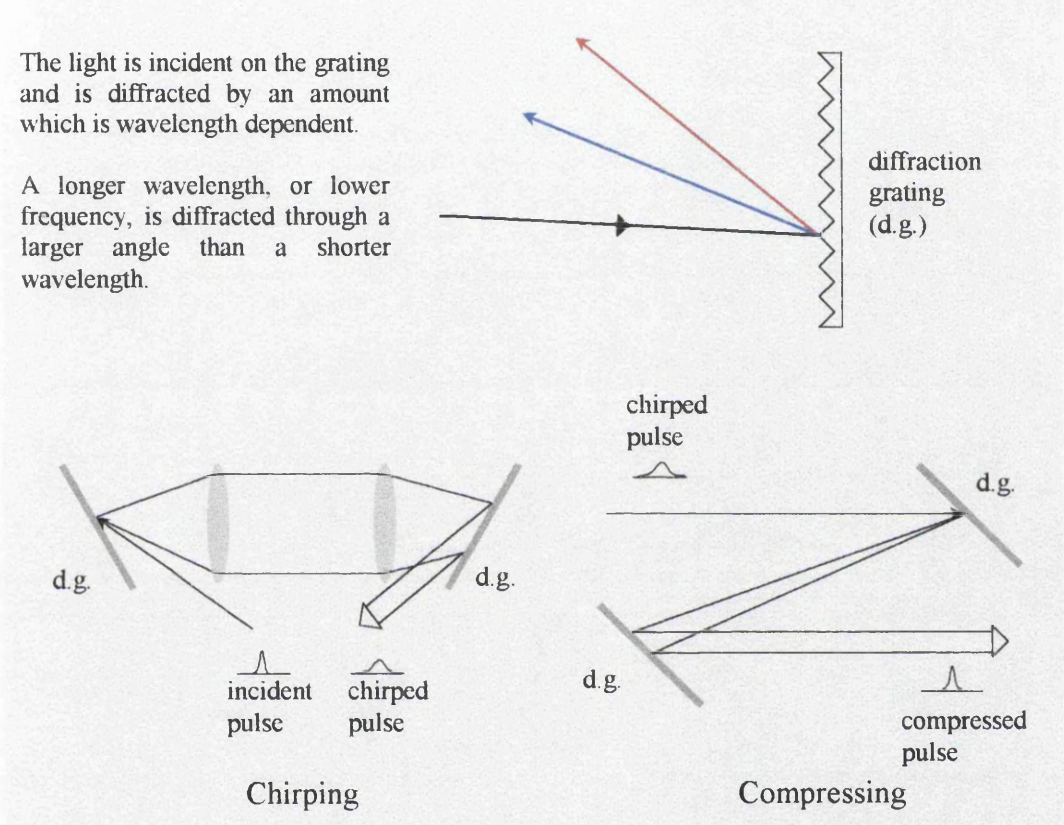

Figure 3i Diffraction of a Light Beam by a Grating

In a dispersive medium, the frequency components of the spectral laser pulse will travel at different speeds and be dispersed, each having an instantaneous velocity defined as the phase velocity, V_p:

$$V_p = \frac{\omega}{k} \qquad \omega = 2\pi\upsilon \qquad k = \frac{2\pi n}{\lambda} \qquad \textit{eqns 3.1.1a/b/c}$$

where ω is the angular frequency, ν the frequency, k the wave number, n the refractive index and λ the wavelength. This is because the refractive index of the medium is frequency dependent. Different materials exhibit different dependences with the

effective path lengths l_{eff}, of the different frequency components having the following relation for passage through a material of length l_0.

$$l_{eff} \approx nl_0 \qquad \textit{eqn 3.1.1d}$$

assuming minimal non-linear contribution.

Chirping and compression were achieved in this study, for the pre-refurbished case, using this principle. A prism pair (type BK 7) was used to chirp the pulse from the tsunami to around 700 fs. The spectrum of the short pulse passed through the prisms in such a way that the different colours followed different paths through the system, with the high frequency components traversing a longer optical path than the low frequency components - the resulting chirped pulse having a similar spectrum to that depicted in figure 3h except that the red trailed the blue frequencies.

The chirped pulse was recompressed using a block of SF10 glass with the thickness of the block effecting the resultant compressed pulse length, related to effective path lengths in equation *3.1.1d.* To achieve a good correlation between the initial and recompressed pulse, a thickness of 145 mm was used. Various thickness of blocks were used to vary the pulse width up to a maximum of a few picoseconds. The property of the SF10 blocks allowed the low frequencies in the trailing edge of the input pulse to travel faster than the leading high frequencies, resulting in a squeezing together of the optical frequencies in the spectral laser pulse. In this case, n effectively increased with increasing frequency.

If the intensity of the beam is high enough for non-linear effects to become significant, then the refractive index n, of the medium is also dependent on the intensity I, according to:

$$n = n_1 + \gamma I \qquad \textit{eqn 3.1.1e}$$

where n_1 and γ are the linear and non-linear refractive index components respectively. The intensity of a pulse depends on time. Therefore we have $n(t)$. It can be shown

[Singhal, 1995; Hutchinson, 1989] that the time dependent frequency of the laser pulse may be expressed as:

$$w(t) = \frac{d\vartheta(t)}{dt} = w_0 - zk_0 \frac{dn(t)}{dt} = w_0 - zk_0\gamma \frac{dI(t)}{dt} \qquad \textit{eqn 3.1.1f}$$

for a wave travelling in the *z*-direction, with phase θ in a medium with gain coefficient γ. Therefore, for a gaussian shaped pulse, *dI/dt* is positive on the leading edge of the pulse and a decrease in optical frequency occurs. On the trailing edge there is a corresponding increase in the frequency (negative *dI/dt*). As noted in equation *3.1.1a* the different frequency components travel at different speeds, so this results in pulse width alterations.

In between stretching and compression, the pulses were amplified using a modified three-stage dye-amplifier pumped by a Q-switched Spectra Physics Nd-YAG laser (neodymium yttrium aluminium garnet) which was synchronised electronically to a photodiode reference signal derived from the Ti:S oscillator. The principles of operation of an Nd-YAG laser and dye lasers are well known and found in most laser text books [e.g. Davis, 1996]. The dye laser was operated in the high emission region of the ti-sapphire crystal Therefore, the population inversion created in the dye system was stimulated by the ti-sapphire signal and effective amplification occured of the tsunami output. Figure 3c.i shows the set-up. The dye used was type LDS 751 used in preference to the higher gain type Rhodamine 700. LDS 751 could amplify across a wider bandwidth region. A 10 cm focal length lens was placed before the first amplifier and served to focus the amplified beam through a 100 μm pinhole to remove amplified stimulated emission (ASE). An interference filter further reduced ASE before entry into a Bethune cell amplifier [Bethune, 1981]. The Bethune cell was used because it offered several advantages over the standard dye cells, primarily avoiding an imprint of poor spatial uniformity onto the beam from the pump beam. Other benefits include good beam quality and ease of alignment. Due to its innovative shape, the gain distribution across the beam in the Bethune cell is uniform.

The resultant beam of approximately gaussian profile - imaged using a charge coupled device (CCD) - and vertical polarisation had an pulse width of ~ 50 fs and energy in excess of 350 μJ which was an increase of the order of 10^5 in energy amplification.

§3.1.2 The Refurbished Laser System

An extensive overhaul of the laser system [Taday *et al*, 1998] described in section *3.1.1* took place during the course of the present study. Chapters 6 and part of 7 and 8 show the related results. A schematic illustration is found in figure 3c.ii on page 38. One can see that the system is fully solid state with the replacement of dye cells with ti-sapphire amplification, which has several desirable characteristics including a very high damage threshold (~ 8 - 10 J cm^{-2}), a high saturation fluence (~ 0.9 J cm^{-2}), a high thermal conductivity and a large peak gain cross-section [Backus *et al*, 1998]. Moreover, ti-sapphire has the broadest gain bandwidth of any known material - ~ 230 nm FWHM - and thus can support extremely short pulses. The evolution of the pulse through the system is summarised in figure 3j [Taday *et al*, 1998]. A brief overview follows.

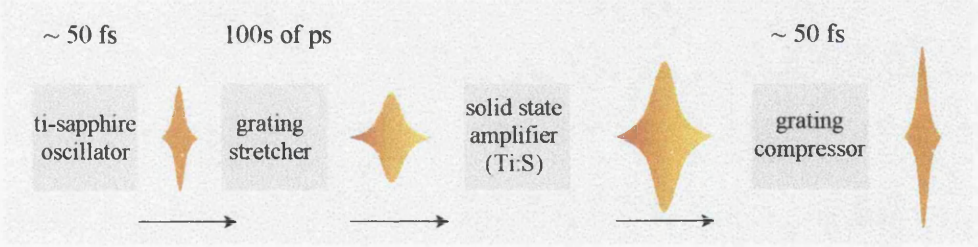

Figure 3j The Laser Pulse Evolution in the Refurbished Femtosecond System

A ti-sapphire oscillator is pumped by an argon-ion laser as in section *3.1.1*. The system was set to produce pulses of duration 50 fs and wavelength 790 nm with about 9 nJ per pulse. The pulses were then stretched to ~ 200 ps using a grating system which operated on the principles highlighted previously - the red frequencies lead the blue frequenciesd. The oscillator was isolated from the stretcher via a Faraday rotator [Davis *et al*, 1996] which limited against undesirable feedback, and prevented potential oscillator damage. The energy per pulse after the stretcher and rotator was reduced to around 0.5 nJ.

The stretched pulses were then amplified in a multipass amplifier system (pre-amp in figure 3c.ii) which consisted of numerous spherical mirrors and a titanium-sapphire rod of length 7 mm (Crystal Systems) pumped with 67 mJ from a Nd:YAG laser (Spectra Physics). After five passes, the train of pulses were extracted using a time-gated polarisation device - polariser-Pockel cell combination [Svelto, 1989] - to reduce the repetition rate from 82 MHz to 10 Hz. This set-up is known as cavity dumping, in that the ultrashort pulses of high intensity are coupled out of the laser cavity at a reduced repetition rate. The selected pulse was then re-injected into the amplifier to boost its energy to ~ 1mJ. The pre-amplifier provided a total net gain of $\sim 4 \times 10^6$ which is an order of magnitude greater than the original system provided. Plans for further amplification are in place, with the use of an additional amplifier which is labelled in figure 3c.ii as a power-amp [Taday *et al*, 1998].

Pulse recompression was achieved using a diffraction grating pair, as described in the previous section. Gaussian profiled pulses around 50 fs were thus produced at the energies given above.

A summary of the performance of the laser beam before and after refurbishment is provided in table 3.i on page 61. Recall that the pre-refurbished system had a fundamental wavelength of 750 nm, while the post-refurbished system operated at 790 nm.

§3.2 Ion Detection and Data Acquisition

As indicated earlier, the laser is coupled to a time-of-flight mass spectrometer (TOF). The ion detection and data acquisition system is illustrated in figure 3k, the main points of which are described in this section.

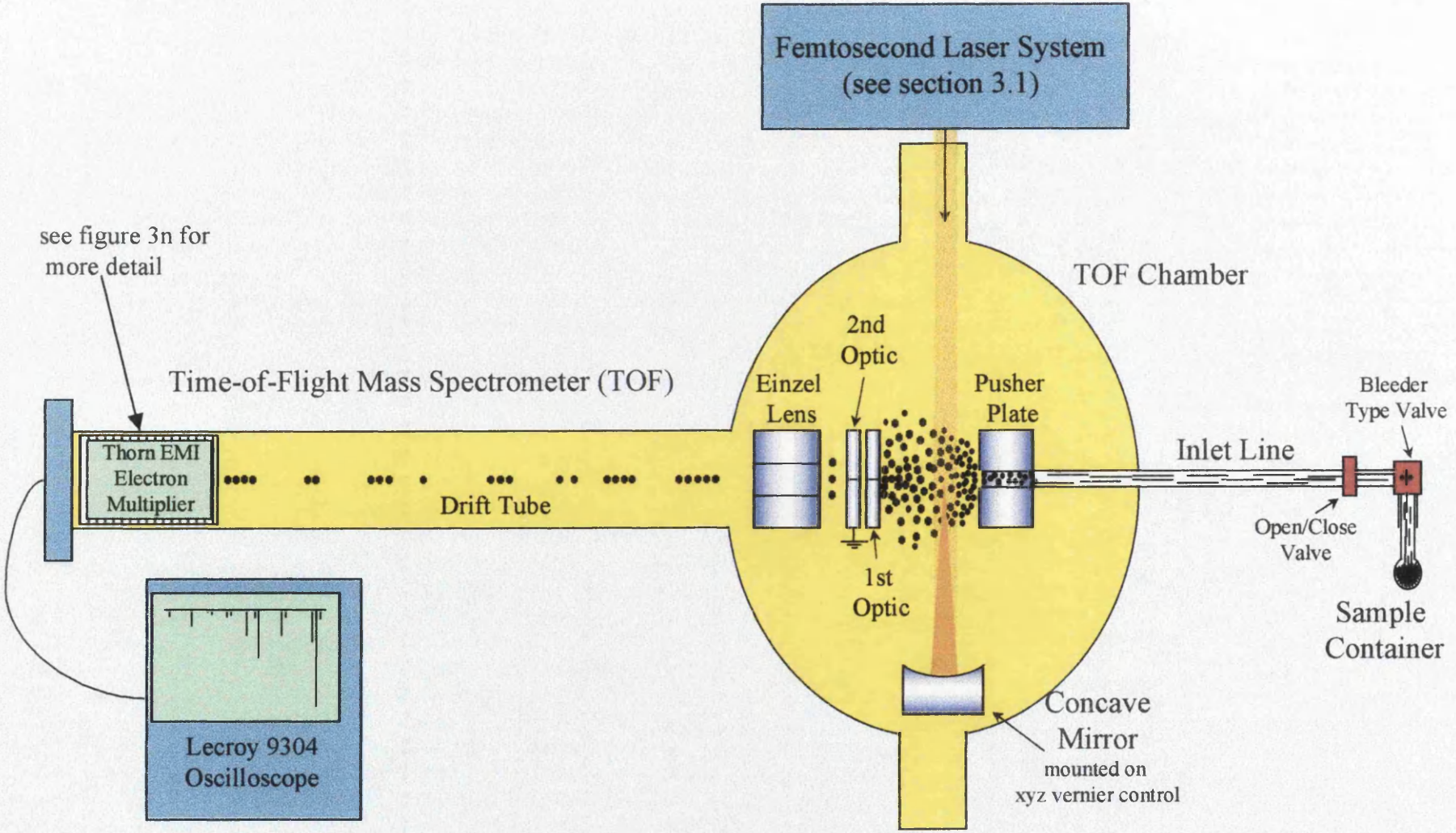

Figure 3k The Ion Detection and Data Acquisition System essentially comprising of a Linear TOF, Electron Mutiplier and Digital Oscilloscope

§3.2.1 *The Linear Time-of-Flight Mass Spectrometer (TOF)*

Mass spectrometry is inherently a destructive means of analysis. A mass spectrometer, by definition, requires ionisation of a sample such that separation by electric or magnetic fields can occur according to the ions' ratio of mass-to-charge (m/z). This leads to mass spectra of type and abundance of ions. The conversion of molecules to parent ions in mass spectrometry is incidental since even the most accurate mass spectrometer cannot measure the mass differences between molecules and corresponding ions. Time-of-flight mass spectrometry operates on the principle that for ions originating at a common spatial and temporal position, their flight times, upon acceleration through an electrostatic field and subsequent passage across a drift region, will be dependent on their m/z ratios. The flight time t, of an ion of mass m and charge z is given by:

$$t = l\left[\frac{m/z}{2eV}\right]^{\frac{1}{2}} \qquad \textit{eqn 3.2.1a}$$

where l is the distance travelled by the ions, V is the potential difference across the accelerating electric field and e the electronic charge. Determining the distance l can be very difficult since in practice the production of ions at varying positions occurs. The initial spatial, temporal and velocity distribution of the ions limits the resolving power of the instrument. The mass resolution of the system is defined by its ability to distinguish between ions of different mass/charge ratios (m/z). A working definition is that two peaks are said to be just resolved if their intensities are each half their respective peak values at the point where the overlap is greatest - see figure 3l.

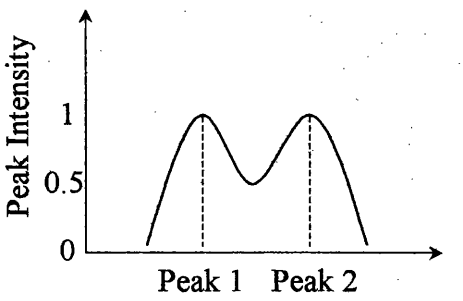

Figure 3l Two Peaks Just Resolved

For an ion of m/z ratio, the resolution R, is given by:

$$R = \frac{m/z}{\Delta(m/z)} \qquad \textit{eqn 3.2.1b}$$

where Δm is the full width at half maximum (FWHM). Typical values for the present study are ~ 300 at 130 Dalton (1 Dalton = 1 atomic mass unit). The intrinsic resolution is higher still. Maximising the resolving power within the limits of the TOF balanced with experimental requirements was important and is discussed below.

The TOF employed for the present study is based on a Wiley-McLaren design [Wiley and McLaren, 1955]. It has been described in some detail elsewhere [e.g. Marshall *et al*, 1992; Smith *et al*, 1998a]. The model is of conventional linear type with a field-free drift region of length 1.2 m.

The Inlet System

Samples to be ionised came in a variety of different forms: solids, liquids or gases, simple compounds or mixtures. In the present system the sample was required to be in its vapour phase prior to ionisation by the laser beam. The samples were connected directly to a bleeder-type valve, thus allowing precise flow control. An on/off valve situated after the bleeder provided a more reliable seal, which was advantageous when evacuating the system or changing samples. Gas bottles were connected via a steel tube, while liquid samples - and very occasionally solids - were contained in glass phials coupled to the entrance site. Occasionally, the phial had to be gently heated to create sufficient vapour. The vapour samples were then admitted effusively into the TOF chamber via a capillary tube connected to a tiny hole in the first pusher plate. To prevent contamination the inlet system was operated at around 120 C using an independent heater. An independent Edwards evacuating pump was also connected to the inlet line. This effectively limited the samples sticking to the walls of the apparatus and was augmented by occasionally flushing the system with an inert gas - usually nitrogen - to dislodge any unwanted accumulation. Indeed, gas flow cleansing was useful throughout the TOF apparatus.

High-Vacuum Environment

The TOF chamber was maintained at an operational pressure of 10^{-5} - 10^{-6} torr (1 torr = 1 millibar = 10^2 Pascals) using an efficient turbopump (type Balzers TPU 350) which operated similar to a jet engine principle. The pressure at the local site of sample introduction was expected to be considerably higher. This was however a correlated increase to the recorded pressure. It was possible to achieve a base pressure as low as 10^{-8} torr when no sample was present. Failure to reach this indicated a leak in the system or a build up of contaminants. Seepages could be tested for using acetone and closed either by adjusting nut-and-bolt joints or applying a sealant. Contamination was ridded as discussed above i.e. gas flushing or heating using baking tape wrapped around the system.

The inlet system and high vacuum environment within the TOF provided an ideal environment in which to probe samples with a laser beam, effectively curtailing the presence of foreign species and creating essentially uni-molecular conditions since the collision probability was small.

Laser Beam Alignment, Ion Optics and the Drift Region

The laser beam was coupled to the TOF via a quartz entrance window. From the rear of the chamber it was focused to a tight spot using an xyz-vernier controlled broadband concave mirror coated with enhanced aluminum for high reflectivity in the UV and near infrared wavelength region - see figure 3m.

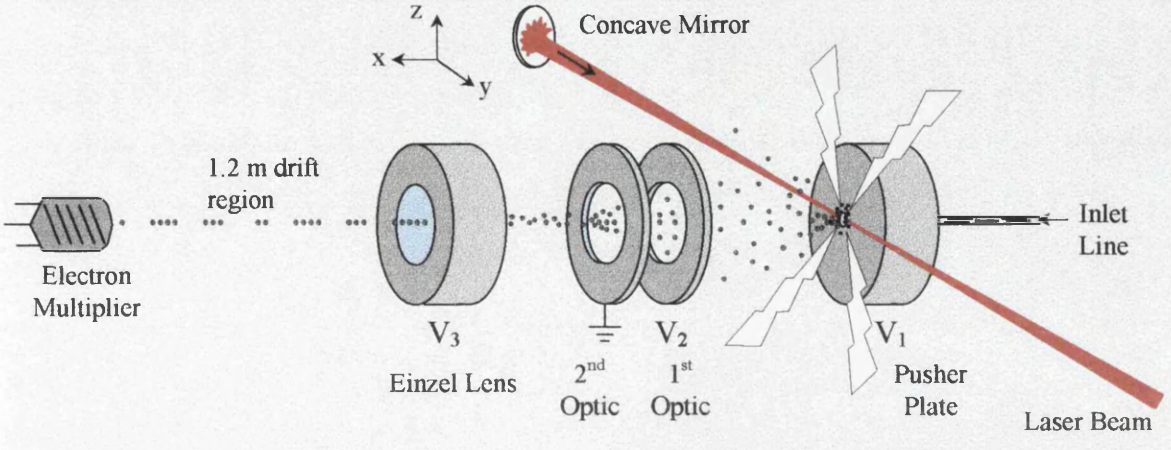

Figure 3m Laser Focal Spot Alignment and the Ion Optics within the TOF

Various mirrors were used of focal lengths 3, 5 and 10 cm. This produced focal spots with radii upwards of a few microns and corresponding intensities up to of the order of 10^{16} W cm^{-2} - see section *3.3.3* for details of the calculations. Previously, lenses had been used to focus the beam. However replacing lenses with mirrors made for a wavelength independent focal point avoiding chromatic aberration and allowing a tighter focal spot and therefore higher laser intensity to be achieved.

With such a set-up, the ions were generated at a well defined spatial (small focal point) and temporal (fast ion creation during short pulse width) starting position within the electrostatic accelerating field. Bearing in mind that flight times along the drift tube (see later) were of the order of tens of microseconds, the ions formed during the femtosecond laser pulse could be taken as beginning at a single point in time. This tended towards the ideal situation for a TOF as indicated earlier. The optimum position of the laser focus was found to be 1mm directly away from the sample entrance hole along the x-axis in figure 3m. It had to command a balance between several parameters. A focal spot closer than 1mm to the pusher plate could result in space-charge effects and the laser beam grazing the plate causing ablation and spurious reflections. On the other hand, further out than 1mm along the x-axis resulted in fewer particles available for ionisation and therefore a lesser ion yield.

Ion optics based on the Wiley-McLaren model [Wiley and McLaren, 1955] were used to efficiently extract, accelerate and channel the positive ions created at the laser focus. In figure 3m, typical values for V_1, V_2 and V_3 were 2.5, 2 and 1 kV respectively ($V_1 > V_2 > V_3$). The einzel lens located after the 2nd optic increased the transmission through the system.

Ions with an initial velocity component other than directly along the positive x-axis could either escape the pull of the electric field or some finite time would elapse before they became aligned to travelling in the positive x-axis direction. The longest period of time for this occurred when the initial velocity was along the negative x-axis. This obviously limited the resolution but was minimised with ion optics set at optimum potentials. However, the initial velocity distribution was considered to be the main source of resolution degradation due to the very well defined initial temporal and spatial conditions at time zero as discussed above. It is however, also worth

noting that the spatial contribution to resolution was greater for higher intensities due to an increased cross section of the gaussian beam profile causing ionisation.

After traversing the electrostatic field the ions passed into a zero field drift tube of length 1.2 m with a flight-time given by balancing the ionic kinetic energy with the electrostatic field energy, as given by equation *3.2.1a*. From such a derivation it is evident that the m/z ratio has an inverse squared correlation with the velocity.

The accuracy with which l and to a lesser extent V can be measured is insufficient to achieve a reliable m/z value for a given a flight time t. Therefore a simple calibration equation is introduced.

$$t^2 = \frac{m}{z}a + b \qquad \textit{eqn 3.2.1c}$$

where a and b are constants which are determined using two well defined estimated ion peaks, $(m/z)_1$ and $(m/z)_2$ with corresponding flight times t_1 and t_2. The usual peaks chosen are the lowest and highest m/z ratios hydrogen and the parent ion respectively. Carbon was also often used as a calibrant. Then m/z follows from:

$$\frac{m}{z} = \frac{\left(t^2 - b\right)}{a} \qquad \textit{eqn 3.2.1d}$$

for a given flight time t.

§3.2.2 The Electron Multiplier and Digital Oscilloscope

Detection of the ions arriving at the end of the drift tube was performed using a Thorn EMI electron multiplier [Thorn EMI Ltd] connected to a Lecroy 9304 digital oscilloscope [Lecroy Corporation] - see figures 3k and 3m.

The electron multiplier works on a cascade principle. A schematic is shown in figure 3n on the next page.

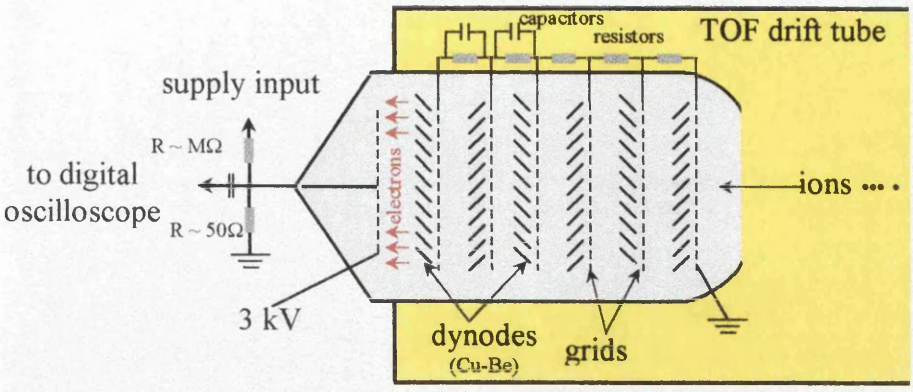

Figure 3n A Schematic of the Electron Multiplier

The grid potentials increase from right to left in the above figure. An incoming ion strikes a dynode and liberates an electron which is then accelerated until it can knock "secondary" electrons from an anode. This anode is a cathode relative to the left-adjacent anode from where more electrons are liberated. This process cascades through several stages resulting in a measurable signal which can be electronically counted. A typical electronic gain of such a device is ~ 10^6 rendering it a highly sensitive instrument.

The electronic signal, proportional to the ion flux, was coupled and displayed on a multipurpose Lecroy 9304 digital oscilloscope. Mass spectra were recorded of ion intensities against their corresponding flight times - which were accurately measurable and used for spectral analysis. The spectra were directly stored onto DOS format floppy disks of capacity 1.44 MB.

A unique feature of time-of-flight mass spectrometry is the capability of providing a complete mass spectrum after excitation with a single laser pulse. Typically however, a spectrum was averaged over a few hundred laser shots to statistically minimise shot-shot fluctuations and to increase the signal-to-noise ratio. A trigger to the oscilloscope was provided by using a portion of the laser light fed into a photodiode via a beam splitter. This was advantageous for on-line analysis.

§3.2.3 A Typical Time-of-Flight Mass Spectrum

A typical FLMS TOF mass spectrum of ion intensity against mass-to-charge ratio is shown in figure 3o for benzene, chosen as an example. Several peaks are labelled as an illustration.

According to equation *3.2.1c/d*, a simple Q-basic computer program was written to calculate m/z values given a calibration and relevant flight-times. After confirmation of correct peak identification, the data was converted to PC computer format and Microsoft Excel was used to further process the data and produce mass spectra of ion abundance against m/z ratios.

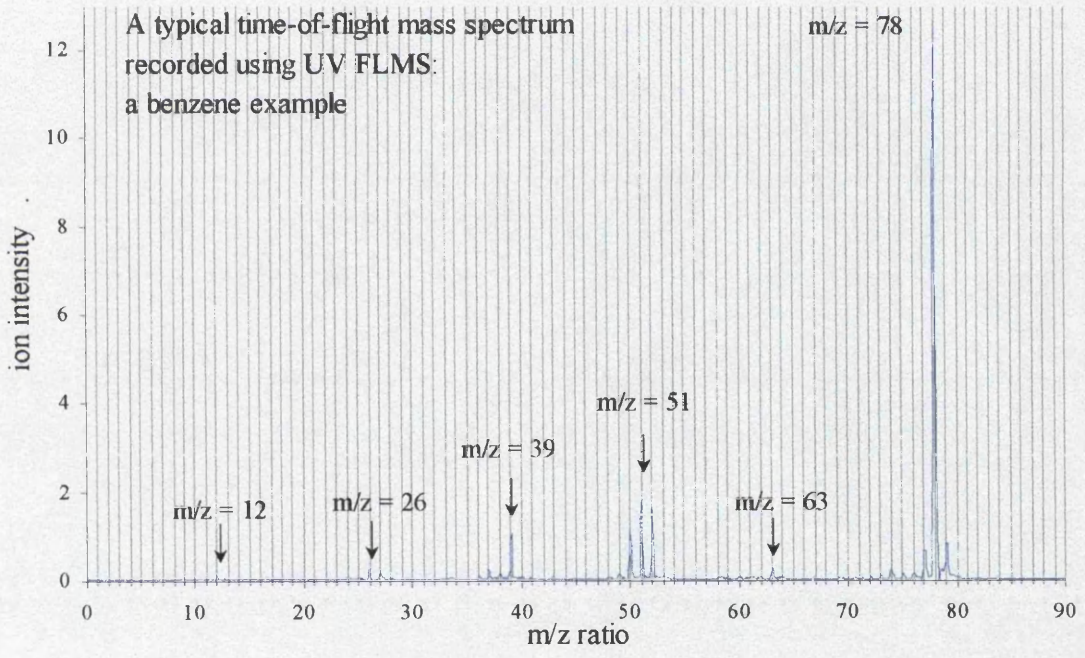

Figure 3o A typical TOF mass spectrum recorded using FLMS

§3.3 Laser Diagnostics

The final section centres on relevant laser beam measurements and associated techniques and related calculations. It is divided into three main sub-sections, namely: (i) pulse width measurement, (ii) pulse manipulation and energy measurement and (iii) details of laser beam intensity calculations.

§3.3.1 Autocorrelation Measurement of the Laser Pulse Width

It was important to monitor/measure the laser pulse width and profile, particularly before and after the stretching and compressing systems. The direct measurement of ultrashort pulses is not yet possible due to relatively slow response times of detectors. This problem is side-stepped using second harmonic generation (SHG) [Singhal, 1995] autocorrelation techniques [Yariv, 1997; Singhal, 1995; Maine *et al*, 1988; Salin *et al*, 1987; Fujimoto *et al*, 1984].

For this study, pulse width diagnostics were achieved with the capability of single shot analysis. The autocorrelator built for this purpose is shown schematically in figure 3p [Langley *et al*, 1993]. The principles of SHG and Michelson interferometry are utilised.

The laser beam of intensity I was collimated from lens l_1 and, on entering the autocorrelator, was divided by a 50:50 beam splitter (bs). In one of the two beams, a corner-cube (cc) reflector was used as an optical delay line, which was variable. Lens l_2 was used to focus both beams onto a non-linear crystal of type BBO. The UV beam generated by the crystal was imaged onto a Pulnix TM 765 CCD camera with the option of connection to a digital oscilloscope (do) which could be triggered using a photo-multiplier tube. A filter (ff) eliminated the fundamental beam frequency.

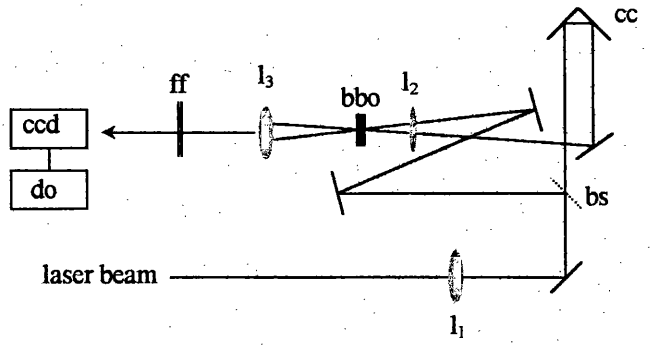

Figure 3p Single Pulse Autocorrelator

Resulting SHG intensity signals were therefore proportional to the product of the overlapping intensities in the non-linear medium with the efficiency of production of the SHG signal proportional to the square of the fundamental intensity I. For no time

overlap between the two pulses, then $I_{2\omega} \alpha (I/2)^2$. For zero time delay, then $I_{2\omega} \alpha I^2$. Between these limits, $I_{2\omega} \alpha (I/2^2 \rightarrow I^2)$ depending on the overlap factor. The FWHM of the resulting SHG intensity profile as a function of delay time is proportional to the pulse width of the laser beam according to the autocorrelation.

Details of the autocorrelation function can be found in Lasers and Electro-Optics [Davis, 1996]. Figure 3q shows a typical single shot autocorrelation trace of an amplified laser pulse.

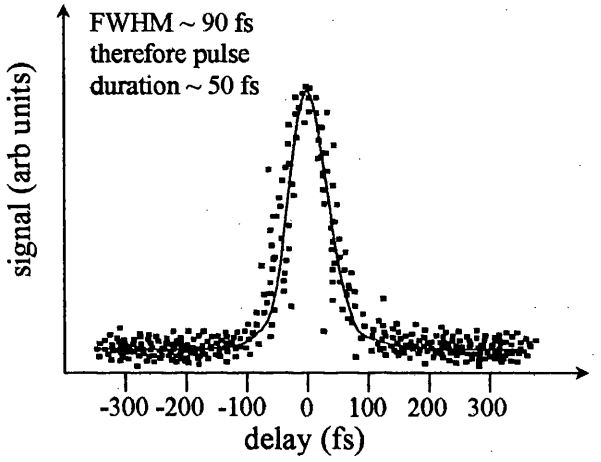

Figure 3q Single shot autocorrelation of an amplified laser pulse

§3.3.2 Bench Optics and Measurement of Pulse Energy

Directing and performing measurements of the laser beam was achieved using a system of optical components placed on an optics bench, and will now be described. Figure 3r is a schematic of the control and diagnostic set-up and should be referred to during the following discussion.

A series of broadband mirrors capable of fine movement directed the beam towards a Pellicle beamsplitter made of optical grade nitrocellulose, which reflected ~ 20% of the beam towards a lens ahead of an energy meter. The remaining 80% continued towards the TOF.

The mirrors were chosen to command a balance between several parameters including reflectivity, bandwidth capability, pulse broadening effects, laser damage resistance,

coating durability, thermal expansion, wavefront distortion, dispersion effects on ultrashort laser pulses and cost. Primarily they were of type broadband UV enhanced aluminium extending to high reflectivity in the near IR wavelength region. Typical reflectivity was greater than 95%.

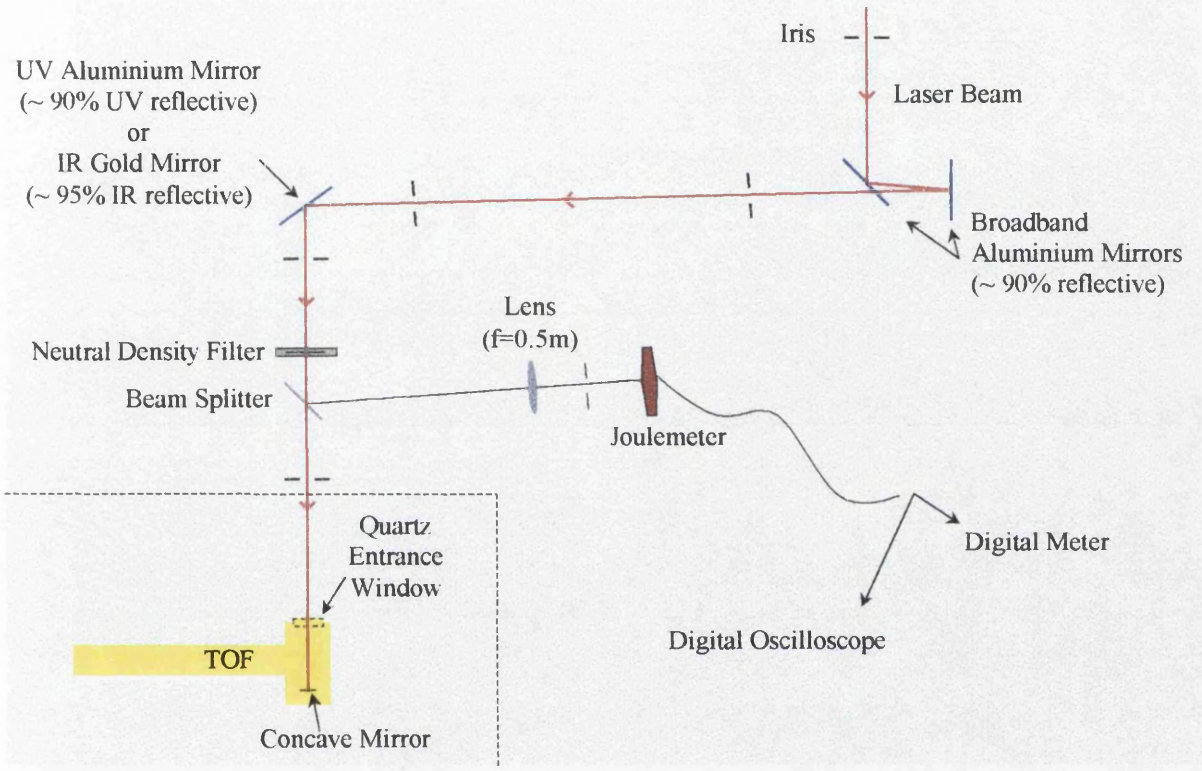

Figure 3r Bench-top optical components used for laser direction and measurement

Pellicle beam splitters combine the advantages of broadband wavelength capability with almost total elimination of multiple reflections commonly associated with thicker glass beamsplitters. Pellicles are manufactured by stretching a ~ 5 μm thick polymer membrane over a flat metal frame. The extreme thinness eliminates multiple reflections by making them coincident with the original beam.

It was of considerable importance to establish laser pulse energies. This was done using a Molectron J3-09 Pyroelectric Joulemeter. The operating principles are as follows. A photosensitive lithium tantalate crystal is rapidly heated upon absorption of laser photons, becoming electrically polarised. This produces a surface charge which is collected and displayed on an oscilloscope screen in units of voltage. The peak height of the signal is proportional to the absolute pulse energy according to a

calibration of 1mV = 1.77 μJ. This calibration was checked frequently by connecting the output of the joulemeter to a digital averaging meter.

Controlled attenuation of the laser beam energy was achieved using a circular neutral density filter (NDF) made of fused silica for good thermal stability. The optical gradient of the NDF varied around a circle for convenient attenuation adjustment by simply rotating the filter. Attenuation was achieved by a thin, reflective aluminium film, allowing the NDF to withstand the laser energies. As such, laser intensity dependent investigations were easily performed.

A frequency doubled UV beam was generated from the fundamental IR beam by placing a type 1 BBO (β-Barium Borate) crystal cut at 28.7° in the beam path. BBO crystals are efficient in second harmonic generation and have a high damage threshold. With the BBO crystal in place, a quartz 750 nm half-wave plate was used ahead of the crystal such that the resulting UV beam emerged vertically polarised, consistent with the fundamental beam. Additionally, for UV light, a glass absorbing filter eliminated the presence of IR light.

A calibration between the energy recorded by the joulemeter and the energy of the focused beam spot in the TOF was estimated by taking into account the transmission through the beam splitter and the attenuation at all the relevant optical components in the beam path prior to focusing. The resultant value of energy focused at the laser spot was used in the beam intensity calculation.

One further point to note is that the laser beam profiles were imaged using a charge coupled device (CCD) of type Pulnix TM 765, which revealed approximately gaussian shaped profiles, particularly with the refurbished laser beam. The autocorrelation measurements confirmed this also.

§3.3.3 Determining the Laser Intensity at the Focused Spot

The following expression was used to calculate the beam intensity I, in watts per square centimetre, at the focused laser spot area A:

$$I(Wcm^2) = \frac{P(W)}{A(cm^2)} \qquad \textit{eqn 3.3.3a}$$

where P is the power in watts according to:

$$P(W) = \frac{E(J)}{\Gamma(s)} \qquad \textit{eqn 3.3.3b}$$

for beam energy E in joules and pulse width Γ in seconds.

The circular spot areas ($A = \pi r^2$) were calculated from the focused spot radii r, according to equations *3.3.3c* and *3.3.3d* which correspond to different pulse profiles before and after the laser refurbishment respectively [Taday, 1997]. Equation *3.3.3c* describes a diffraction limited [Svelto, 1989] spot while *3.3.3d* is for a gaussian formation:

$$r = \frac{1.22 f\lambda}{D} \qquad \textit{eqn 3.3.3c}$$

$$r = \frac{2 f\lambda}{\pi D} \qquad \textit{eqn 3.3.3d}$$

for focal length f of the concave mirror (3, 5 and 10 cm), wavelength λ (790, 750 and 375 nm) and pre-focussed collimated beam diameter D (~ 5-10 mm) seen to have a circular shape. The parameters of wavelength, energy, focal length and beam diameter affect the laser intensity.

The pulse width also affected the beam intensity. As described in section 3.1, the fundamental pulse width for IR wavelengths was ~ 50 fs. At 375 nm, this lengthened to 90 fs. Increasing the pulse width for a given wavelength lead to a decreasing laser intensity.

Table 3.i shows how varying the above parameters affected the laser intensity. The lowest pulse widths and highest energies are used in the calculations. Note that 790 nm corresponds to post-system refurbishment, while 750 and 375 nm correspond to

pre-system refurbishment. Equations *3.3.2c* and *3.3.2d* are applied where relevant. Only at 790 nm were different concave mirrors used. Notice how the intensity is greater after the system overhaul. Also notice that higher intensities were possible with 750 c.f. 375 nm primarily due to the greater energy available at the higher wavelength but also due to the slightly shorter pulse widths in the IR region. Equal energies would have lead to higher intensities at the lower wavelength due to a smaller spot radii.

λ(nm)	Γ(fs)	E (μJ)	P (GW)	f(cm)	D (mm)	r (μm)	A (μcm^{-2})	I (W cm^{-2})
375	90	10	0.1	10	10	4.57	0.66	1.6×10^{14}
750	50	50	1.2	10	10	9.15	2.63	3.8×10^{14}
790	50	400	8.0	10	5	10.0	3.14	2.5×10^{15}
				5	5	5.0	0.79	1.0×10^{16}
				3	5	3.0	0.28	3.0×10^{16}

Table 3.i Calculations of Laser Intensity at the Beam Spot for varying conditions

CHAPTER 4

IONISATION AND DISSOCIATION OF BENZALDEHYDE

§4.0	**Introduction**	63
§4.1	**Experimental**	67
§4.1.1	*The Spectrophotometer*	67
§4.1.2	*The Femtosecond Laser System and the Mass Spectrometer*	67
§4.2	**Results and Discussion**	68
§4.2.1	*Ionisation-Dissociation (ID) versus Dissociation-Ionisation (DI)*	68
§4.2.2	*Soft Ionisation versus Fragmentation*	72
§4.2.3	*Double Charged Benzaldehyde*	73
§4.2.4	*Multiphoton Ionisation and Saturation*	75
§4.2.5	*Tunnelling*	77
§4.2.6	*A Fast Dissociation Channel*	78
§4.2.7	*Non-Statistical Photon Absorption*	80
§4.3	**Conclusions**	81

§4.0 Introduction

Benzaldehyde photo-processes have generated considerable interest [Silva *et al*, 1996 and references within]. As a structural relative of benzene, it is of considerable interest for investigation, and as a molecule in its own right, the potential for experimental studies and theoretical analysis is manifold. Benzaldehyde is used in the food, beverage, pharmaceutical, perfume, soap, and dyestuff industries. Figure 4a shows a schematic of the molecule's structure [McMurry, 1984] which reveals its cyclic-aromatic nature with an adjoining aldehyde group (CHO).

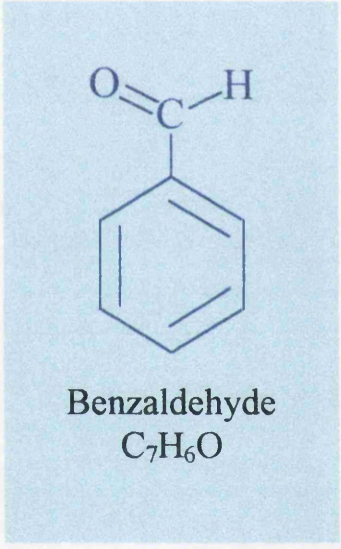

Figure 4a The Benzaldehyde Molecule

Benzaldehyde's ionisation potential is 9.52 eV [Long *et al*, 1983]. Its broad UV absorption spectrum was recorded using a spectrophotometer with a resolution of 0.5 nm. The spectrum can be seen in figure 4b. The singlet excited states are clearly evident. Electronic excitation to the first singlet excited state (S_1) gives rise to a weak absorption band system at 371.5 nm (~ 3.33 eV). The second absorption band to the S_2 state occurs at 275 nm (~ 4.51 eV) while by far the strongest absorption peaks occur between 220 - 245 nm (~ 5 eV, S_3) and at 194 - 195 nm (~ 6.4 eV, S_4) [Silva *et al*, 1996; Long *et al*, 1983; Yang *et al*, 1983]. The triplet manifold is less well categorised although intersystem crossing via T-states has been reported [Hirata *et al*, 1980; Berger *et al*, 1973].

Figure 4c is a diagram showing some of the energetically allowed multiphoton fragmentation pathways in the neutral and ionic manifold of states. The appearance potentials are taken from references Yang *et al* [1985, 1983]. The absorption spectrum is superimposed as well as the absorption of nine photons at 750 nm and five photons at 375 nm.

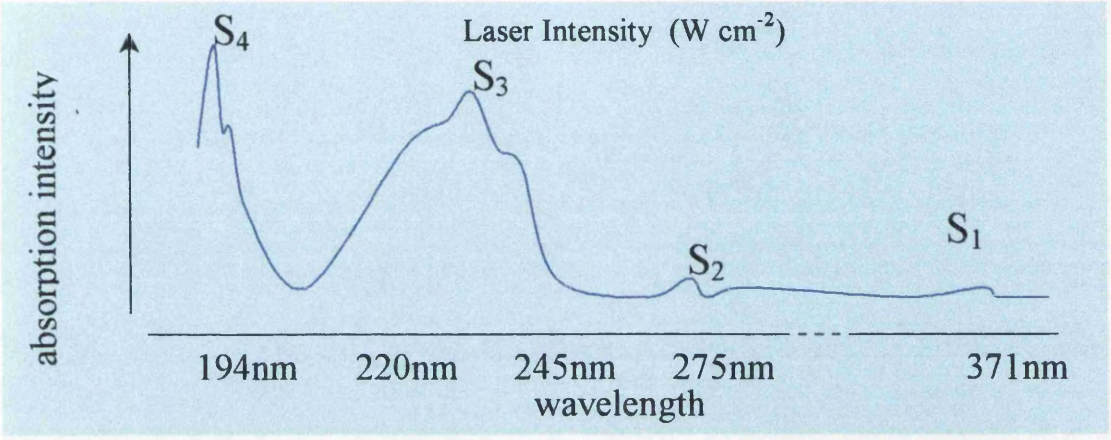

Figure 4b The UV Absorption Spectrum of Benzaldehyde

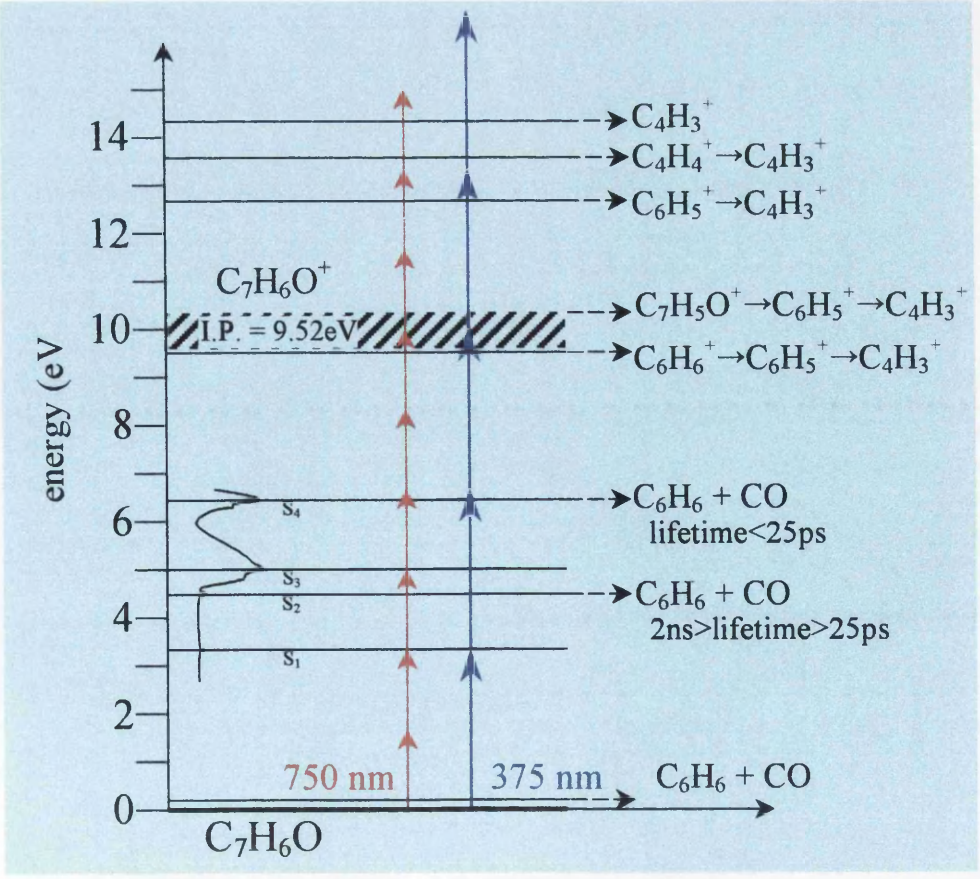

Figure 4c Some Benzaldehyde Fragmentation Pathways

The laser mass spectrometry of benzaldehyde has been investigated at varying laser pulse widths, intensities and wavelengths. A primary process in benzaldehyde photolysis involves the formation of benzene and carbon monoxide, as shown below. This occurs via the S_2 and S_4 states below the parent ionisation threshold, thus suppressing molecular ion production [Silva *et al*, 1996; Yang *et al*, 1985,1983; Long *et al*, 1983; Antonov *et al*, 1981; Hirata *et al*, 1980; Berger *et al*, 1973]. The products can be further excited by absorbing additional photons, which can lead to further ionisation or fragmentation.

$$C_7H_6O + n\text{h}\nu \rightarrow C_7H_6O^* \rightarrow C_6H_6 + CO$$

Dissociation from the S_2 singlet occurs on a time-scale less than 2 ns [Long *et al*, 1983] but greater than 25 ps [Yang *et al*, 1985]. The S_4 singlet is thought to dissociate even faster [Silva *et al*, 1996].

A general theme emerging from these studies is as follows: nanosecond laser pulse widths yield small or non-existent parent ions, with a strong dominance of lighter mass fragments. This is consistent with molecular fragmentation followed by ionisation, occurring below the parent ionisation threshold, and is known as dissociation-ionisation (DI) or ladder-switching [Boesl *et al*, 1980]. This is in contrast to ionisation-dissociation (ID) in which any fragmentation occurs via the parent ion. In this case a ladder-climbing mechanism applies [Gedanken *et al*, 1982]. ID and DI are described in detail in chapter 2, section *2.3.4*, and are considered to be the two distinct mechanisms by which multiphoton absorption in molecules can lead to fragmentation [Kilic *et al*, 1997; Yang *et al*, 1985; Gedanken *et al*, 1982]. Molecular pre-dissociation often competes with ladder-climbing, the latter becoming more dominant as the laser pulse duration decreases [Yang *et al*, 1985] due to dissociative lifetimes becoming comparable to the laser pulse widths.

Several authors have shown mass spectra for benzaldehyde at 20 ns with very low intensity parent or high-mass peaks [Antonov *et al*, 1981, 1980; DeCorpo *et al*, 1980; Seaver *et al*, 1980]. Long *et al* [1983] report a similar result, namely that total dominance of lighter fragment ions occurs, indicating pre-dissociation competing

strongly with direct photo-ionisation, specifically from the S_2 state. In this pulse length regime, the choice of wavelength is seen to significantly influence whether ladder-switching or ladder-climbing occurs. Yang *et al* [1983] in an investigation of benzaldehyde using laser pulse widths of 8 ns, found competition between ID and DI pathways at 266 nm (one photon energy coincides with the S_2 band) which was also dependent on laser intensity. The molecule in the excited S_2 singlet would either dissociate or be effectively bypassed via optical up-pumping. However at 355 nm (one photon energy coincides with an S_1 state), irradiation at both ns and ps largely lead to ID domination over the entire laser intensity range. They concluded that wavelength selection was a more important parameter in protecting the molecule against DI, than laser intensity.

In the picosecond pulse width region, parent-like dominance over its moieties is largely found, in contrast to the nanosecond findings. A specific above threshold dissociation pathway is:

$$C_7H_6O + m\text{h}\nu \rightarrow C_7H_6O^+ \rightarrow C_7H_5O^+ + H$$

As with nanoseconds, a wavelength influence on ionisation dynamics is found. In another study Yang *et al* [1985] described the "immediate" dissociation of $C_7H_6O^+$ in the above pathway at 25 ps and 266 nm, whereas increasing the wavelength to 355 nm resulted in larger parent ion peaks. "Immediate" in this sense is presumed to mean less than 25 ps. They also suggested that the role of ladder-climbing increased as the laser pulse decreased from nanosecond to picosecond durations.

This chapter [Smith *et al*, 1998a] extends the previous measurements in the nanosecond and tens of picosecond regimes. It describes recent experimental findings for benzaldehyde photo-chemistry, utilising time-of-flight techniques with short, intense laser pulse durations ranging from 50 fs to 2.7 ps at wavelengths 750 and 375 nm, and beam intensities up to 2×10^{14} W cm^{-2}. This technique is known as Femtosecond Laser Mass Spectrometry (FLMS). At these short pulse widths and high laser intensities, the question is addressed as to whether ID is the generally preferred dissociative mechanism, similar to the results reported for other molecules carried out

in this intensity regime [Kilic *et al*, 1997; Kosmidis *et al*, 1997; Ledingham *et al*, 1997]. The role of wavelength upon molecular fragmentation and ionisation is also considered. And in particular, it is of interest to investigate the fast hydrogen loss dissociative pathway mentioned earlier [Yang *et al*, 1985]. Furthermore, in the 10^{14} W cm^{-2} laser intensity region, it is important to consider saturation of the ionisation signal and to question the basic multiphoton description of the ionisation mechanism and energy intake by the molecular system.

§4.1 Experimental

§4.1.1 The Spectrophotometer

Figure 4d is a schematic of the apparatus used to record the UV absorption spectrum of benzaldehyde. A liquid sample was introduced to a small quartz phial and vapourised using an infrared source, before being placed in a spectrophotometer of type Perkin Elmer Lambda 9, set at 0.5 nm resolution. A simple arrangement of UV source-sample-detector and interface to a pc sufficed to record the spectrum.

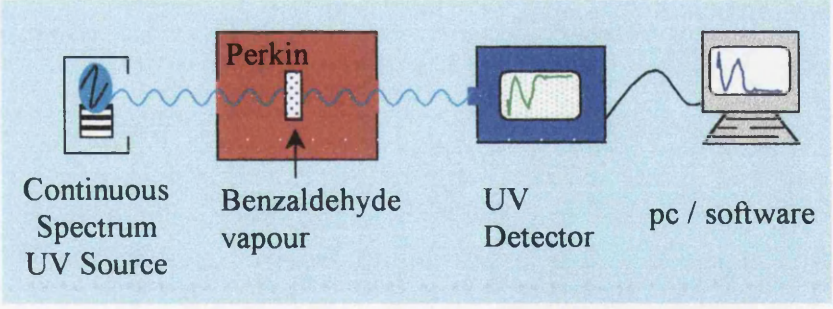

Figure 4d Absorption Spectrum Acquisition

§4.1.2 The Femtosecond Laser System and the Mass Spectrometer

The experimental set-up consists of a femtosecond laser system, [Langley *et al*, 1994] a time-of-flight mass spectrometer (TOF) [Ledingham *et al*, 1995a] and a LeCroy 9304 digital oscilloscope. The apparatus is described in considerable detail in chapter 3. Briefly a mode-locked titanium-sapphire oscillator was pumped by an all-lines 'Beamlok' argon-ion laser, prior to amplification in a three-stage dye laser (dye

specification LDS 751). Pulses of 50 - 90 fs width were generated. Longer pulse lengths up to 1.32 ps (375 nm) and 2.7 ps (750 nm) were produced by lengthening the pulses via passage through SF10 blocks of various thickness. A series of broad band mirrors guided the laser pulses towards the TOF. A concave mirror within the TOF served to focus the beam to spot sizes of 5 and 10 microns for 375 and 750 nm respectively. As such laser intensities up to approximately 2×10^{14} W cm^{-2} were achieved at wavelengths 750 nm (fundamental) and 1×10^{14} W cm^{-2} at 375 nm (frequency doubled). Such calculations are illustrated in chapter 3, section *3.3.3*.

The TOF is of conventional linear design with a field-free drift region of 1.2m. Benzaldehyde vapour was admitted effusively via a needle valve before passing through a tiny hole into the TOF main chamber. The position of the laser spot with respect to this hole was critical [Kilic *et al*, 1997]. Ions thus created were accelerated and channelled by ion optics based on a Wiley-McLaren design, before collection using a Thorn EMI electron multiplier coupled to the digital oscilloscope. Mass spectra of ion yield against their corresponding time-of-flight were thus recorded. The ions' flight times are a measure of their mass-to-charge ratio (m/z) - see section *3.2.1*.

§4.2 Results and Discussion

§4.2.1 Ionisation-Dissociation (ID) versus Dissociation-Ionisation (DI).

Figure 4e shows the ionisation-dissociation mass spectra at 750 and 375 nm for varying laser intensities up to 1.2×10^{14} W cm^{-2} at 90 fs pulse duration. Ion yields are plotted against their corresponding flight times. The spectra are normalised for amplifier gain and gas pressure in the TOF such that direct comparisons can be made between them. It is readily seen that the parent ion dominates in all the spectra. The predominant initial appearance of parent molecular ions at the lowest laser intensities suggests a common parent precursor in an above threshold dissociation mechanism. Furthermore the consistent dominance of the benzaldehyde parent ions over its moieties as the laser flux increases, also supports an ID route. This parent supremacy was true for all pulse lengths used in the experiment.

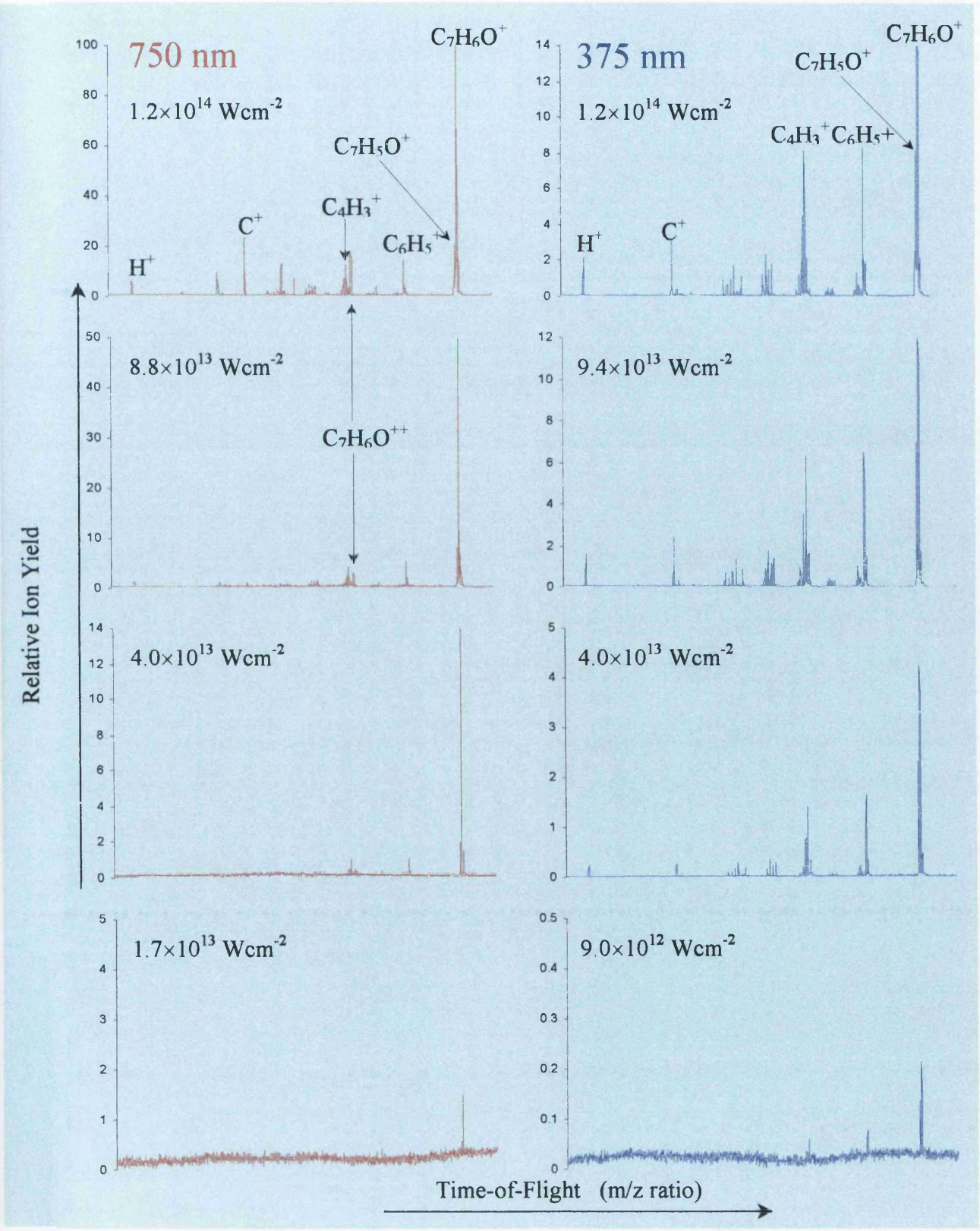

Figure 4e Benzaldehyde Mass Specta at 750/375 nm and 90 fs

Yang *et al* [1985] illustrated mass spectra recorded under similar experimental conditions at a wavelength of 355 nm and a laser pulse width of 25 ps. This is shown as a schematic in figure 4f. The parent peak is again predominant at all laser intensities, indicative of an ID route as Yang *et al* concluded. However, by inspection of figure 4f, the dependence of the ion intensities as a function of laser power are markedly dissimilar for the different fragments. This points to an opening of DI pathways for some of the moieties.

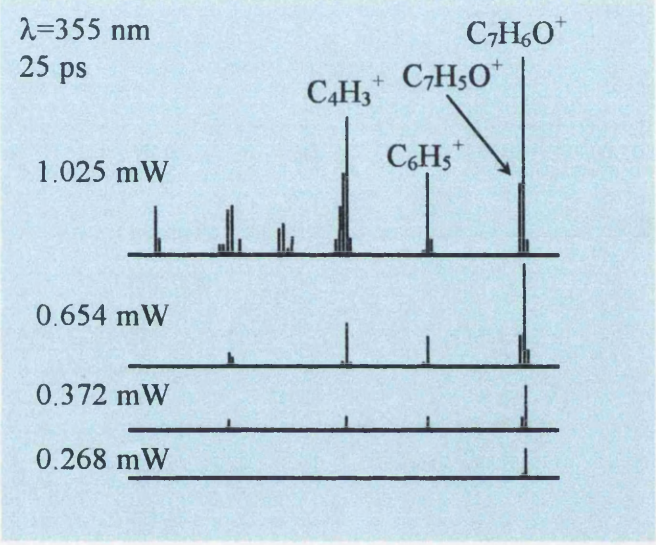

Figure 4f Benzaldehyde Mass Spectra at 355nm and 25 ps [Yang *et al*, 1985]
Reproduced with kind permission of the authors and the American Chem. Soc.

In contrast to Yang *et als'* findings, figure 4g shows the ion yield as a function of laser intensity, at a pulse width of 90 fs, for the main fragment mass peaks. Vertical multiplication factors are indicated, which serve to separate the ion plots. The ions are multiplied by these factors prior to drawing the graphs. It can be seen that the daughter ions have the same slope as the parent ion at both wavelengths (apart from a double charged benzaldehyde ion and the C^+ and H^+ ions at 750 nm). This is strongly suggestive of a common parent precursor in an ID model [Ledingham *et al*, 1997] and a distinct lack of DI activity. If the DI route were dominant, then the gradients of the fragment moieties, whose appearance potentials are normally different from the parent ion, would not necessarily follow that of the parent, as is the case evident from figure 4f.

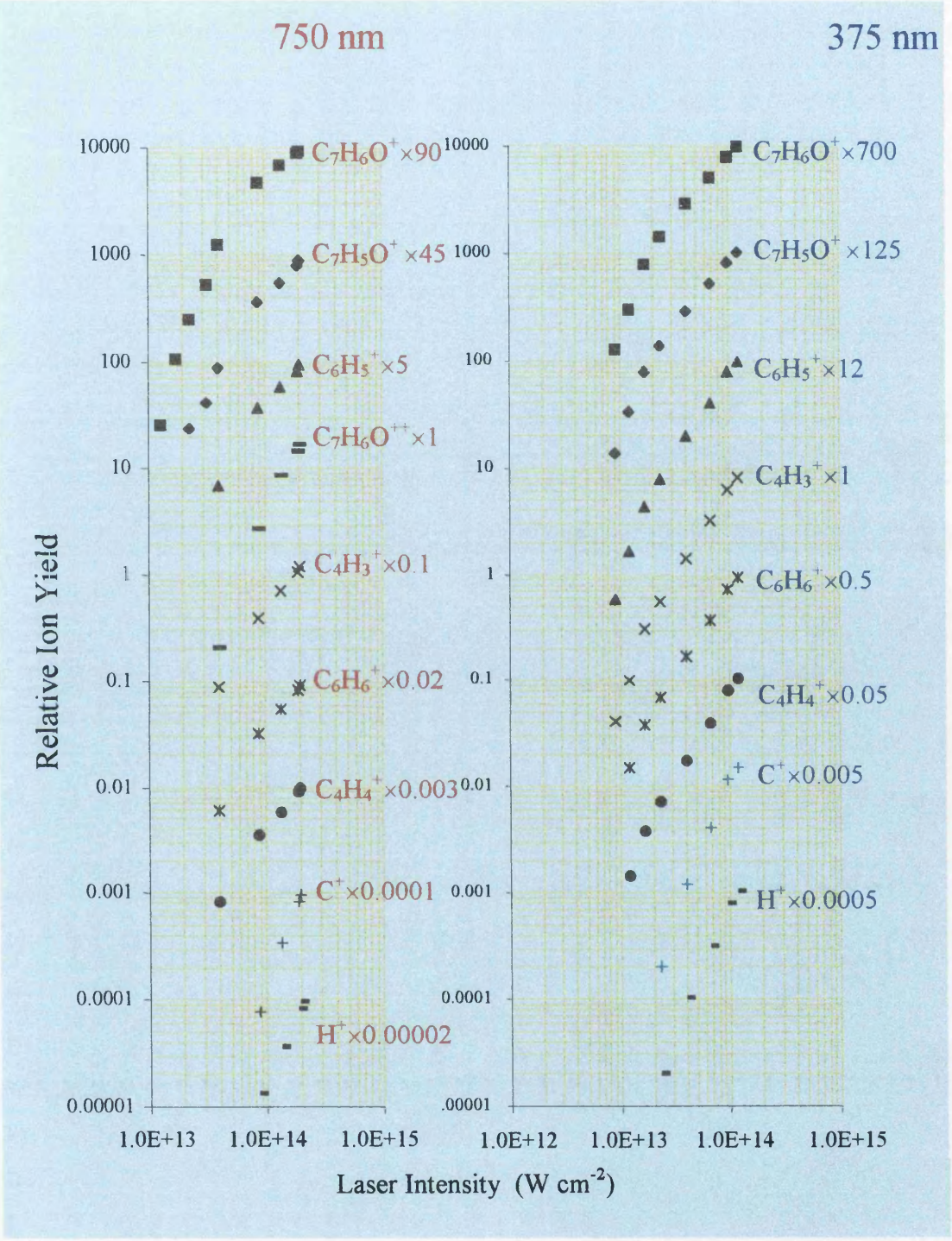

Figure 4g Laser Intensity Dependence at 90 fs and 750/375 nm

The principal DI route is the production of C_6H_6 + CO as indicated in the introduction. When these neutral molecules are irradiated individually as ground state gases under similar experimental conditions, by far the predominant peaks in the mass spectra are the parent ions at mass 78 (C_6H_6) [Smith *et al*, 1998b] and 28 (CO)

respectively. In the present work these peaks are very small which suggests that these neutral fragments are largely missing. This implies that the DI dissociative pathway is a minor one.

§4.2.2 Soft Ionisation versus Fragmentation

To produce an exclusive parent ion is to ionise softly. For analytical purposes, that is to identify the molecule(s) being studied, soft ionisation is to be favoured. Figure 4e clearly shows this effect for the lower laser intensities, particularly at the longer wavelength. As fragmentation increases with beam flux, parent ion dominance is still seen to occur. Such observations have important implications with respect to chemical analysis, especially for multi-component samples. For example in environmental air monitoring, [Smith *et al*, 1998c] in which a number of molecules simultaneously present may be detectable as a series of clean spikes on the mass spectra displaying minimal daughter fragments, and therefore limiting the scope for misinterpretation.

Conversely when structural information is sought then significant molecular fragmentation is desirable. This is best obtained using higher laser intensities and the shorter wavelength, as figure 4e illustrates, although parent ion dominance is still seen to occur despite this significant daughter ion formation. However, the UV photons do seem less suitable, in this case, for analytical purposes due to a lower production of intact parent ions. In fact over the intensity range, the 375 nm daughter fragments show a factor of about four times greater intensity than at 750 nm. This has been observed by the Glasgow group as a characteristic of fragmentation in a number of molecules at high laser fluxes and short pulse widths e.g. NO_2, [Singhal *et al*, 1998] CO_2, CS_2 [Graham *et al*, 1998], CH_3I, benzene, toluene, naphthalene, [Smith *et al*, 1998b] and 1-3 butadiene.

Therefore, for such molecules, FLMS at longer wavelengths is preferred for chemical analysis. Chapters 5 and 6 consider this further.

§4.2.3 Double Charged Benzaldehyde

Figure 4e reveals the considerable presence of a double charged benzaldehyde ion, $C_7H_6O^{++}$, at 750 nm which appears at $\leq 10^{14}$ W cm^{-2}. Figure 4h presents a mass spectrum in more detail with expansion and labelling at regions of interest. A slight hint of a triple charged parent ion may be present, but is barely distinguishable above the background noise. A small contribution to the double parent ion at a mass-to-charge-ratio of 53 is thought to occur from $C_4H_5^+$, although minimal since no such corresponding peak occurs at 375 nm, where increased fragmentation compared to 750 nm is apparent. Further evidence is available to confirm the appearance of the double charged parent ion. As previously stated, the gradient of the $C_7H_6O^{++}$ laser intensity dependence in figure 4g is greater than the other ion dependences. This is suggestive of considerably increased photon absorption, which may be expected to reach the double charged manifold.

Another technique can be employed to confirm or otherwise the existence of multiply charged components. It follows from the fact that there are naturally occurring isotopic mixtures present in substances. Out of the three atomic types in benzaldehyde, carbon is the only one with a significant isotopic presence. The $^{13}C/^{12}C$ amounts are 98.9 % ^{12}C and 1.1 % ^{13}C [De Hoffman, 1996]. Therefore, for a molecular sample with seven carbon atoms (C_7H_6O), it is expected that an isotope with an extra neutron (^{13}C) should be present at around 8 % abundance (7 × 1.1 %). By measuring peak areas in the mass spectrum of figure 4h, this isotopic ratio is found to be approximately correct, not only for m/z = 106 ($C_7H_6O^+$) and 107 ($C_6{}^{13}CH_6O^+$) but also for m/z = 53 ($C_7H_6O^{++}$) and 53.5 ($C_6{}^{13}CH_6O^{++}$) which indicative of a dominant double peak at m/z = 53 ($C_7H_6O^{++}$).

However, the ambiguity of coincident peaks at $C_7H_6O^{++}$ and $C_4H_5^+$ (coincident within the limits of the resolution of the mass spectra) could be further eliminated by using single deuterated benzaldehyde (C_7H_5DO) which would give a definite double ionised parent peak at a mass-to-charge ratio of 53.5. This powerful technique has been used for single deuterated benzene (C_6H_5D) revealing a large unambiguous parent double at m/z = 39.5 - see chapter 6, section *6.2.2* for details.

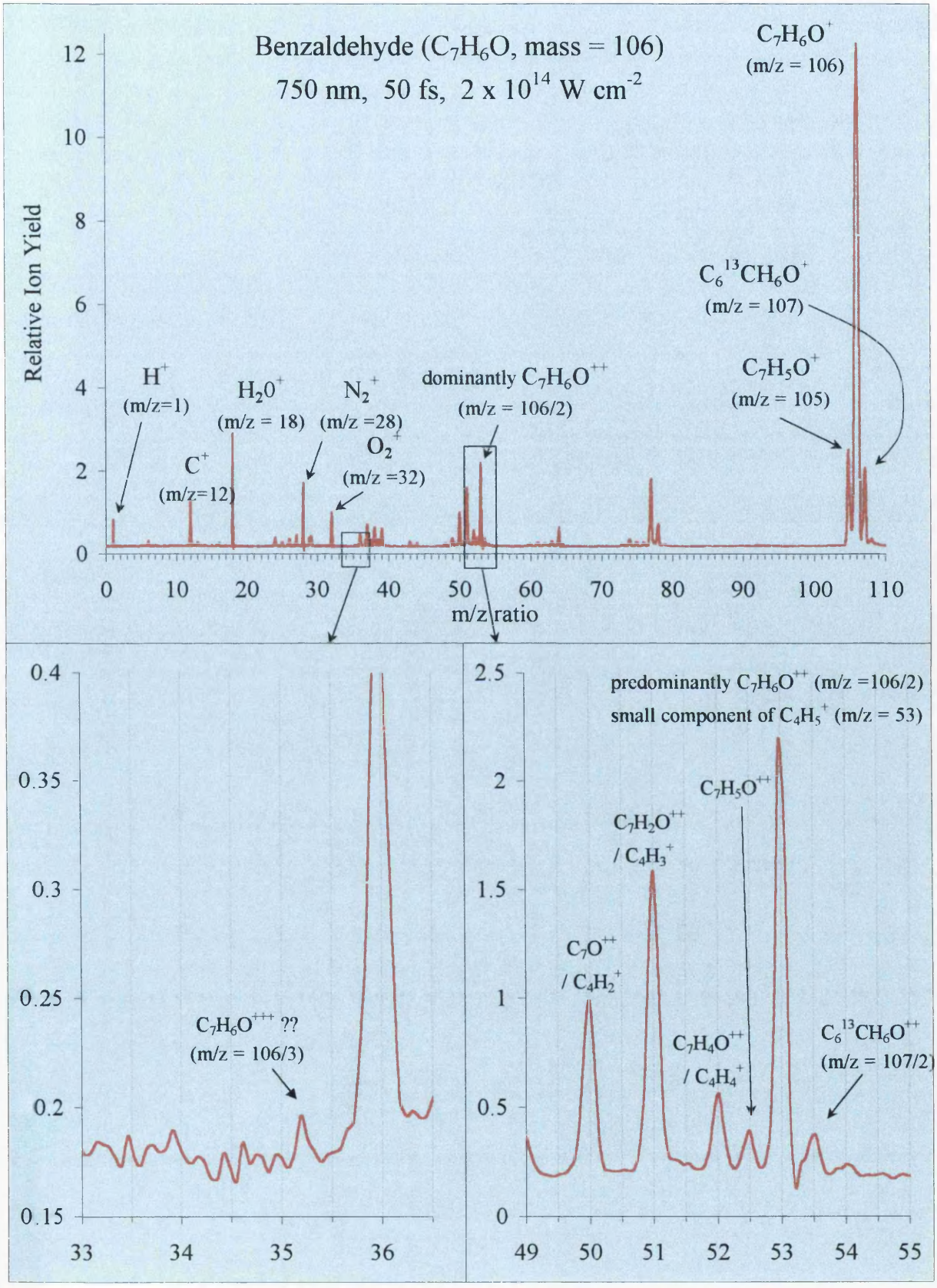

Figure 4h Benzaldehyde Mass Spectrum with insets of multiply ionised regions

The double ionised parent peak is also a prominent feature in a number of other molecules investigated to date. These include CO_2, CS_2 [Graham *et al*, 1998], CH_3I, benzene, toluene, naphthalene [Smith *et al*, 1998b] and 1-3 butadiene. The presence of such double ionised entities is thought to be of considerable importance and raises many interesting questions. Under such conditions the ions must have substantial structural stability, this being a prerequisite for detection, with flight times in the TOF of the order of microseconds. The interesting new appearance of multiply ionised medium mass molecules irradiated using FLMS, is described in some detail in chapters 5 and 6, with specific emphasis on the aromatic molecules benzene, toluene and naphthalene. Chapter 7 considers general aspects of this multiple ionisation.

§4.2.4 Multiphoton Ionisation and Saturation

For benzaldehyde, the appearance of the parent molecular ion implies absorption of at least 3 photons at 375 nm and 6 photons at 750 nm over the intensity range studied - see figure 4c. From the gradients of figure 4g, a dependence of 2 for 375 nm and 3 for 750 nm is measured. This is consistent with a 3 (375nm) and 6 (750nm) multiphoton absorption process approaching saturation, which may be expected at such high laser intensities [He *et al*, 1997a]. The mechanism of multiphoton ionisation is discussed in chapter 2, section 2.3.

In the region of 10^{14} W cm^{-2}, saturation of the parent ion signal is approached, which has been described as maximum sensitivity FLMS [Singhal *et al*, 1998]. This relates to a unity ionisation probability, which physically corresponds to all molecules within the sensitive volume being ionised, this volume being intimately related to the focused laser spot dimensions at the local region of ionisation. Experimentally this is a reduction in the rate of change of ion yield as the laser intensity increases and can be seen as a characteristic bend at the uppermost curve locality - see figure 4g. Any increase after this is mainly due to an expansion in the ionising focal volume of the laser beam. This effect is more visible with 750 nm where slightly higher intensities were achievable, and is again observed in chapters 5 and 6 for the aromatic molecules benzene, naphthalene and toluene. The experiment was carefully set up as to avoid any contribution from electronic saturation of the electron-multiplier tube in the TOF,

which generally shows up as a rounding of ion peak - loss of resolution - in the mass spectra, especially for the large parent signals.

Figure 4i shows the total ion yield (summing all peaks in the mass spectra) as a function of laser intensity at pulse width 90 fs and wavelengths 750 and 375 nm. Saturation is again apparent from the experimental yield curves and is also expected from the general considerations of multiphoton ionisation cross sections [He *et al*, 1997b] at laser intensities in excess of 10^{13} W cm^{-2}. This confirms that the decreasing parent ion gradients evident in figure 4g are demonstrating a true saturation effect, and are not simply due to increasing fragmentation with laser intensity.

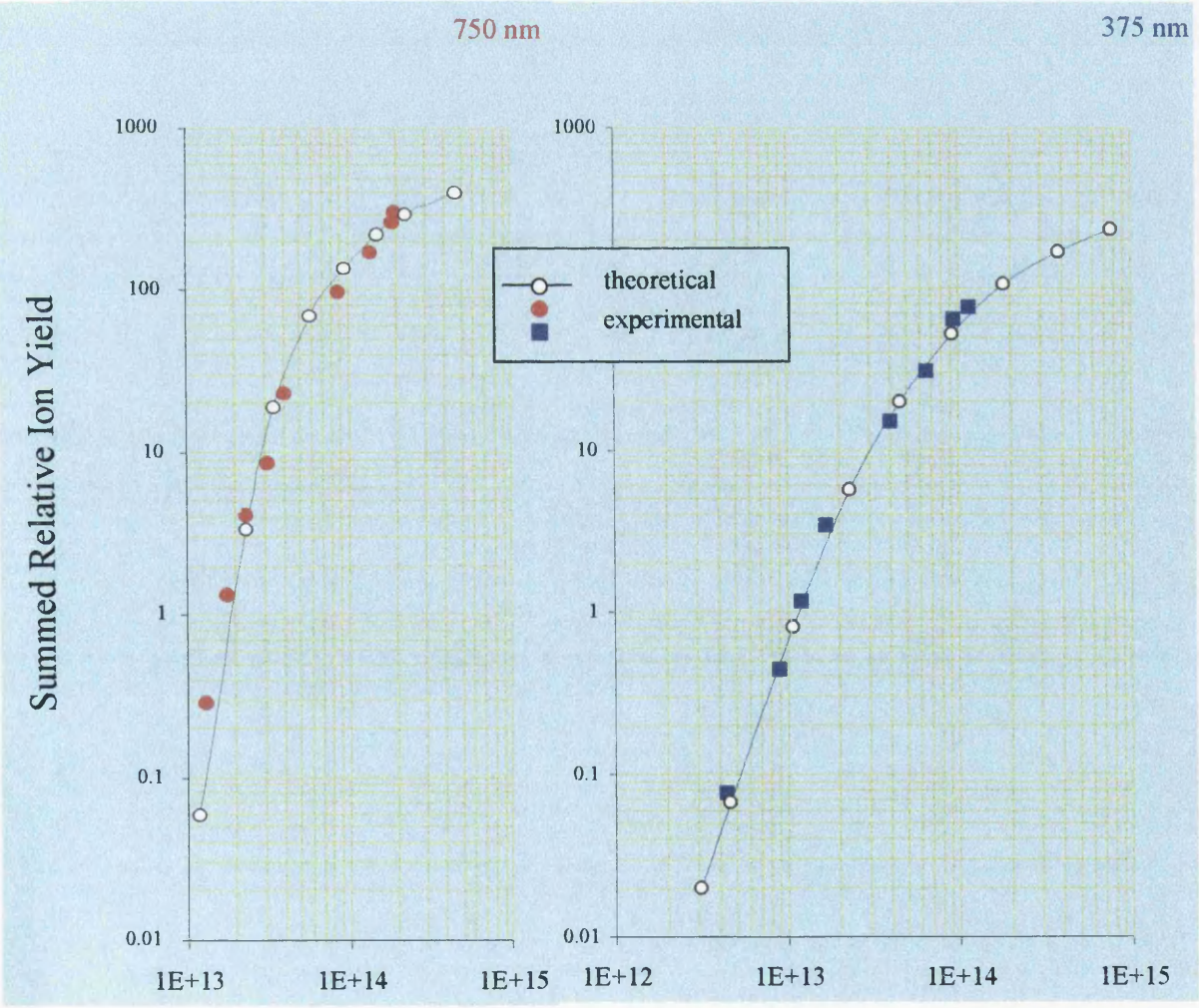

Figure 4i The Summed Laser Intensity Dependence at 90 fs and 750/375 nm

As stated earlier, the multiphoton transition for benzaldehyde proceeds with the absorption of 6 photons to reach the parent ion while 375 nm ionisation requires 3 photons. The predicted yields for the cross sections are shown in figure 4h as a solid curve and the agreement with the data is excellent. In calculating the theoretical curves, the effects due to the beam spot size, the time profile of the laser pulse and the finite acceptance volume of the time-of-flight mass spectrometer were taken into account. The cross sections for the six photon (non-resonant) absorption for 750 nm and the three photon absorption for 375 nm were treated as variable parameters in the fitting and were found to be 1.38×10^{-180} $cm^{12}sec^5$ and 1.5×10^{-82} cm^6sec^2 respectively. Chapter 2 deals with the theoretical treatment of cross sections and reference should be made to this for further explanation - section *2.3.5*.

§4.2.5 Tunnelling

Several authors have argued that when the laser beam intensity reaches ~ 10^{14} - 10^{15} W cm^{-2}, it is possible that tunnelling ionisation can occur [Codling *et al*, 1994,1993; Walsh *et al*, 1994, 1993; Chin *et al*, 1993, 1992; Augst *et al*, 1991, 1989; Gibson *et al*, 1990].

Chapter 2, section 2.4 discusses the relevant theoretical aspects. Although the experimental data is well described by a multiphoton mechanism, using such short intense laser pulses, it is possible that field ionisation (tunnelling) can provide a more complete description of the process in the higher intensity range [Vijayalakshmi *et al*, 1997; Codling *et al*, 1993].

The Keldysh parameter [Keldysh *et al*, 1965] has given a semi-quantitative indication of the mechanism of ionisation. It is defined by:

$$\gamma = \left(\frac{E_i}{1.87 \times 10^{-19} I \lambda^2} \right)^{\frac{1}{2}} \qquad \textit{eqn 4.2.5a}$$

where E_I is the zero-field ionisation potential of the molecule expressed in eV, I is the laser intensity in W cm^{-2} and λ is the laser wavelength in nm. Values of $\gamma \leq 0.5$ have

been postulated as a pragmatic threshold for tunnelling with total multiphoton ionisation corresponding to $\gamma \geq 5$ [Ilkov *et al*, 1992]. In the present experiment, all values of γ are greater than unity (smallest $\gamma \sim 1$ at the highest beam intensities). Keldysh parameters of value close to unity may be construed as being in the intermediate range between tunnelling and multiphoton ionisation.

In the present case, although predominantly a multiphoton process, field ionisation may contribute to the total ionisation rate, particularly in the uppermost intensity region examined in the present case i.e. approximately $> 10^{14}$ W cm^{-2}. The relative importance of these mechanisms needs to be examined further, especially for medium-to-large mass molecules, with limited studies to date. Chapter 6 provides more insight into such phenomena.

§4.2.6 A Fast Dissociation Channel

This section considers the effects of laser pulse width variation on molecular ionisation and/or dissociation pathways. For the 750 nm wavelength, the length of the pulses were varied between 90 fs to 2.7 ps, and for 375 nm, from 90 fs to 1.3 ps. Short laser pulse widths can allow valuable insights into molecular transitional and ionisation/dissociation state lifetimes. Moreover by changing the pulse width in this very fast regime it is possible to determine particular state lifetimes to within an upper and lower limit set by the availability of the pulse tuning. Of course the pulse width range must be compatible with the transitional state under study. Nanosecond laser studies were less successful in this respect, largely due to pre-dissociative states having lifetimes shorter than the laser pulse widths.

In Figure 4j, at each wavelength, four mass spectra are shown for the benzaldehyde parent and hydrogen loss peaks for different pulse widths. The ratios of the parent to hydrogen loss peaks as the pulse width varies are illustrated in Figure 4k.

It is clear that the relative parent intensity grows as the pulse width decreases, an effect which is more significant at 750 nm. It must be emphasised that the ratios of parent to hydrogen loss peaks at all pulse widths are only weakly dependent on the

laser intensity. The points of figure 4k represent the mean ratio value, with the error bars being a measure of this intensity dependence as a standard deviation. Therefore the relationship of the graph is considered real. The data of figures 4j and 4k suggest a hydrogen loss pathway with a dissociation time of less than 1 ps. This is construed from analysing the 750 nm curve of figure 4k, revealing it to be approximately a summation of two exponentials with half-lives of the order of 600 - 700 fs below a pulse width of ~ 1000 ps and 1500 fs above. However this is unlikely to be the only mechanism of producing the H loss fragment, otherwise pulse widths less than this lifetime would lead to even less dissociation to $C_7H_5O^+$ than that apparent from the figures.

This represents an extension to Yang *et al's* [1985] conclusion that the fragmentation of the parent ion into $C_7H_5O^+$ occurs on a time-scale of less than 25 ps. Concordant behaviour is found for the ratio of NO_2^+/NO^+ under similar experimental conditions [Singhal *et al*, 1998].

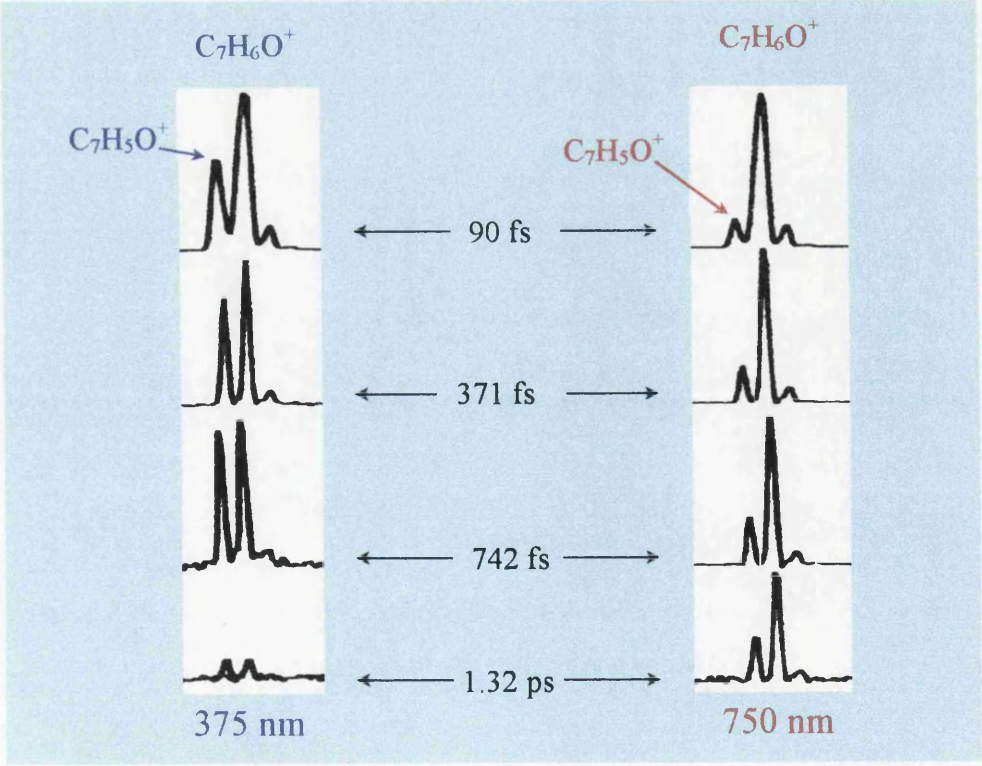

Figure 4j Parent and Hydrogen Loss Ion Peaks for Varying Pulse Widths

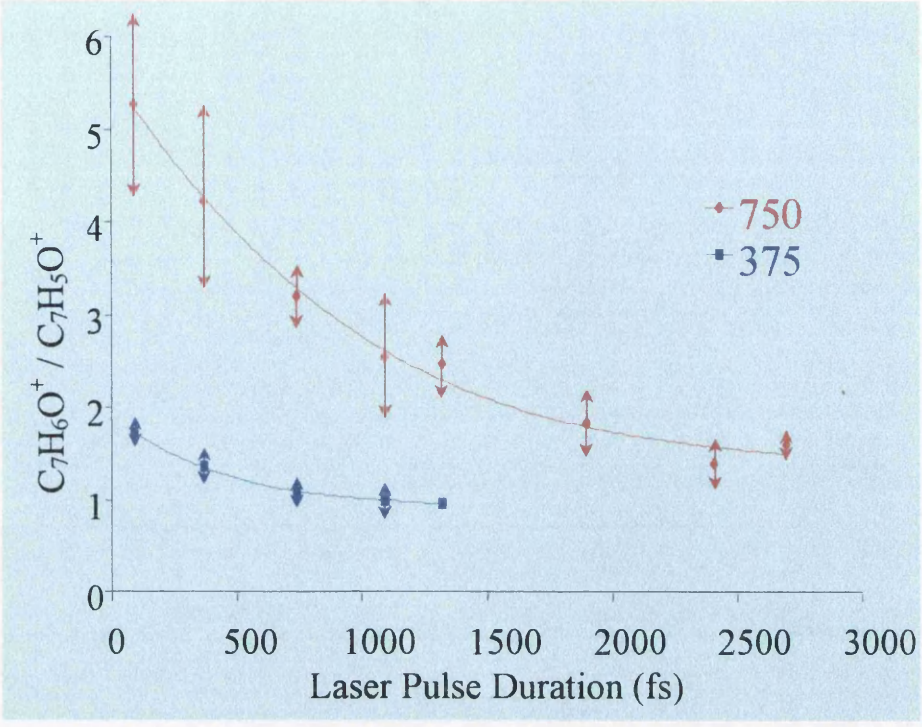

Figure 4k $C_7H_6O^+ / C_7H_5O^+$ as a Function of Pulse Width at 750/375 nm

§4.2.7 Non-Statistical Photon Absorption

As previously mentioned, and visible in figure 4e, increasing laser intensity leads to increasing molecular fragmentation. This can be explained by the appearance of new fragmentation channels as the rate of photon absorption increases, as well as by the saturation of existing ones. At such high molecular internal energies, dissociation may take place in a somewhat explosive manner, with the interactive processes also being affected by the laser pulse width. Pulse duration is thought to intrinsically influence energy flow within the molecular system, and thus determine to a large extent the operational ionisation and/or dissociation pathways. Upon photon absorption in the short pulse regime, a breakdown in the statistical nature of molecular energy distribution occurs [Weinkauf *et al*, 1994; Antonov *et al*, 1981] compared to nanosecond pules in which the energy randomly distributes itself over the entire molecule. As such, bottlenecks in energy transport may be set up within the molecule which could induce site-specific molecular bond activity. This may result in local fragmentation depending on the particular bond cleavage strength. This could lead to energy expensive ions with high appearance potentials being formed ahead of less

expensive ones with lower appearance potentials. Such bottlenecks may be released by increasing the pulse width towards the nanosecond excitation regime, although this may have a detrimental effect with respect to analysis.

For benzaldehyde, a possible region for local energy entrapment is the aldehyde group [Antonov *et al*, 1981]. This CHO group shown in figure 4a is the only non-symmetric part of the molecule. Within the aldehyde cluster itself, the bottleneck could form around the C=O bond, and as pulse width increases, spread out to other parts of the cluster, such as the C-H cleavage. In this model the more tightly bound C=O cleavage would resist dissociation more than the C-H bond. This may explain the increased production of $C_7H_5O^+$, as a primary daughter ion, as pulse width increases. Further information on the loss of the hydrogen atom from benzaldehyde to form $C_7H_5O^+$ could be found using singly deuterated benzaldehyde, with the hydrogen atom in the aldehyde cluster being substituted by deuterium, and therefore having a mass of 107 (C_7H_5DO). The primary daughter ion would either have a mass of 105 ($C_7H_5O^+$) or 106 ($C_7H_4DO^+$) depending on the local site of ionisation in the pathway described in section 4.2.6.

§4.3 Conclusions

The potential for FLMS in both theoretical and applied science is considerable. The technique has been applied to benzaldehyde [Smith *et al*, 1998a]. This has allowed an investigation into the operational ionisation and/or dissociation pathways, as well as associated dissociation lifetimes of transitional molecular states. The majority of dissociation has been shown to occur above the molecular ionisation threshold in a predominant ID model; in other words ladder-climbing followed by ladder-switching from within the parent ionisation continuum. A particular pathway is the dissociation of $C_7H_6O^+$ to $C_7H_5O^+$ on a time-scale of the order of less than a picosecond.

Consistent with the ID model, the molecular ion is predominant in all the mass spectra. Exclusive parent production is seen to be possible at 750 and 375 nm but is best achieved using longer wavelengths and lower laser intensities. For chemical analysis, FLMS is particularly effective in this region. The Glasgow group have

already shown that FLMS may become a universal system for the analytical detection of molecules [Ledingham *et al*, 1998a, 1997, 1996/7, 1995/6, 1995a, 1995b; Smith *et al*, 1998a, 1998b; Kilic *et al*, 1997; Kosmidis *et al*, 1997; Singhal *et al*, 1996].

Conversely fragmentation can be maximised using shorter wavelengths (375 nm) and higher intensities, where for a given pair of mass spectra at 750 and 375 nm, at similar laser pulse widths and intensities, fragmentation is significantly increased for the lower wavelength. This is preferred for structural studies of molecules.

In the current intensity range the ionisation mechanism has been found to be predominantly multiphoton with experimental and theoretical results in close agreement. However, at saturating intensities in the region of 10^{14} Wcm^{-2}, the ionisation may not be absolutely multiphoton in the sense that tunnelling may contribute to the total ion yields. Chapters 6 and 7 consider molecules subjected to intense beams of the order of 10^{15} W cm^{-2}. The multiphoton versus tunnelling altercation is further evoked with tunnelling, as expected, contributing more significantly to the ionic yields for higher laser intensities.

At a wavelength of 750 nm and at an appearance laser intensity around $\leq 10^{14}$ Wcm^{-2}, a double ionised benzaldehyde parent ($C_7H_6O^{++}$) has been observed. Essentially, no such peak was found in corresponding 375 nm mass spectra. This significant new result is thought to be of considerable importance, and has been observed by the author for a number of other medium mass molecules. The forthcoming chapters include results of multiply ionised benzene, deuterated benzene, toluene, naphthalene, 1,3-butadiene and carbon disulphide.

Finally, bottlenecks in energy migration within the molecular system have been considered. Such ionisation and site-specific dissociation, or non-statistical photon interaction, could significantly aid understanding with respect to energy and charge flow in molecules. Indeed the random energy distribution associated with nanosecond laser pulses may provide an additional explanation as to how increased fragmentation occurs in this pulse width region, with a greater number of molecular bonds being accessed compared to femtosecond excitation. FLMS is leading to a greater control

over fragmentation than previously obtained. Selective local dissociation may be another factor in its favour. This drives towards being able to control chemical dynamics.

CHAPTER 5

FLMS OF BENZENE, TOLUENE AND NAPHTHALENE

§5.0	**Introduction**	85
§5.1	**Experimental**	89
§5.2	**Results and Discussion**	90
§5.2.1	*Features of the Mass Spectra*	90
§5.2.2	*Laser Intensity Dependence*	96
§5.2.3	*Uniform Chemical Analysis*	98
§5.2.4	*Saturation of the Multiphoton Process*	100
§5.2.5	*Changing the Pulse Width*	100
§5.3	**Conclusions**	102

§5.0 Introduction

This chapter considers the application of femtosecond laser mass spectrometry (FLMS) to the aromatic molecules benzene, toluene and naphthalene [Smith *et al*, 1998b]. Particular emphasis is placed on drawing a comparison between the molecules'changing mass spectrometry from the development of nanosecond to femtosecond pulse width lasers. Structural schematics of the molecules can be seen in figure 5a.

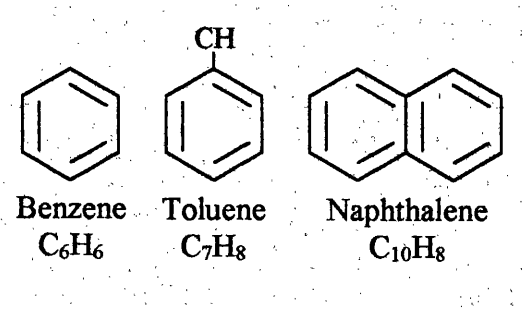

Figure 5a Some Aromatic Molecules

The trace-sensitive detection and identification of atoms and molecules is an area of considerable importance with the potential for widespread and diverse application. Lasers are particularly suited for such trace chemical analysis [Ledingham *et al*, 1992]. The technique, in which a laser coupled to a mass spectrometer, ionises a gaseous sample preceding detection, is the basis of resonance ionisation mass spectrometry (RIMS) which was discovered about twenty years ago but largely developed in the early 1980s [Fassett *et al*, 1988; Hurst *et al*, 1988; Lubman *et al*, 1987; Bekov *et al*, 1983]. RIMS provides a selective, ultra-sensitive technique to analyse atoms, providing information on relative component abundance as well as identification. Applied to molecules, the procedure is known as resonance enhanced multiphoton ionisation (REMPI) [Boesl *et al*, 1994]. Further explanation of these techniques can be found in chapter 2, §2.3.

REMPI and RIMS, and their non-resonant equivalents, generally make use of tuneable lasers in the ultraviolet (UV) wavelength regime, with nanosecond length pulses. Such experiments have had much success, particularly in fundamental studies of atomic and

molecular structure. However for the purposes of chemical fingerprinting, certain inherent problems have arisen.

Firstly the molecules, after laser excitation, have often been found to rapidly dissociate in preference to parent ion formation. This is due to the dissociative excited states having lifetimes shorter than the laser pulse widths, often resulting in extensive fragmentation and small or non-existent parent ions, [Boesl *et al*, 1991; Gedanken *et al*, 1982; Dietz *et al*, 1982; Zandee *et al*, 1979] leading to ambiguous chemical identification.

Secondly, to increase selectivity and sensitivity, the laser wavelength is usually tuned to resonantly ionise discrete energy levels in the sample species. In order to perform a more general analysis on different molecular species, the laser can be de-tuned to ionise the sample non-resonantly. This results in decreasing ion yields and the differing ionisation potentials may cause a non-uniform probability of detection. Therefore, although advantageous for specific investigations, REMPI is restrictive in a broad analytical sense, in which a sample may have an unknown composition.

In recent years, the femtosecond laser has been used to overcome such difficulties. FLMS has developed in conjunction with ultrafast lasers. The Glasgow group have illustrated that the potential of FLMS is substantial [Smith *et al*, 1998a, 1998b, 1998c; Ledingham *et al*, 1998a, 1998b, 1997, 1996/7, 1995/6, 1995a, 1995b; Singhal *et al*, 1998, 1996; Kilic *et al*, 1997; Kosmidis *et al*, 1997]. The short pulse widths coupled to high beam intensities [Hutchinson *et al*, 1989] (10^{12}- 10^{15} W cm^{-2}) has allowed rapid optical up-pumping through pre-dissociative states, such that molecular ionisation levels are reached. This ladder-climbing mechanism [Gedanken *et al*, 1982] is in competition with ladder-switching [Boesl *et al*, 1980] with the former becoming more dominant as the pulse duration decreases [Yang *et al*, 1985]. This leads to predominant parent peaks in the mass spectra making for successful analysis and identification of the species under investigation. Dissociation can occur to some degree via the parent ion continuum, and is found to be dependent on the beam characteristics. Such features are described for benzaldehyde in chapter 4 [Smith *et al*, 1998a].

Intense, short pulse width lasers have also been shown to have the potential to overcome the nanosecond analytical non-uniformity. He *et al* [1997a] have shown that highly uniform, quantitative and sensitive analysis of atoms is possible with ion sputtering coupled to intense laser beams (~ 10^{15} W cm^{-2}) of pulse widths around 35 ps. The large bandwidths of such lasers make it difficult to tune to a specific molecular resonance. Nonetheless high sensitivity is still achieved using the short intense laser pulses, which is advantageous for general analysis. Schutze *et al* [1996, 1995] have applied non-resonant multiphoton ionisation (NRMPI) to semiconductor materials such as GaAs. Using a technique known as picosecond laser desorption mass spectrometry (ps-LDMS) at beam intensities around 10^{13} W cm^{-2}, they showed that the same degree of ionisation for all species under investigation was possible in the saturation regime, and indicated that standard-free sensitive surface quantification could be achieved.

The general application of laser mass spectrometry to aromatic molecules has been extensive, with particular emphasis to the prototype molecule benzene. Boesl [1991, and references therein], Neusser *et al* [1984] and Schlag *et al* [1983] have reported results for benzene, naphthalene and toluene in the nanosecond region at beam intensities around 10^{7-8} W cm^{-2}. They found that soft ionisation - exclusive parent ion production - was possible in the three molecules, but considerable wavelength tuning was required to achieve this. Careful control of the laser intensity was also necessary to preserve the excited molecule and thus prevent rapid dissociation down to small mass fragments and a corresponding loss of a significant parent signature.

In agreement with the above [Weinkauf *et al*, 1994; Antonov *et al*, 1981; Zandee *et al*, 1979] it was reported that for benzene and other molecules, fast relaxation processes (e.g. photo-dissociation) can compete with further photon excitation, a process which is highly wavelength selective. This model for ladder-switching is well known to occur in aromatic systems.

Recently, using intense lasers, studies by DeWitt *et al* [1997, 1995] have reported photo-ionisation/dissociation for benzene, toluene, naphthalene and some other related

aromatics. 780 nm laser pulses of length 170 fs were used with TOF methods at beam intensities up to 3.8×10^{13} W cm^{-2}. Limited dissociation was observed in the molecules studied, with consistent parent ion dominance in the mass spectra. A comparison in the nanosecond regime revealed no parent ions at 532 nm, 3.5 ns and a power density of 1×10^{9} W cm^{-2}. However, it was possible to produce a parent ion at 266 nm and 2.5 ns in the same intensity region, although substantial fragmentation occurred upon increasing the laser power further. Interestingly, using a near-infrared (IR) wavelength of 780 nm, at 5 ns and $\sim 3 \times 10^{8}$ W cm^{-2}, no detectable signal was present. Presumably the power density was insufficient to ionise the sample. Strong focussing would be required to create a sufficient flux of photons to ionise in the IR region at nanosecond pulse widths. Niu *et al* [1998] investigated differences between UV and IR MALDI (matrix assisted laser desorption ionisation) using laser pulses less than 10 ns. They found that the protein ions produced in the infrared experienced less fragmentation than those in the ultraviolet wavelength region.

The high intensities associated with femtosecond lasers can limit the problem of insufficient ionising beam fluxes, and allow a comparison between UV and IR wavelengths, at similar pulse widths. As described in chapter 4, an investigation into benzaldehyde using an ultrafast laser revealed that at 750 nm there was much reduced fragmentation compared to the results at 375 nm. In another study, Singhal *et al* [1998] reported that for NO_2, parent ion yields at 750 nm were significantly greater than those corresponding to 375 nm. The conclusion follows that for analytical purposes, the higher wavelength seems more suitable.

This chapter presents results from a FLMS investigation of the aromatic molecules benzene, toluene and naphthalene. An intense femtosecond laser (up to 4×10^{14} W cm^{-2} and 50 - 90 fs) was used to probe the samples in a time-of-flight mass spectrometer (TOF) at wavelengths of 750 and 375 nm. This is an order of magnitude increase in laser intensity over recent measurements by DeWitt *et al* [1997,1995]. Of particular interest is the question of whether the soft ionisation reported above continues into this higher intensity regime, and if fragmentation in the UV wavelength region is relatively increased

compared to 750 nm, which could have considerable analytical implications. Following from this, the potential for uniform chemical analysis is considered and the optimum beam parameters to achieve this are discussed.

It is also of principal importance to extend the observations of chapter 4 with respect to an investigation into the appearance, or otherwise, of multiply ionised parent ions, similar to that reported for benzaldehyde ($C_7H_6O^{2+}$). Also discussed in the previous chapter, saturation of the ion signal is considered.

§5.1 Experimental

The experimental set-up consists of a femtosecond laser system and a time-of-flight mass spectrometer (TOF). A detailed description is located in chapter 3, and is similar to that reported in chapter 4. The laser system consisted of a titanium-sapphire oscillator pumped by an argon-ion laser with the resulting beam amplified in a dye laser and using chirped pulse amplification and optical pulse compression techniques to produce pulses of width 50 – 90 fs. It was possible to vary the pulse width up to a maximum of around 2 ps using SF10 blocks. Auto-correlation techniques at 750 nm were used to measure the pulse widths. Wavelengths of 750 nm and frequency doubled 375 nm were generated with intensities up to a maximum of $\sim 4 \times 10^{14}$ W cm^{-2} (750 nm) and $\sim 1 \times 10^{14}$ W cm^{-2} (375 nm). The TOF is of linear design based on a Wiley-McLaren model. Samples were admitted to the TOF chamber via a needle valve. The laser beam was focussed to a tight spot using a 10 cm focal length concave mirror such that the location of the focus was in the immediate vicinity of the sample molecular stream, thus defining an ionisation volume.

Coupling the system to an electron multiplier and digital oscilloscope, allowed the production of mass spectra of ionic yield versus time-of-flight. The flight time is related to the mass-to-charge ratio. The mass spectra have typical resolution of ~ 300 at 130 D - see section *3.2.1*.

§5.2 Results and Discussion

§5.2.1 Features of the Mass Spectra

Figures 5b – 5d show mass spectra for the molecules benzene, toluene and naphthalene respectively, taken at 750 nm and 50 fs, and 375 nm and 90 fs, for varying laser power densities. Relative ion intensities are plotted against their mass-to-charge ratios (m/z). The spectra are consistently normalised for gas pressure and amplifier gain such that quantitative comparisons can be made. This normalisation extends to comparisons between the three molecules, that is in cross-examining benzene (figure 5b), toluene (figure 5c) and naphthalene (figure 5d).

In terms of optimum chemical analysis, soft ionisation is desirable. This is found for all three molecules at both wavelengths in the lower beam intensity range. Fragmentation increases with the laser intensity, although parent ion dominance remains.

At a wavelength of 750 nm, exclusive parent production can be achieved at higher intensities ($\sim 3 - 5 \times 10^{13}$ W cm^{-2}) compared with 375 nm ($\sim 1 \times 10^{13}$ W cm^{-2}). It was not possible to match the 375 nm beam intensities with the highest intensities of the 750 nm beam, but comparing similar laser beam fluxes over the intensity range studied, fragmentation is clearly seen to be more prominent with the UV wavelength. Daughter ion formation can thus be suppressed to a greater relative degree at 750 nm. This has considerable implications for the purpose of analysis. However, for structural studies, molecular dissociation can provide useful information. High intensity UV excitation is appropriate in this event. It is noted though, that the UV mass spectra still maintain a predominant parent, despite the increased dissociation. This is contrary to nanosecond behaviour, where molecular moieties usually dominate the mass spectra at the cost of parent ions [Boesl, 1991].

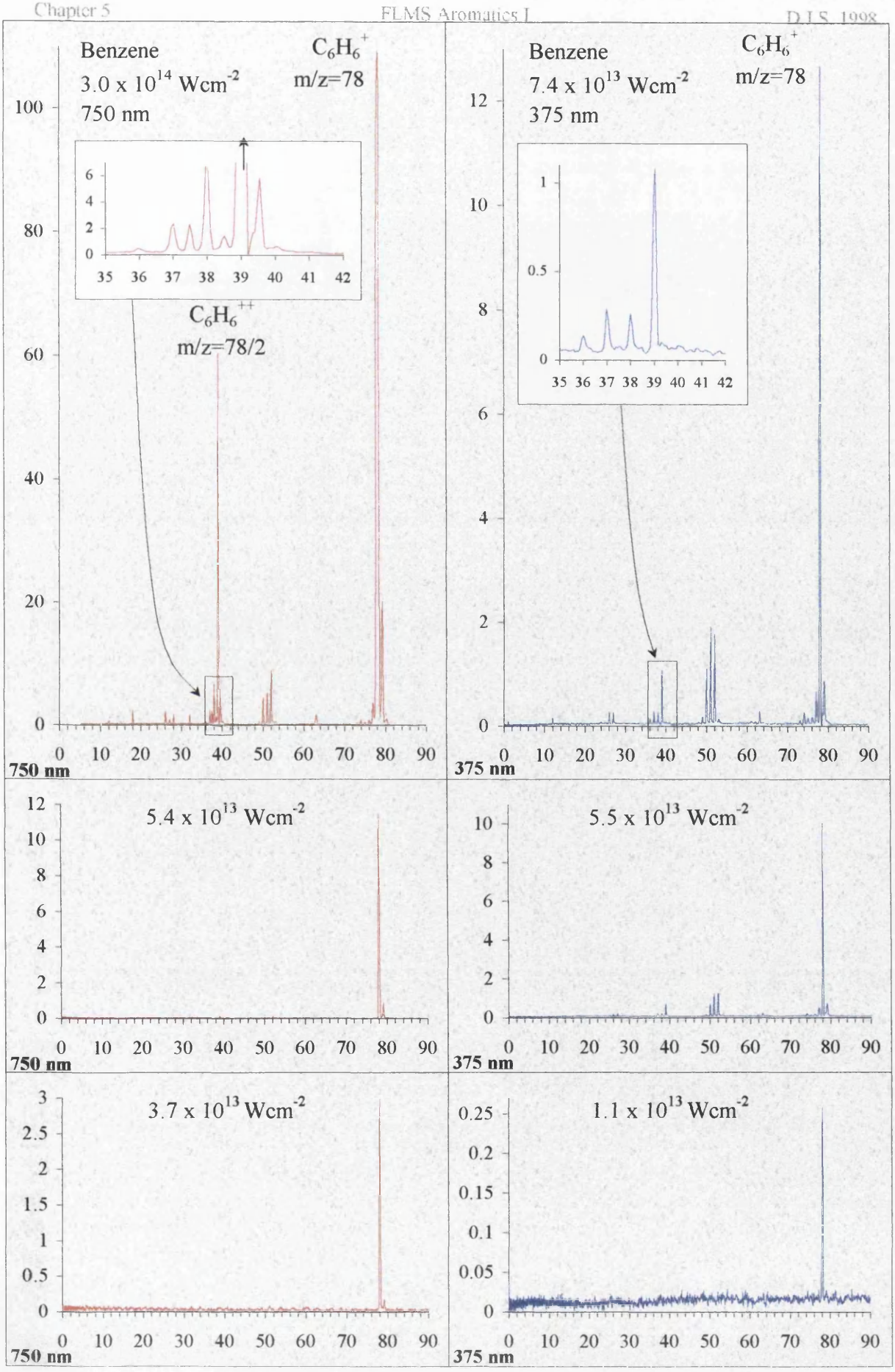

Figure 5b Benzene Mass Spectra at 750/375 nm and 50/90 fs respectively: Relative Ion Yield vs mass-to-charge ratio (m/z)

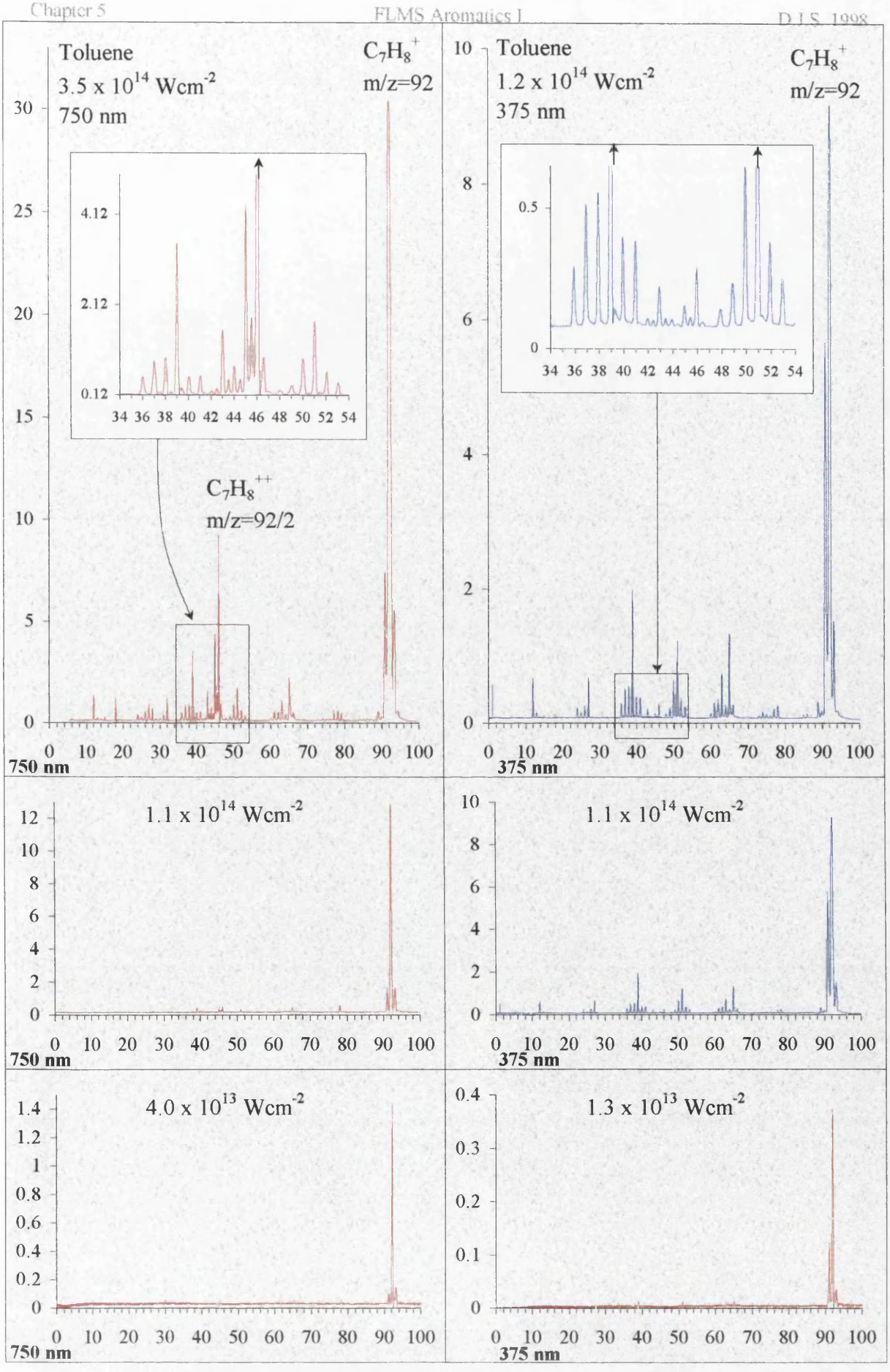

Figure 5c Toluene Mass Spectra at 750/375 nm and 50/90 fs respectively: Relative Ion Yield vs mass-to-charge ratio (m/z)

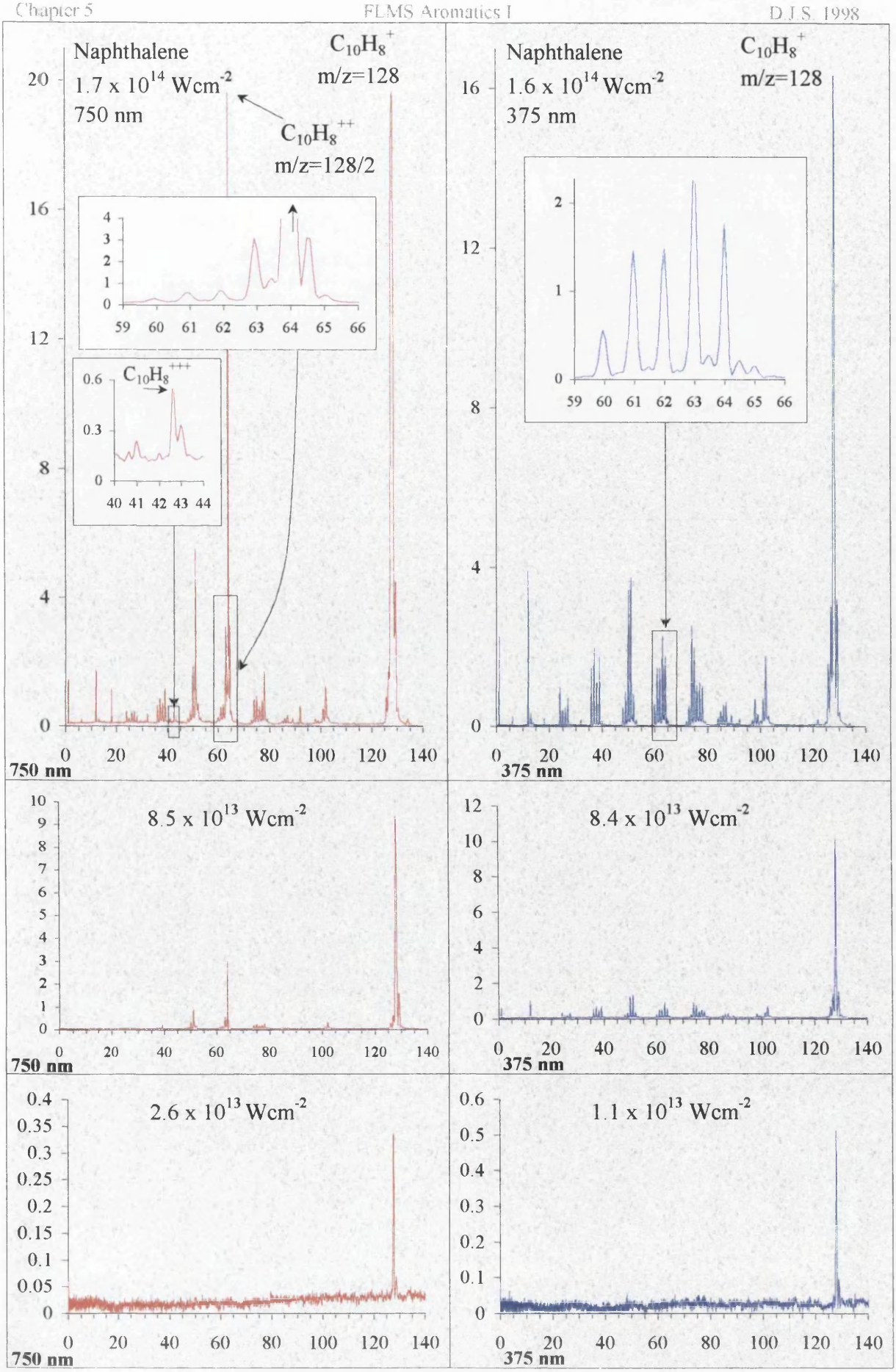

Figure 5d Naphthalene Mass Spectra at 750/375 nm and 50/90 fs respectively: Relative Ion Yield vs mass-to-charge ratio (m/z)

The molecules (M) irradiated with the near-IR beam not only show little relative fragmentation, but are seen to produce a clear double ionised parent in figures 5b – 5d - with appearance thresholds around 10^{14} W cm^{-2}. This is concordant with the observations of chapter 4, in which the appearance of double ionised benzaldehyde is noted. Indeed, similar characteristics have been seen, by the Glasgow group, for a number of other molecules including CO_2, CS_2 [Graham *et al*, 1998], CH_3I, and 1,3-butadiene.

In the present case for benzene, toluene and naphthalene, the unambiguous presence of an envelope of double ionised satellite peaks, occurring at half mass numbers, can be seen in the insets of figures 5b – 5d. A particularly strong satellite peak for each of the molecules is found at one half mass above the prominent M^{2+} which must be double ionised ^{13}C parent molecules - a ^{13}C molecule being an isotope with one ^{12}C atom replaced by ^{13}C. This naturally occurring isotopic mixture has been discussed in the previous chapter - *see §4.2.3.* Suffice it to say that for a molecule containing "x" carbon atoms, a ^{13}C isotope will generally be present with a percentage abundance of "$x \times 1.1$" [e.g. De Hoffman, 1996].

In detail for figure 5b, the strongest peak for benzene occurs at a mass/charge ratio (m/z) of 78, with a satellite at mass 79. The satellite corresponds to $C_5{}^{13}CH_6^+$ and has the correct $^{13}C/^{12}C$ isotopic ratio of about 7% for a molecule with six carbon atoms. At 750 nm, the next strongest peak is at m/z = 39. This could either be $C_6H_6^{2+}$ or the fragment $C_3H_3^+$. However it also has a satellite at m/z = 39.5 with the ratio of this peak to the peak at m/z = 39 similar to the isotopic ratio above. Hence the peak at m/z = 39 must predominantly be $C_6H_6^{2+}$. Laser intensity dependences have also been used to confirm the appearance of multiples - see section *5.2.2.* The existence of $C_6H_6^{2+}$ has been further verified using deuterated benzene (C_6H_5D) which shows a very strong, unambiguous double ionised parent peak – see chapter 6, section 6.2. In the inset of figure 5b for 750 nm, an envelope of half-mass peaks can also be seen. These ions are further considered in the next chapter. In contrast to the above, the comparative 375 nm spectra demonstrate substantially diminished or absent corresponding peaks, albeit increased fragmentation. This further indicates that the multiple component at 750 nm is significant because if

these peaks were single ionised fragments instead of dominantly multiply ionsed species, then one would expect them to be even more intense in the UV spectra, which is evidently not the case.

In figure 5c the spectrum for toluene is shown. A predominant single parent ion is evident, as expected using the technique of FLMS. The double ionised envelope, including a dominant multiple parent ion ($C_7H_8^{2+}$), is again a strong feature of the 750 nm spectrum and is in a region of the mass spectrum which does not correspond to any single fragment ions and hence is unambiguous. The insets show this to be a weaker effect in the 375 nm spectrum despite increased dissociation at the neighbouring C_3 and C_4 fragment groups. The peaks at m/z = 46.5 and 46, within experimental error, show the correct $^{13}C/^{12}C$ isotopic ratio for a molecule with seven carbon atoms (~ 8%).

The naphthalene spectrum in figure 5d shows similar characteristics to figures 5b and 5c. A strong $C_{10}H_8^{2+}$ peak is evident which can be distinguished from the fragment $C_5H_4^+$ because of its accompanying satellite at m/z = 64.5 with the correct isotopic ratio (~ 11%). These peaks are not so evident in the 375 nm spectrum even although the fragmentation is greater. There is also a strong peak at m/z = 51 for the 750 nm spectrum, which is evident because of the reduced surrounding fragmentation. This has been partly attributed to the double ionised C_8H_6 fragment. Triple charged ions, M^{3+}, have also been observed for this molecule in the intensity range above approximately 10^{14} W cm^{-2} at m/z = 128/3. This is seen in an inset at 750 nm at the highest intensity.

As previously stated, the laser intensities at 375 nm did not match the high intensities of 750 nm and so a direct comparison of the appearance, or otherwise, of multiply charged ions could not be made in this region.

§5.2.2 Laser Intensity Dependence

It is particularly instructive to plot the ionic yields as a function of laser intensity. This has been done for benzaldehyde - section 4.2. Similar dependences are shown in figure 5e for benzene, toluene and naphthalene respectively, at UV and IR wavelengths.

A consistent normalisation is again performed. Single and double ionised parent peaks are included as well as one or two typical single charged fragment peaks. As fragmentation is minimal, few peaks were available to plot such curves. The following observations from figure 5e are considered.

It is evident that by enlarge the gradients of the 750 nm curves are steeper than those of 375 nm, which can also be seen in figure 5f not yet discussed. This suggests that up to the first ionisation potential, the absorption process proceeds via a multiphoton model. Specifically, a dependence of approximately 2 at 375 nm and 3 at 750 nm is found for the three molecular parent ions, benzene, toluene and naphthalene. This conforms to a 3 (375 nm) and 6 (750 nm) multiphoton absorption process for benzene (I.P. = 9.24 eV) and toluene (I.P. = 8.5 eV) and a 3 (375 nm) and 5 (750 nm) multiphoton absorption process for naphthalene (I.P. = 8.12 eV) – assuming some degree of saturation during absorption. The ionisation potentials are taken from reference Weast [1972]. For the higher intensities, a tunnelling mechanism may have some contribution to make to the ionic yield - more on this in chapter 6.

The daughter ions (single charged) for both wavelengths evidently follow the slope of the parent ions. This, coupled to predominant parent ions in the mass spectra, is strongly suggestive of an ionisation-dissociation (ID) mechanism in which the short intense laser pulses bypass nanosecond pathways (pre-dissociative states) below the molecular ionisation continuum. The minimal dissociation occurs mainly from above-threshold, that is, via the parent ion.

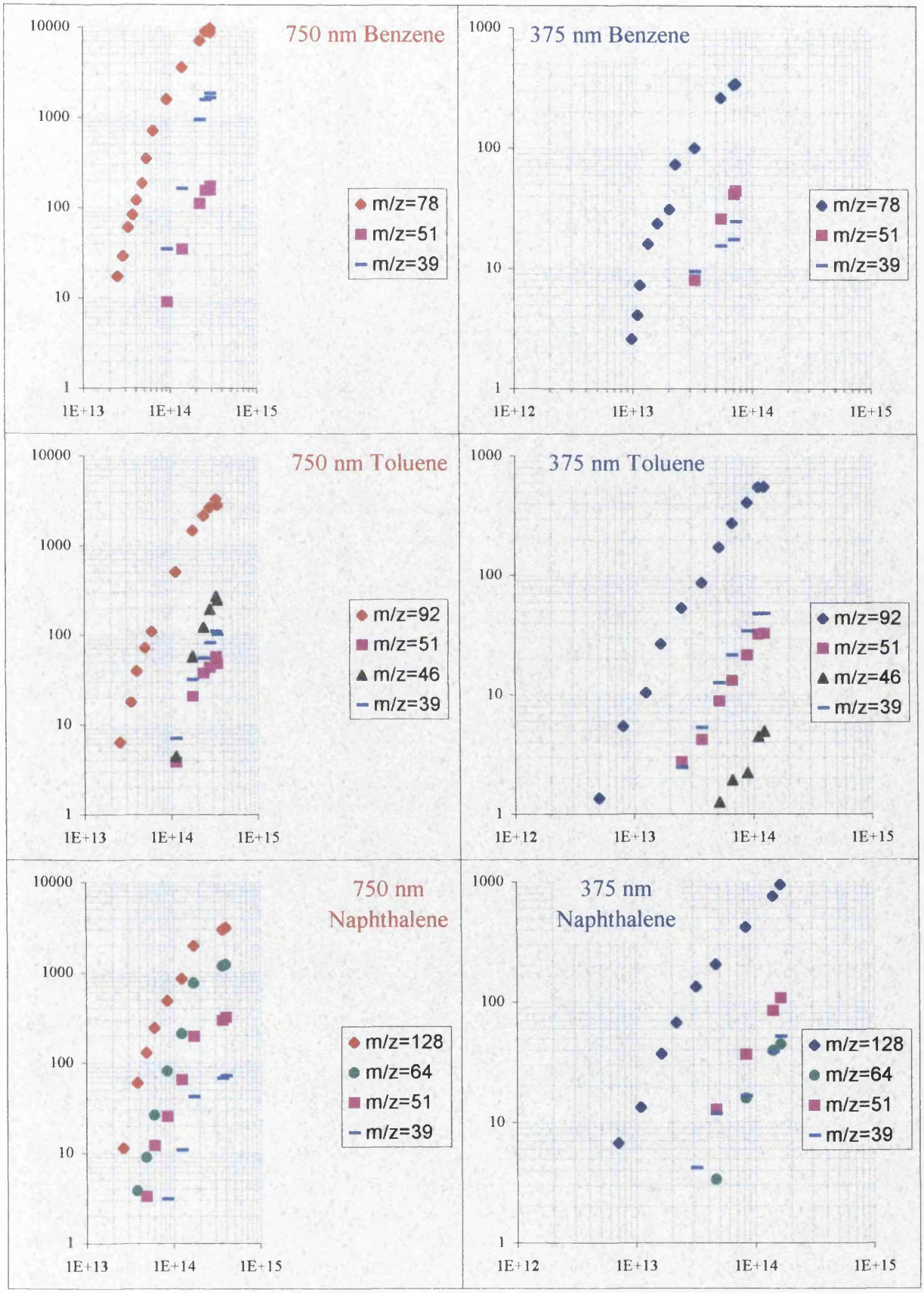

Figure 5e Laser Intensity Dependences for 750/375 nm at 50/90 fs respectively: Relative Ion Yield vs Laser Intensity

As previously discussed the peaks at m/z values equal to half that of the parent m/z value, are dominantly double ionised parents at 750 nm and single ionised daughter peaks at 375 nm. This corresponds to m/z = 39 (benzene), m/z = 46 (toluene) and m/z = 64 (naphthalene). It can be argued that these peaks in the relevant mass spectra are slightly steeper than the single charged curves at 750 nm which may be expected for a sequential ionisation process in which multiply charged states would require additional photons to be accessed.

§5.2.3 Uniform Chemical Analysis

With particular reference to chemical analysis and molecular ion formation, the choice of wavelength can be made less important by choosing an appropriate laser intensity.

Figure 5f illustrates how the parent ion yield (peak areas) varies with beam intensity for benzene (5f.*i*), toluene (5f.*ii*) and naphthalene (5f.*iii*), at both wavelengths. Normalised ion quantities are plotted as a function of laser beam intensities at 750 and 375 nm.

The intersection of the 750 and 375 nm curves is important, representing an equal probability of parent molecular ion production for the different wavelengths. Wavelength de-sensitivity in terms of parent ionic yields is apparent. This corresponds to an optimum operating intensity of about 7×10^{13} W cm^{-2} for the three molecules. Such wavelength independence characterises FLMS as a more flexible and general analytical approach.

However, the higher wavelength may still be more suitable for molecular identification due to the associated reduced fragmentation.

It is also important to point out that at the optimum operating laser intensity, the quantitative ion production for the three molecules is very similar. This indicates a tendency towards uniform molecular detection, which has already been observed for atoms in a similar intensity region by He *et al* [1997a]. FLMS thus has the potential for standard-free quantitative analysis. This is a significant finding.

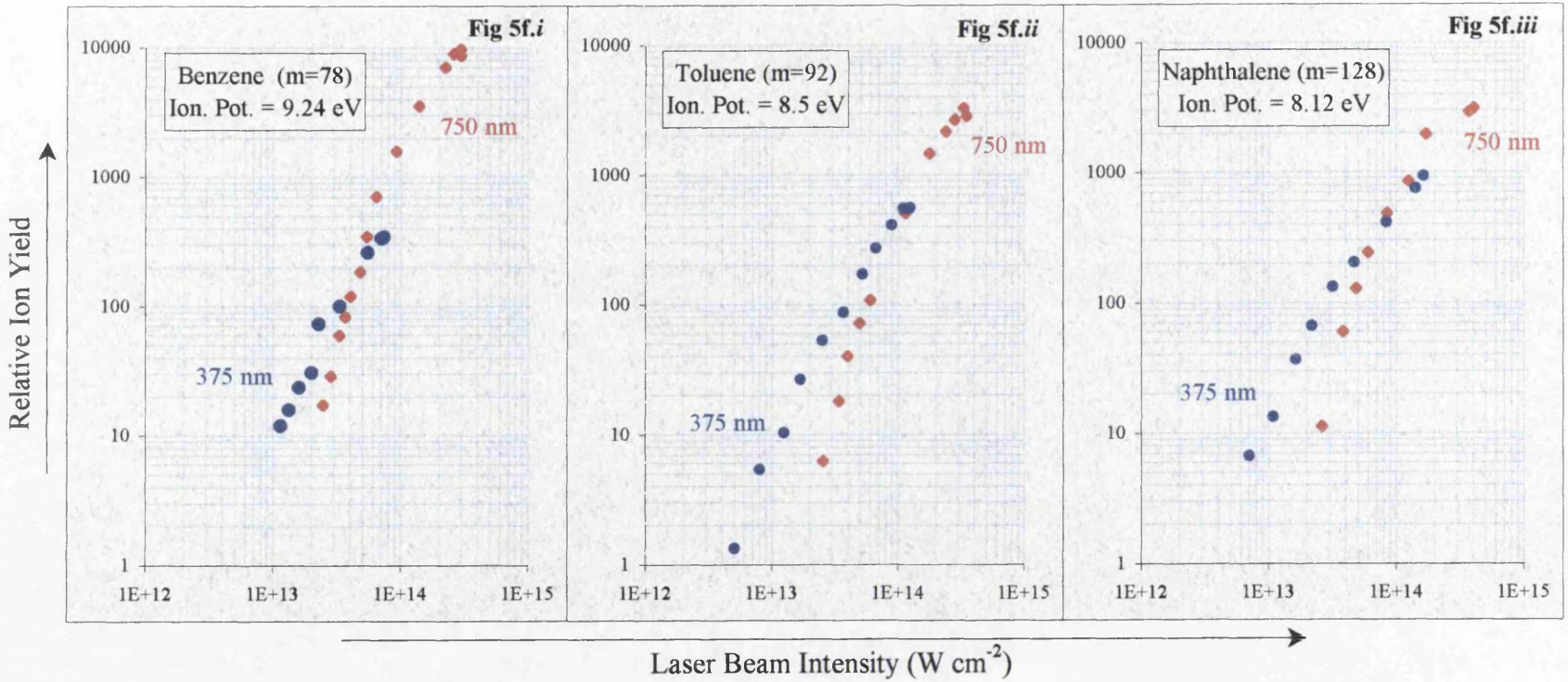

Figure 5f The Laser Intensity Dependence for benzene (5f.*i*), toluene (5f.*ii*) and naphthalene (5f.*iii*) parent molecular ions at 750/375 nm and 50/90 fs respectively: Relative Ion Yield vs Laser Intensity.

§5.2.4 Saturation of the Multiphoton Process

A degree of saturation of the ionisation signal is apparent in figures 5e and 5f at the higher laser intensities. Similar observations were noted in chapter 4 for benzaldehyde, section *4.2.4*. Saturation can be seen as a reduction in the rate of change of ion yield as the beam intensity increases. The increasing ion yields with lesser gradients can be attributed to an effective increase in the ionising focal volume of the laser beam, as the wings of the spatial beam profile become more significant. This is due to the laser wings' ionising ability increasing with increasing laser intensity, an effect which becomes more noticeable as the rate of ionisation by the main beam slows because saturation is approached [Trappe *et al*, 1993; Sogard *et al*, 1988]. This is tending towards unity ionisation probability, with the sensitivity of FLMS being maximised.

§5.2.5 Changing the Pulse Width

Varying the pulse width from approximately 50 fs – 2.5 ps did not materially affect the results for the molecules studied although all dissociation channels have not yet been investigated in detail. In other words, rapid up-pumping through the molecular system was maintained within this pulse width range to produce mass spectra with concordant features to figures 5b - 5d for benzene, toluene and naphthalene respectively. Figure 5g illustrates this with consistently normalised mass spectra for the prototype molecule benzene recorded at various pulse widths. The results of varying the pulse width for toluene and naphthalene are in concert with benzene. Wavelengths in the UV (375 nm) and IR (750 nm) are shown. A greater pulse variation was possible using the IR than the UV wavelength due to the greater powers available with the former. Laser beam parameters are indicated on the spectra. Laser intensity decreased rather sharply as pulse width increased. To isolate any pulse width effect, spectra are included for similar intensities at different pulse widths.

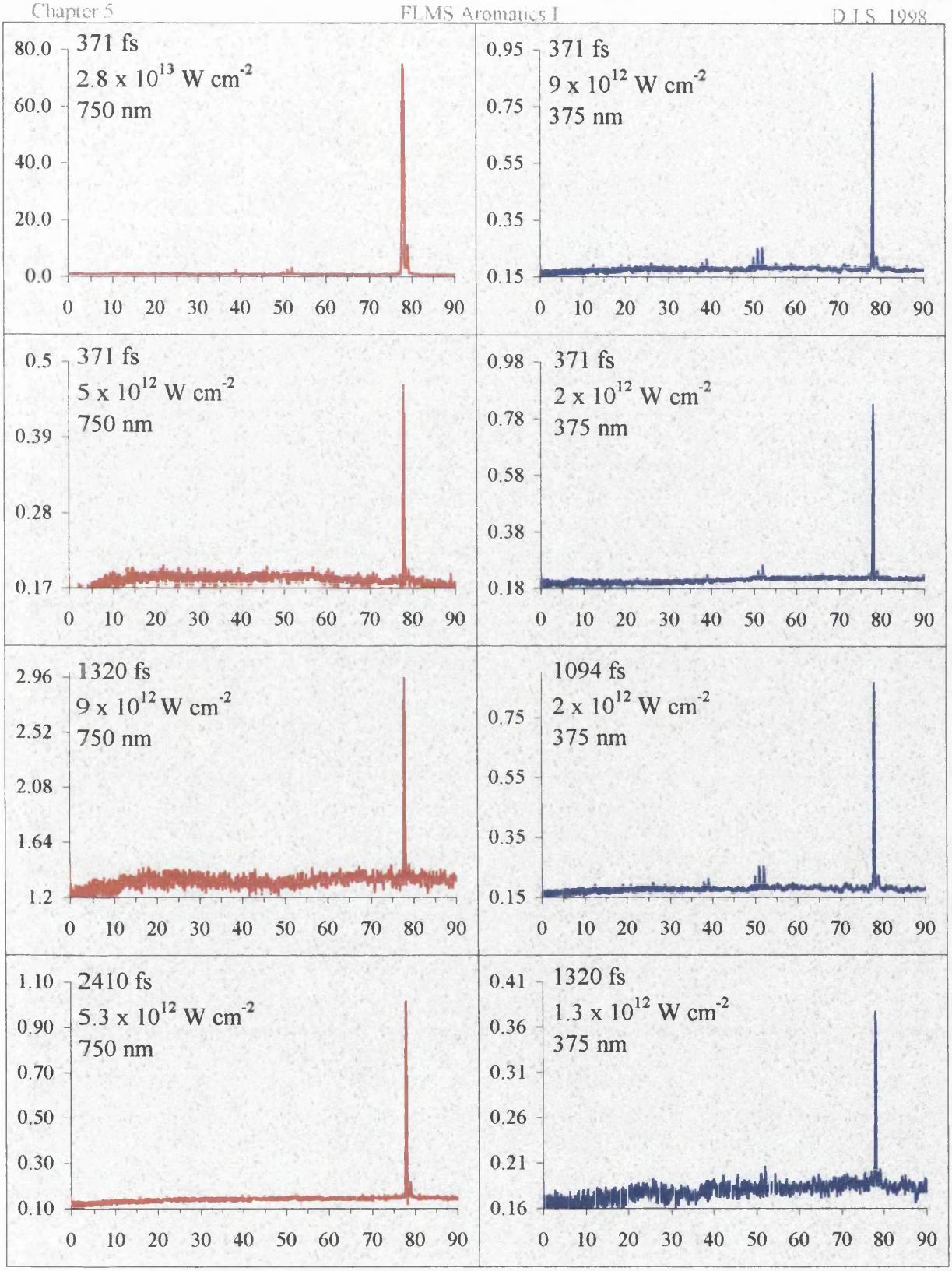

Figure 5g Benzene Mass Spectra at 750/375 nm for Various Pulse Widths
Relative Ion Yield vs mass-to-charge ratio (m/z)

It is clear that the parent ion is predominant in all the mass spectra. Soft ionisation or exclusive parent production is visible. Minimal fragmentation appears for moderate laser intensities, with greater relative fragmentation at 375 nm compared to 750 nm.

The laser intensity and wavelength, rather than the pulse width (within the ultrafast range studied) seem to be the governing factors in whether or not dissociation occurs, from above the parent ionisation threshold. Therefore disregarding a pulse width influence, and observing the normalised ionic yields of figure 5g, it can be seen that increasing the intensity leads to an increased production of parent ions. No double ionisation is observed because the intensities are below the appearance threshold of $\sim 10^{14}$ W cm^{-2} as previously discussed at 750 nm.

§5.3 Conclusions

FLMS has been applied to the molecules benzene, toluene and naphthalene at the wavelengths 750 and 375 nm, using laser beam intensities up to 4×10^{14} W cm^{-2}. Findings are concordant for the three molecules as discussed below. Similar results have also been reported in chapter 4 for the molecule benzaldehyde, indicating the general consistency of the technique.

The aims of the experiment determine the choice of laser parameters. FLMS has been shown to be useful for analysis due to its efficiency in producing dominant parent molecular ions at 750 and 375 nm, but particularly in the IR wavelength regime, in agreement with DeWitt *et al* [1997,1995]. Less relative fragmentation is observed at IR compared to UV wavelengths for a given laser intensity in the range studied. This effect is common to all the molecules studied by the Glasgow group. Other groups have also recognised the potential of FLMS, especially in the analysis of organo-metallic molecules [Willey *et al*, 1997; Grun *et al*; 1996].

The increased UV fragmentation is a very important observation, which has been seen by other authors for the intense irradiation of small molecules [Cornaggia *et al*, 1990], but is

difficult to explain. It is possible that higher charged states are reached by the UV photons which in turn dissociate to C_nH_m fragments, perhaps characteristic of UV radiation in the nanosecond regime.

At 750 nm, the appearance of multiply charged molecular ions has been observed with little associated molecular fragmentation. Such effects were minimal at 375 nm, where greater fragmentation occurred. The appearance threshold for these effects has been found to be around 10^{14} W cm^{-2} in the IR, which is in agreement with the appearance threshold of double ionised benzaldehyde reported in chapter 4 - see section *4.2.3.* Although it was mentioned that to reach the first ionisation level, photons were absorbed via multiphoton processes, it is possible that tunnelling ionisation [Codling *et al*, 1994] is becoming important as the intensity increases. An envelope of double ionised cations is a very strong feature at these intensities. This corresponds to a Keldysh parameter (γ) [Keldysh, 1965] of about 1.0 for the IR photons. The fact that these effects of increased multiple ionisation and minimal dissociation were not observed to the same degree for the UV photons, might simply reflect that the smallest Keldysh parameter for 375 nm was about 2.0. A Keldysh value of 2.0 corresponds to predominant multiphoton ionisation, while $\gamma \sim 1.0$ concurs with a greater contribution from the tunnelling mechanism, although multiphoton activity remains significant– see chapter 2, section 2.4 for Keldysh theoretical considerations.

Chapter 6 details a further investigation into this interesting multi-charged phenomenon for the molecules included in the present chapter, as well as deuterated benzene, using higher power lasers ($\sim 10^{15}$ W cm^{-2}) at an increased wavelength of 790 nm. The choices of beam parameters reflect the experimental goals. An infrared wavelength is chosen to further aim at reduced molecular dissociation, and the greater beam intensities to aim for an increased production of multiply charged ions.

The results of dominant parent ions, minimal fragmentation and production of multiples are largely in contrast to nanosecond REMPI findings. Nanosecond soft ionisation can only be achieved by strictly controlling the laser beam characteristics of wavelength and

intensity to avoid extensive dissociation and a corresponding loss of a parent ion signature. FLMS represents a more flexible method of producing dominant stable parent ions, with changes in intensity and wavelength playing a less important role when the appropriate range is reached (~ 10^{12+} W cm^{-2} presently). FLMS effectively bypasses nanosecond routes. However, once the very short pulse width region has been entered, laser intensity and wavelength do minimally affect the results in terms of the yield of dominant parent ions and degree of fragmentation. On the other hand variations of the pulse width within the femtosecond region have not affected the results.

For analytical purposes, a degree of wavelength independence has been identified. For laser intensities tending towards 10^{14} W cm^{-2}, the molecular ion yield has been found to be similar for both 750 and 375 nm. Moreover, at these intensities approaching saturation, it has been shown that uniform parent molecular detection is obtained for the three molecules, benzene, toluene and naphthalene. This points to a possible quantitative procedure for molecular detection without the use of standards.

CHAPTER 6

FURTHER EXPLORATION OF FLMS APPLIED TO AROMATIC MOLECULES

§6.0	**Introduction**	106
§6.0.1	*Analysis and Multiply Charged Ions*	106
§6.0.2	*Background*	107
§6.0.3	*Aims*	114
§6.1	**Experimental**	115
§6.2	**Results and Discussion**	115
§6.2.1	*Toluene*	117
§6.2.2	*Benzene and Deuterated Benzene*	119
	Double Ionised Species	123
	Triple Ionised Species	126
	Laser Intensity Dependences	127
§6.2.3	*Ionisation Mechanisms and Pathways for Single and Multiple Ion Production.*	130
§6.3	**Conclusions**	132
	Appendix 1	135
	Appendix 2	138

§6.0 Introduction

The present chapter further considers the application of femtosecond laser mass spectrometry (FLMS) to aromatic molecules [Smith *et al*, 1998a, 1998b, 1998c; Ledingham *et al*, 1998a, 1998b] building on some interesting findings discussed in chapters 4 and 5. Specifically, chapter 6 reports on a subsequent investigation into the appearance, or otherwise, of multiply charged parent molecular ions with minimal associated fragmentation.

§6.0.1. Analysis and Multiply Charged Ions

In terms of the analysis of molecules, it has been shown in the previous two chapters that FLMS is an extremely useful tool. Results have been presented thus far for aromatic molecules, although FLMS has been successfully applied to a range of other molecules – see for example chapter 7. Thus far the prerequisites for optimum detection have been found to be at a laser wavelength in the near-infrared (IR) region (~ 750 nm) at short pulse widths (~ 50 fs) in the beam intensity range around 10^{14} W cm^{-2}. Under such conditions, the parent signature dominates the mass spectra with minimal dissociation. Moreover, uniform molecular analysis has been shown to be possible at an operating laser intensity around 7×10^{13} W cm^{-2}.

At a threshold intensity of approximately $\leq 10^{14}$ W cm^{-2}, the appearance of double charged parent ions has been observed. In pure analytical terms, this unexpected finding may not be ideal, since the analyst may only be interested in single charged parent signatures. It is also important to realise that the onset of double ionisation lies at an intensity above that required for uniform detection, and as such may have significant implications with respect to successful analysis.

§6.0.2 Background

The multiple ionisation of, or high harmonic generation in molecules is an extremely interesting phenomenon in its own right and is generating considerable interest in current physics. The experimentation into molecules subjected to intense laser fields, and the molecules' response, is still in its initial stages and has mainly centred on small species. Several good reviews have been published [Protopapas *et al*, 1997; Codling *et al*, 1997, 1994, 1993; Giusti-Suzor *et al*, 1995; Freeman *et al*, 1991].

The initial experiments on atomic/molecular species using intense lasers occurred in the early 1960s lead by Mainfray and Manus [1991] and others [Lompre *et al*, 1976; L'Huillier *et al*, 1984, 1983]. The results appeared to be governed by an n photon perturbative ionisation rate, R_n given by:

$$R_n = \sigma_n I^n \qquad \textit{eqn 6.0.2a}$$

where I is the laser intensity and σ_n is the generalised n-multiphoton ionisation cross section - see *§2.3.5* for further details.

However as early as 1965, Keldysh [1965] recognised that an alternative mechanism to multiphoton ionisation could occur under certain conditions. His work has been influential in the paradigm shift towards this alternative. Chapter 2 describes the Keldysh theory in some detail, and has been briefly considered in chapters 4 and 5 – see sections 2.4, *4.2.5* and *5.3* respectively. Suffice it to say that under conditions associated with atoms or molecules subjected to intense laser fields (picosecond to femtosecond, $10^{13\text{-}16}$ W cm^{-2}) perturbation theory becomes inadequate to describe the resultant non-linear dynamics. The laser electric fields are no longer small compared to the binding molecular fields of the valence electrons, which can lead to new physical effects. The normal coulomb potential of the atom or molecule can become so distorted that electrons tunnel through the barrier formed by the atomic/molecular potential and the instantaneous electric field of the laser. Figure 6a illustrates this resultant distortion for the summation

of a typical atomic potential (the molecular case is similar) with a high intensity dc electric potential.

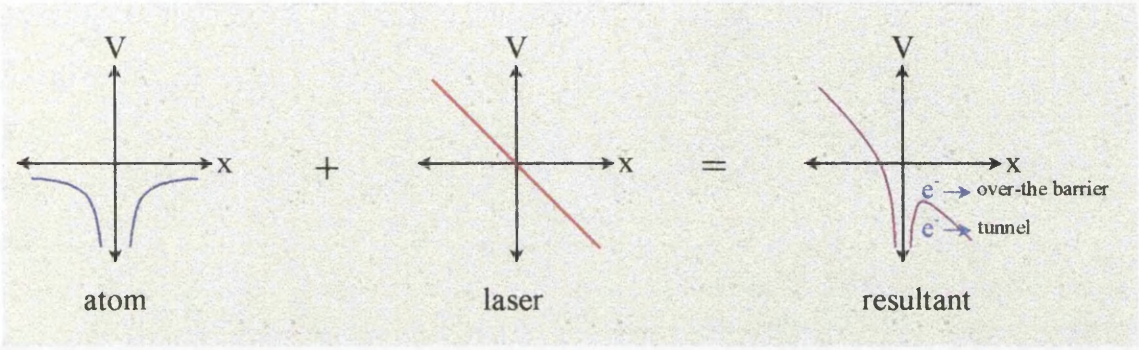

Figure 6a The Summation of an Atomic Potential and a dc Laser Field Potential

For this phenomenon to occur, the barrier must remain more or less static for long enough to allow the electron to penetrate it, that is for ionisation to result. The process is more suited to longer wavelengths (lower frequencies) as well as high intensities. A lower frequency increases the probability of the electron escaping because the "wiggle" motion imparted to the electron allows it to occupy the region where it is most likely to escape beside the potential barrier for longer periods of time than that associated with a higher frequency motion.

A semi-quantitative criterion for tunnelling has been defined by Keldysh:

$$\gamma = \left(\frac{E_i}{1.87 \times 10^{-19} I \lambda^2} \right)^{\frac{1}{2}} \qquad \textit{eqn 6.0.2b}$$

where E_i is the zero-field ionisation potential of the atom or molecule expressed in eV, I is the laser intensity in W cm^{-2} and λ is the laser wavelength in nm. Values of $\gamma << 1$ correspond to tunnelling while $\gamma >> 1$ define a dominant multiphoton mechanism. Values falling between these thresholds are in the intermediate region where both mechanisms are likely to occur. Recently a more pragmatic definition has been postulated with tunnelling concurring with values of $\gamma < 0.5$ [Ilkov *et al*, 1992]. It is important to note

that such criteria for ionisation mechanisms cannot be considered absolute. The interpretation of results obtained has varied considerably from agreement with the above to the observation of pure multiphoton ionisation in the tunnelling regime [Lompre *et al*, 1976] and vice-versa [Gibson *et al*, 1990]. Ledingham's group have shown that NO_2 [Singhal *et al*, 1996] and benzaldehyde [Smith *et al*, 1998a] dynamics, under subjection to lasers at different wavelengths at intensities in the range ~ $10^{13\text{-}14}$ W cm^{-2}, can be adequately described by multiphoton processes. This is despite Keldysh parameter values approaching the tunnelling threshold.

An alternative to tunnelling exists if the atomic or molecular coulombic potential is sufficiently suppressed by the laser field such that the electron can escape over the barrier rather than tunnel through - see figure 6a. Such a phenomenon usually requires a field strength higher than that required for tunnelling. This tends towards an unbound ground state and is known as over the barrier ionisation (OTBI) - see chapter 2, section 2.4. OTBI occurs when the external laser field surpasses a critical point, Σ_c [Augst *et al*, 1991] given by:

$$\Sigma_c = \frac{E_i^2}{4Z} \qquad \textit{eqn 6.0.2c}$$

corresponding to a threshold laser intensity, I_{th} of:

$$I_{th} = 4\times10^9 \frac{E_i^4(eV)}{Z^2} \qquad \textit{eqn 6.0.2d}$$

where E_i is the ionization potential and Z the ionic charge.

As an example and for simplicity, consider Xenon (ionisation potential = 12.1 eV). Applying the above equation the intensity for OTBI is found to be: I_{th} = 8.6 × 10^{13} W cm^{-2}. This OTBI threshold may be considerably greater than the saturating intensity of Xenon in which all the atoms and molecules within the laser focal volume are ionised. In fact, Protopapas *et al* [1997] pointed out that a saturating intensity for Xenon is around 2.5 × 10^{13} W cm^{-2} using a laser pulse width of 36 ps and a wavelength of 1.064 μm.

Therefore total multiphoton ionisation of the target species may pre-empt tunnelling or OTBI, due to the rise time of the laser pulse and corresponding ascending laser intensity along the pulse profile. Consequently for tunnelling to manifest, the laser pulses may be required not only to be very intense, but also to be ultrafast with a sharp rise in the temporal profile. This can avoid a multiphoton process ionising the sample species ahead of non-perturbative interaction. Manipulation of the leading edge of the laser pulse may be required and is best achieved using a technique known as interferometric shaping [Giles *et al*, 1995]. The principle of this method is to split the laser pulse into two pulses of unequal intensity, delay the main pulse and recombine them such that the low intensity pre-pulse can interfere constructively or destructively with the leading edge of the main pulse. This produces an increase or decrease in its rise time. Such a method affords rapid and controlled adjustments of the pulse profile and limits unwanted changes in the pulse characteristics.

Lambropoulos [1985] concluded that substantial ionisation during the rise time of the pulse of a strong laser is inevitable in the picosecond, and perhaps even femtosecond range. It was therefore stated that no neutral atoms or molecules could be exposed intact to a peak power much above 10^{14} W cm^{-2}, due to the pulse evolution argument.

It is important to realise that a further increase in laser intensity beyond saturation can lead to more ionisation, albeit at a reduced rate. Primarily, this is due to an effective expansion in the interaction focal volume of the laser spot due to the beam wings significantly contributing to the ionisation rate [Trappe *et al*, 1993; Sogard *et al*, 1988; Lambropoulos, 1985]. This is discussed in chapter 5 (*§5.2.3*) being illustrated in the plots of ion yield versus laser intensity as a reduced but still increasing ionisation rate. Multiphoton ionisation would most likely still pre-empt tunnelling at this reduced ionisation rate as the intensity of the wings increase.

Again it is emphasised that detailed explanations of the ionisation mechanisms outlined above are located in chapter 2. Although more geared towards atomic processes, molecular dynamics can be modelled on such mechanisms. This is particularly true when

the molecules themselves are behaving with somewhat atomic characteristics. Walsh *et al* [1994, 1993] and Chin *et al* [1993, 1992] have pointed out that simple molecules (diatomic and triatomic) can be quasistatically tunnel ionised as if they were structureless atoms with an ionisation potential equivalent to that of the molecules. Similarly, Liang *et al* [1994] have suggested that diatomic molecules can produce harmonics in a manner similar to that of an atom with the same ionisation potential. Ledingham's group [1998a] have also discussed atom-like behaviour of polyatomic molecules.

However, due to additional degrees of freedom, molecules can exhibit phenomena not associated with atoms; for example, above threshold dissociation (ATD), bond-softening/hardening and coulomb explosions. Details of these mechanisms can be found by referring to Codling *et al* [1997 and references therein]. It is not the aim of the present work to elucidate the theories in detail. A theoretical overview of the response of molecules to high electric fields is presented in the second chapter - see chapter 2, sections 2.2 onwards. It is however, important to note that the laser parameters (e.g. intensity, pulse width, pulse rise-time or shape, wavelength) are influential on the mechanisms of ionisation and the resultant molecular dynamics. In this sense the beam characteristics can aid understanding and ultimately control chemical dynamics.

Following pioneering work by Codling and Frasinski there has been increasing emphasis on studying the interaction of short intense laser radiation with molecules, particularly those of a diatomic or triatomic nature. This is a natural evolutionary step from atomic analysis. General themes are emerging from such studies of small molecules and are briefly outlined below [Talebpour *et al*, 1998, 1997a, 1997b, 1997c; Codling *et al*, 1997, 1994, 1993; Vijayalakshmi *et al*, 1997; Posthumus *et al*, 1997a, 1997b, 1996; Cornaggia *et al*, 1996, 1994, 1991, 1990; Safvan *et al*, 1996; Brabec *et al*, 1996; Normand *et al*, 1996, 1991; Dietrich *et al*, 1996, 1992; Constant *et al* , 1996; Giusti-Suzor *et al*, 1995; Seideman *et al*, 1995; Purnell *et al*, 1994; Liang *et al*, 1994; Hatherly *et al*, 1994; Ravindra Kumar *et al*, 1994a, 1994b; Kyrala, 1993; Lavancier *et al*, 1991; Frasinski *et al*, 1987; L'Huilleir *et al*, 1984].

A field ionisation, coulomb explosion model with ionisation preceding any dissociation, has had some success in fitting the data.

Many of the above authors have observed the phenomenon of multiple ionisation in small molecules, both as multi-charged molecular parent species and multi-charged atomic ions from molecules. As the focussed laser intensity increases above an approximate threshold of 10^{14} W cm^{-2}, double ionisation can occur with higher ionised multiples appearing with ascending intensity. The ions are rapidly formed by the swift removal of outer valence electrons and become aligned with the high electric field [Normand *et al*, 1996]. This is followed by rapid separation (Coulomb explosions) leading to multi-ionised species. The mechanism of electron removal is not well understood. Rapid sequential near-vertical ionisation may occur with successive stripping of electrons as the bonds lengthen somewhat, on a femtosecond time-scale, from their equilibrium positions to greater inter-nuclear distances. This sequential ion production [Cornaggia *et al*, 1991] matches the laser intensity evolution along the pulse profile with multiphoton ionisation likely taking place ahead of field ionisation as discussed earlier.

The process is not thought to be described by a slow sequential stripping of the electrons because the first unstable molecular ion would likely dissociate before further ionisation occurred, leading to a non-production of the high harmonics observed.

Additionally, Codling *et al* [1997 and references therein] observed that the phenomenon of multi-electron ionisation-dissociation (MEDI) takes place in simple molecules in intense fields. The Reading group speculated that the process may best be described by coulomb explosions combined with ionisation enhancement occurring at critical inter-nuclear distances. In this model electrons are stripped from the molecule until the first repulsive charge state is reached, whereupon dissociation begins as the molecule stretches to the aforementioned critical distance where the probability of higher ionisation is greatly enhanced [Normand *et al*, 1996; Constant *et al*, 1996; Seideman *et al*, 1995].

The ionic kinetic energies largely observed may be explained by the above, that is: (i) rapid sequential ionisation at various points along the coulombic potential curve; (ii) coulomb explosions at critical inter-nuclear distances. Both explanations are consistent with the ionic kinetic energies being considerably less than expected if a non-sequential (vertical) explosion had taken place at equilibrium inter-nuclear distances comparative to that of the neutral molecule. In that situation, many electrons are simultaneously removed from the molecule which can subsequently result in an extreme coulomb explosion.

Whatever the mechanism(s) of molecular ionisation and/or multi-electron ionisation-dissociation (MEDI) of small molecules, the process is indeed a complex one, and is poorly understood at present. Difficulties abound. For example, the molecular ionisation and dissociation time-scales are of the same order [Codling *et al*, 1994]. Also, although kinetic energy measurements can be instructive, [e.g. Cornaggia *et al*, 1990; Frasinski *et al*, 1987] interpretative energetic problems do exist; for example in the detailed analysis of coulomb explosions [Codling *et al*, 1994; Cornaggia *et al*, 1994, 1991].

Clearly more definitive experiments are required, involving interferometric control and good characterisation of the laser parameters, as well as more detailed and careful analysis of the ionisation and dissociation dynamics.

It is likely that the theoretical treatment of molecules in intense laser fields will increase in difficulty as the molecules become more complex. Although, as indicated, most experiments to date have concentrated on small molecules, studies of medium mass molecules is becoming an area of active interest. The evolutionary experimental process is continuing from atoms to simple-to-complex molecules, hand-in-hand with the development of ultrafast intense lasers and superior experimentation. Such investigations are performed not only for theoretical reasons [e.g. Sanderson *et al*, 1997; Cornaggia *et al*, 1995] but also because FLMS has considerable potential as a sensitive analytical technique as reported in chapters 4 and 5 and in, for example, the following references [Smith *et al*, 1998a, 1998b, 1998c; Ledingham *et al*, 1998a, 1998b, 1997, 1996/7, 1995/6,

1995a, 1995b; Kilic *et al*, 1997; Kosmidis *et al*, 1997; He *et al*, 1997a, 1997b, 1996; Willey *et al*, 1997; Weickhardt *et al*, 1997; DeWitt *et al*, 1997, 1995; Levis *et al*, 1996; Schutze *et al*, 1996, 1995; Purnell *et al*, 1994]. Additionally there is the potential for such experimental work to efficiently generate stable molecular high harmonics as a source of fast, intense, tuneable and coherent radiation.

§6.0.3 Aims

Following from the previous chapter, the present centres on a subsequent higher power application of FLMS to aromatics. The phenomenon of multiple ionisation is further discussed with the associated mechanism of ionisation being considered as well as speculation on the likely pathways for the production of the observed ions.

Thus far, soft ionisation has been possible and unambiguous significant double ionisation (second most intense peak behind the parent) observed for the three aromatics benzene, toluene and naphthalene at 750 nm, with the onset of the doubles at a threshold intensity of $\leq 10^{14}$ W cm^{-2}. Triple ionised naphthalene has appeared at $\sim \geq 10^{14}$ W cm^{-2}. As yet triples have not been observed for benzene and toluene up to a maximum laser intensity of 4×10^{14} W cm^{-2}. Consequently this chapter focuses on benzene and toluene. Deuterated benzene (C_6H_5D) is also studied, primarily to further quantitatively isolate unambiguous multiply charged ions.

To such ends, the laser intensity is extended from chapter 5 and now peaks at 3×10^{15} W cm^{-2} (c.f. 4×10^{14} W cm^{-2}) at a higher wavelength of 790 nm (c.f. 750 nm). These alterations attempt to create conditions which allow the phenomenon of multiple ionisation to become more prevalent than previously found, while maintaining dominant parent ion peaks, and perhaps further reducing molecular dissociation.

UV wavelength FLMS is not employed in the present chapter because of its increased associated fragmentation, significantly reduced multiply ionised peaks and slightly decreased peak laser intensities, compared to IR wavelength FLMS.

§6.1 Experimental

The experimental set-up is similar to that reported in chapters 4 and 5 – see sections *4.1.2* and *5.1* respectively. It consists of a femtosecond laser system and a linear time-of-flight mass spectrometer (TOF). An extensive laser refurbishment has taken place. The essential features of this remodelling are described in chapter 3, *§3.1.2*.

Suffice it to say, a 50 fs argon-ion laser pumped a titanium-sapphire oscillator to produce a 790 nm, 9 nJ pulse. A chirped amplification system amplified this energy to the mJ level before the pulses were drawn out to about 200 ps in an all-reflective stretcher comprising of a grating (1500 lines per mm) and a concave mirror (radius of curvature 730 mm). Further amplification then occurred in a multi-pass amplifier. The resultant beam was then re-injected into the chirped amplifier to boost its energy to approximately 2 mJ, after which it was compressed to 50 fs using a pair of 1500 lines per mm gratings in a parallel arrangement. The output of the laser system was monitored using a single shot auto-correlator. The resultant laser pulse of wavelength 790 nm and width 50 fs, had a maximum focused beam intensity of the order of 3×10^{15} W cm^{-2} in the interaction region.

The TOF was of linear design based on a Wiley-McLaren model. It was coupled to, and operated with, the femtosecond system in the same manner as previously discussed.

§6.2 Results and Discussion

Several methods can be used to confirm the presence of multiply ionised peaks in mass spectra recorded using FLMS. Such techniques are outlined below.

i) A multiply ionised peak may appear at an unambiguous m/z ratio where single charged ions are unlikely to exist. This can either be in a region of the mass spectra between, for example, neighbouring carbon groups (C_x and C_{x+1}) and/or at an m/z ratio falling at a half integer value. Furthermore, if an envelope of peaks

exist, some of which fall at m/z ratios of half mass numbers, then the adjacent peaks falling at m/z ratios of whole numbers are likely to have a multiply ionised component.

ii) A deuterated molecule (a molecule with a hydrogen atom replaced with deuterium) may be used to produce an unambiguous double ionised parent with m/z equal to a half integer value. Comparing results with the original molecule can facilitate further identification of peaks and peak abundances – see *§ 6.2.2* for an example and further explanation.

iii) For a molecule with X carbon atoms, a $^{13}C/^{12}C$ isotopic ratio will naturally exist with ^{13}C present at an approximate abundance of $X \times 1.1$ %. Therefore multiply ionised parent ions can be confirmed by measuring the consistency, or otherwise, of such a ratio in going from the single ionised parent plus satellite peak to the multiple ionised parent plus satellite peak. This method has been applied in chapters 4 and 5.

iv) A plot of ion yield against laser intensity may be instructive in identifying multiples due to the higher ionised species possibly having a greater gradient than single ionised species.

v) Wavelengths in the IR and UV will produce differing amounts of fragmentation and multiple ion production. Despite increased dissociation using UV FLMS, the multiply ionised peaks are substantially diminished or absent compared to corresponding peaks in the IR spectra. If such peaks were to be attributed to fragmentation and not multiple ionisation then one would expect them to be minimal in the IR and strong in the UV. This is not the case – see *§5.2.1.*

vi) The peaks appear to be narrower in the multiply compared to the singly ionised case.

§6.2.1 Toluene

The mass spectrum for toluene is shown in figure 6b recorded at a wavelength of 790 nm, a pulse width of 50 fs and a laser intensity of 3×10^{15} W cm^{-2}. The spectrum is very similar to the corresponding figure, figure 5c, in the fifth chapter at a lower wavelength (750 nm) and intensity (3.5×10^{14} W cm^{-2}). The essential features of a dominant parent ion, minimal fragmentation and a strong presence of a double ionised C_7H_8 ion are concurrent. The double ionised envelope mentioned in chapter 5 is expanded in greater detail in the present chapter.

Clear evidence can be seen for the unambiguous presence of $C_7H_8^{2+}$ and surrounding multiple satellites. Such peaks are shown in the expanded window of figure 6b, some of which fall at half-mass numbers. The isotopic ratio of $C_6{}^{13}CH_8^+$ / $C_7H_8^+$ (the ratio of the peaks at m/z = 93 to m/z = 92) is approximately 8 %. This is as expected for a molecule containing seven carbon atoms (7 × 1.1 %) and is precisely found by measuring the relevant peak areas. The peaks at m/z =46.5 and m/z =46 have a similar isotopic ratio which is indicative of them being strongly in concert with m/z = 93 and m/z =92. Further confirmation of an envelope of double peaks comes from the fact that the peaks in the inset correspond to an area of the spectrum between the C_3H_n and C_4H_n fragment groups, where single ionised fragments cannot exist. In this respect, toluene is a particularly suitable molecule in which to study double ionisation.

It is worth noting that all the labelled peaks in the inset of figure 6b will have a small isotopic abundance of ^{13}C at a percentage similar to the above amount of 8 %. It is not practical to measure such ratios in the smaller peaks. This is a general statement applying to all the molecules studied.

Triple ionised toluene ($C_7H_8^{3+}$) is not observed in the laser intensity range up to 3×10^{15} W cm^{-2}. Therefore, studying toluene under the present experimental parameters compared to those employed in chapter 5, has yielded similar results, although the multiply charged aspect is being considered in greater detail here.

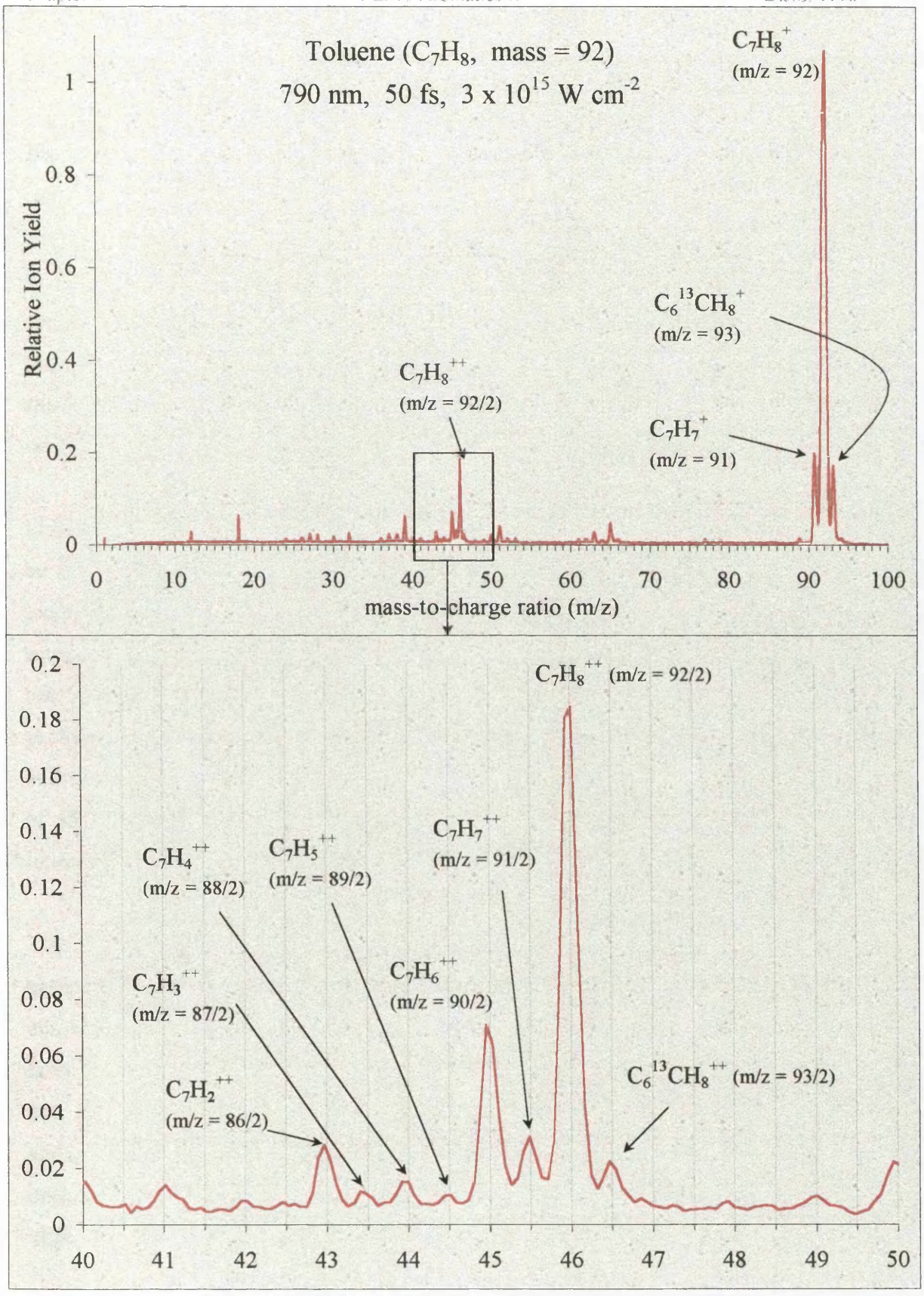

Figure 6b High Intensity Toluene Mass Spectrum with inset at double ionisation region

§6.2.2 Benzene and Deuterated Benzene

The mass spectra of benzene and deuterated benzene are shown in figures 6c and 6d respectively recorded under similar experimental conditions to toluene. The peak laser intensity for benzene is slightly lower (1.5×10^{15} W cm^{-2}) than for deuterated benzene (3×10^{15} W cm^{-2}). The spectra are consistently normalised such that quantitative comparisons can be made between them. This normalisation also extends to toluene shown in figure 6b. Note the minimal fragmentation and predominant parent ion in both spectra, consistent with the benzene spectra reported in chapter 5 (figure 5b) at a lower wavelength and intensity, and concurrent with general FLMS findings to date.

Identification of the labelled peaks in the right hand side insets of figures 6c and 6d can be found in table 6.i on page 122. Naming of the ion peaks is achieved using the techniques (i)-(iv) outlined on pages 115/116. Although a UV investigation was not actually performed in the present case, in light of results in chapter 5, technique (v) was not completely neglected. A detailed explanation of the analysis of the envelopes of ion peaks presented for benzene (figure 6c) and deuterated benzene (figure 6d), is given below. This includes in-depth description of how the systematic peak-by-peak labelling of all the ions was achieved, together with the methods used to estimate the relative intensities of coincident species.

This coincidence of different peaks is worthy of further comment. For two or more ions having the same m/z ratio – within the resolution limits of the spectra - and therefore contributing to one peak, the abundance of each component is estimated and indicated in table 6.i, as stated above. Several coincident permutations are possible of different single and multiply charged, and deuterated and non-deuterated ions appearing at the same apparent m/z ratio. The resolution of the mass spectra is not sufficient to separate out an undeuterated from an equivalent deuterated peak, whose m/z ratios are very slightly different.

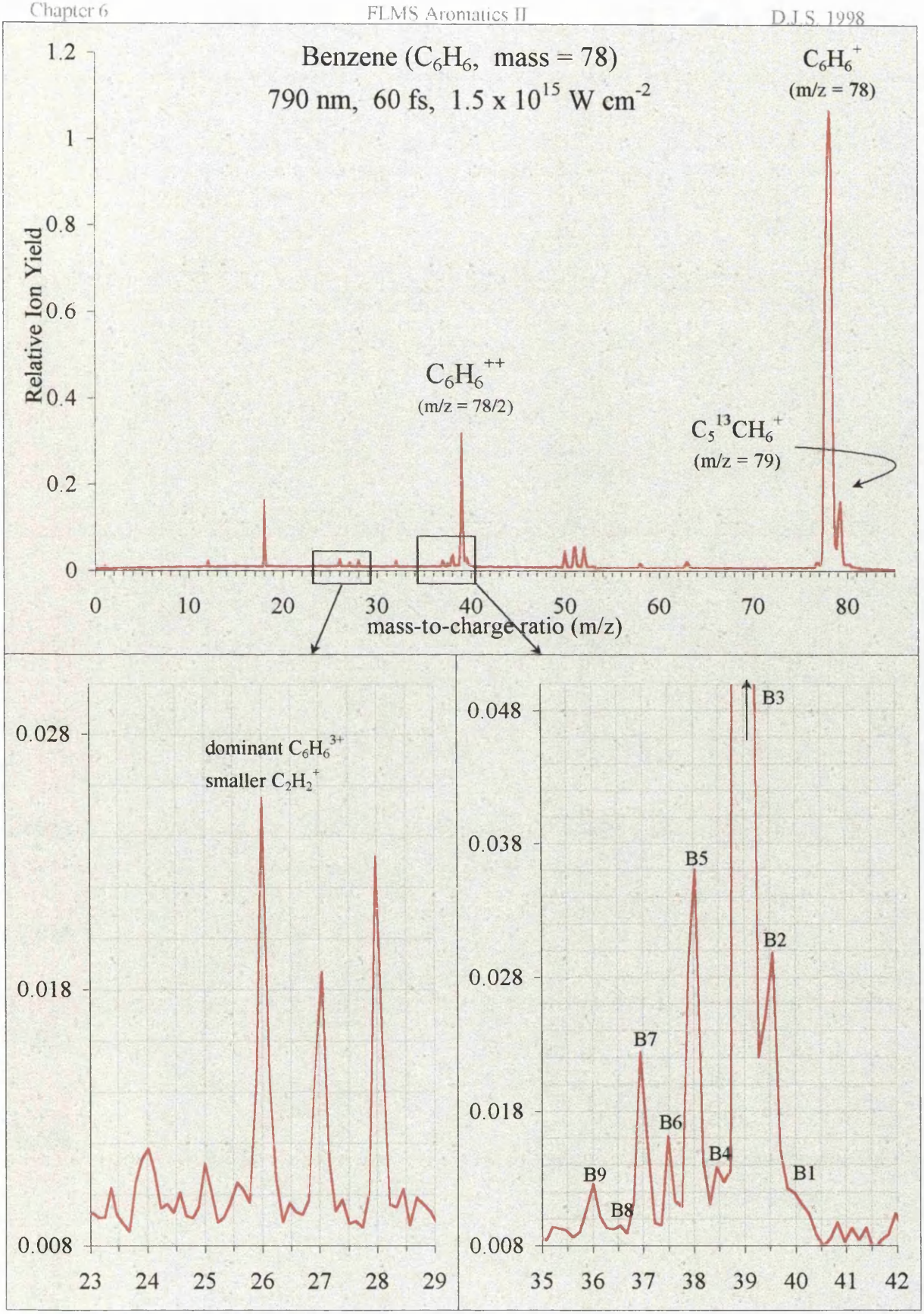

Figure 6c High Intensity Benzene Mass Spectrum with insets at multiply ionised regions

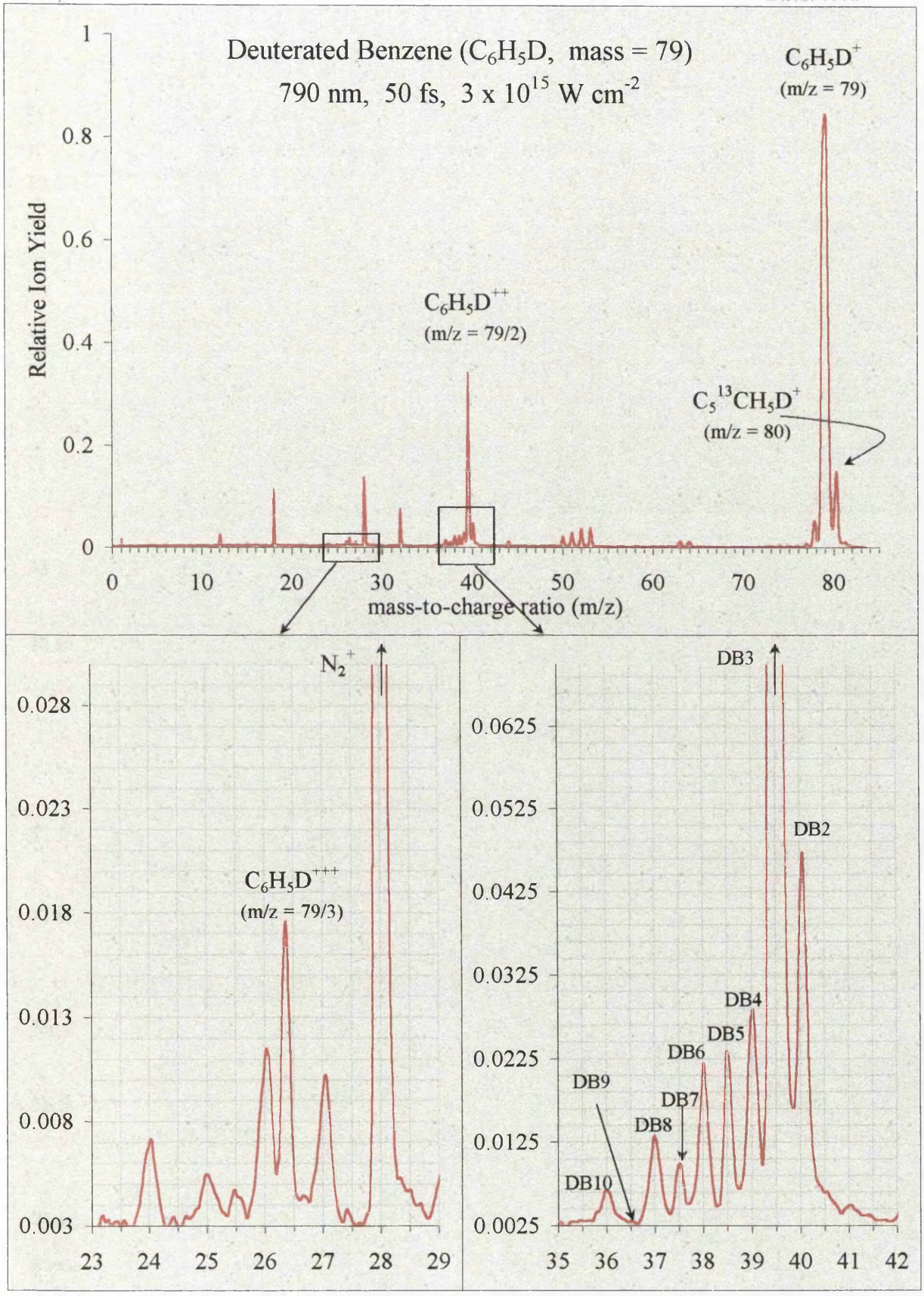

Figure 6d High Intensity Deuterated Benzene Mass Spectrum with insets at multiply ionised regions

m/z ratio	peak	Benzene (C_6H_6)	peak	Deuterated Benzene (C_6H_5D)
40.0	B1	small $C_3H_4^+$	DB2	60% $C_5{}^{13}CH_5D^{2+}$ 40% ($C_3H_2D^+$, $C_3H_4^+$) [$C_3H_2D^+ > C_3H_4^+$]
39.5	B2	100% $C_5{}^{13}CH_6^{2+}$	DB3	100% $C_6H_5D^{2+}$
39.0	B3	90% $C_6H_6^{2+}$ 10% $C_3H_3^+$	DB4	50% $C_6H_4D^{2+}$ 50 % ($C_3H_3^+$,C_3HD^+, $C_6H_6^{2+}$) [$C_3H_3^+ > C_3HD^+ > C_6H_6^{2+}$]
38.5	B4	100% $C_6H_5^{2+}$ but small	DB5	60% $C_6H_5^{2+}$ 40% $C_6H_3D^{2+}$
38.0	B5	65% $C_6H_4^{2+}$ 35% $C_3H_2^+$	DB6	70% $C_6H_2D^{2+}$ 30% ($C_6H_4^{2+}$, $C_3H_2^+$, C_3D^+) [$C_6H_4^{2+}/C_3H_2^+$ 65% to 35 % with small C_3D^+]
37.5	B6	100% $C_6H_3^{2+}$	DB7	small $C_6H_3^{2+} > C_6HD^{2+}$
37.0	B7	$C_3H^+ \geq C_6H_2^{2+}$	DB8	$C_3H \geq C_6H_2^{2+}$ and C_6D^{2+} negligible
36.5	B8	negligible	DB9	negligible
36.0	B9	100% C_3^+	DB10	100% C_3^+

Table 6.i Benzene and Deuterated Benzene Peak Identification. Peak types and abundances are indicated. This table cross-references with figures 6c and 6d, and the detailed calculations are explained in the text.

Double Ionised Species

Clear evidence exists in favour of a double ion production. Doubles were also observed in chapter 5 for benzene. The double ionised envelopes containing the parent 2^+ species and surrounding satellites are expanded in the right hand side insets of figures 6b and 6c for benzene and deuterated benzene respectively. They can be seen to be similar.

An important point to note when dealing with the double ionised envelopes is that an ionic peak from an undeuterated molecule has an equivalent peak in the corresponding deuterated molecule by replacing a hydrogen with a heavier deuterium atom. This works out as an increase in m/z ratio of 0.5 for the double peaks. The labelling system portrays equivalent peaks with equal numbers. For example the double ionised benzene molecule ($C_6H_6^{2+}$ labelled as B3) located at an m/z ratio of 39 in figure 6b has a concordant deuterated peak ($C_6H_5D^{2+}$ labelled as DB3) at m/z = 39.5 in figure 6c.

Another point to note is it that the size of the normalised single and double parent ions for the two molecules are approximately equal. This is a key fact in the analysis because it allows direct quantitative comparisons of ionic intensities.

Additionally, the system employed to label the peaks is a model based on an assumption of so-called concordant peaks having similar probabilities of production in both molecules.

The numbers in bold correspond to particular mass-to-charge ratios for benzene (B) and deuterated benzene (DB). The peaks are portrayed matching the general order of analysis.

39.5 DB Unambiguously $C_6H_5D^{2+}$.

39.0 B This peak could either be $C_6H_6^{2+}$ or $C_3H_3^+$. However the intensity of 39.0 B matches, or is just greater than the intensity of unambiguous 39.5 DB (~ 10 % greater). Therefore it follows that 39.0 B is predominantly the

double ionised component. This is consistent with the fact that the peak at 39.0 B is considerably greater than any other nearby peak. A 90 % to 10% mixture seems reasonable for $C_6H_6^{2+}$ and $C_3H_3^+$ respectively.

40.0 B Very small presence of $C_3H_4^+$.

39.5 B Unambiguously $C_5{}^{13}CH_6^{2+}$.

40.0 DB This peak could have contributions from the double ionised ^{13}C DB molecule ($C_5{}^{13}CH_5D^{2+}$) or the single ions $C_3H_2D^+$ and $C_3H_4^+$. The double ionised unambiguous undeuterated equivalent peak at 39.5 B has an approximate intensity of 0.0282. Therefore it is expected that the double component of the concordant deuterated peak will also be 0.0282. But the height of this 40.0 DB peak is ~ 0.0475. Therefore the single ionised component of the peak is given by 0.0475 – 0.0282 = 0.0193 i.e. $C_3H_2D^+$ and $C_3H_4^+$ contribute this intensity. This is 60 % double and 40 % single components. $C_3H_2D^+$ is likely to be greater than $C_3H_4^+$ due to a more likely "symmetric" fragmentation of $C_6H_5D^+$ to $C_3H_3^+$ and $C_3H_2D^+$. Also $C_3H_4^+$ is small in benzene (40.0 B).

38.5 B Unambiguously $C_6H_5^{2+}$.

39.0 DB The intensity of 39.0 DB is 0.0285 and the intensity of the equivalent undeuterated peak at 38.5 B ($C_6H_5^{2+}$) is 0.014. Therefore the concordant double component, $C_6H_4D^{2+}$, of 39.0 DB is around 0.014. A simple subtraction gives the intensity of the other coincident 39.0 DB components to be 0.0145. These could be $C_3H_3^+$, C_3HD^+ or $C_6H_6^{2+}$. Due to symmetry, $C_3H_3^+$ is more likely than C_3HD^+ and will have the same intensity as $C_3H_2D^+$ located at DB 40. And note that C_6H_6 is present as a 2 % quantity in C_6H_5D. This gives the approximate abundances in table 6.i. Due to the somewhat complex nature of this conclusion, and in light of uncertainties, a quantitative analysis is not fully performed.

38.5 DB Either $C_6H_3D^{2+}$ or $C_6H_5^{2+}$. Predominantly the former since $C_6H_5^{2+}$ is small in benzene. Observing the size of $C_6H_5^{2+}$ in benzene (38.5 B) as ~ 0.014, one can conclude that it may have the same intensity in 38.5 DB.

The size of the 38.5 DB peak is ~ 0.0235. This leads to the percentages in the table.

38.0 B 38.0 B intensity = 0.036. This can either be $C_6H_4^{2+}$ or $C_3H_2^+$. Deuterated equivalent ($C_6H_3D^{2+}$) at 38.5 DB = 0.0235 intensity which is 65% $C_6H_3D^{2+}$. Therefore the undeuterated equivalent in 38.0 B ($C_6H_4^{2+}$) is 65% present.

37.5 B Unambiguously $C_6H_3^{2+}$.

38.0 DB Intensity of undeuterated equivalent ($C_6H_3^{2+}$, 37.5 B) = 0.016. Intensity of 38.0 DB = 0.0225. Therefore 38.0 DB $C_6H_2D^{2+}$ intensity = 0.016 to leave $C_3H_2^+$, C_3D^+ and $C_6H_4^{2+}$ contributing 0.0065 to the peak intensity. It is likely that $C_3H_2^+$ is greater than C_3D^+ with ratio of $C_6H_4^{2+}$ to $C_3H_2^+$ being similar to that found in benzene at 38.0 B. This gives the component intensities shown in table 6.i.

37.5 DB C_6HD^{2+} or $C_6H_3^{2+}$. Small amounts of each, but the latter more likely due to symmetry considerations.

37.0 B Can either be C_3H^+ or $C_6H_2^{2+}$. Deuterated equivalent C_6HD^{2+} (37.5 DB) small, therefore C_3H^+ is perhaps more likely.

36.5 B No peak.

37.0 DB This can either be C_3H^+, $C_6H_2^{2+}$ or C_6D^{2+}. But there is no double concordant peak for benzene (36.5 B). Therefore, the deuterated equivalent C_6D^{2+} (37.0 DB) can be taken as zero. Similar to 37.0 B, C_3H^+ perhaps just greater than $C_6H_2^{2+}$.

36.5 DB No peak.

36.0 B C_3^+ or C_6^{2+}. C^{3+} likely be the only peak present.

36.0 DB C_3^+ or C_6^{2+}. Due to zero presence of double peak at neighbouring 36.5 DB, then peak taken as total C_3^+. This uses the argument that the presence of unambiguous double ionised components at half-mass peaks are suggestive of double activity in the neighbouring peaks.

Now let's consider the isotopic ratio approach to confirm some of the above findings. Consider benzene first. The $^{13}C/^{12}C$ ratios for the single parent (m/z = 79 to m/z = 78)

and double parent ions (m/z = 39.5 to m/z = 39) are consistent at a value of approximately 7% which is implicative of the peak at m/z = 39 being dominantly $C_6H_6^{2+}$, in agreement with the relevant figures in table 6.i. The peak at m/z = 39.5 is of course 100 % $C_5{}^{13}CH_6^{2+}$.

Secondly consider deuterated benzene. At first glance the isotopic ratios of $C_5{}^{13}CH_5D^+$ / $C_6H_5D^+$ (m/z = 80 to m/z = 79) and $C_5{}^{13}CH_5D^{2+}$ / $C_6H_5D^{2+}$ (m/z = 40 to m/z = 39.5) may not seem in concert at values of approximately 7 % and 12 % respectively. One expects a value of 7 % for a molecule containing six carbon atoms. The additional percentage in the double ionised case is due to more than one peak at the same m/z ratio. The ^{13}C presence is still expected to be 7 %. The peak at m/z = 39.5 is unambiguously $C_6H_5D^{2+}$ as noted above. Therefore the peak at m/z = 40 must have 5 % (12 – 7) abundant coincident species with the 7 % abundant $C_5{}^{13}CH_5D^{2+}$. Possible species are $C_3H_2D^+$ and $C_3H_4^+$ responsible for around 40 % (5/12 × 100) of the ion peak at m/z = 40. This is in agreement with the intensities stated in table 6.i and explained above.

Triple Ionised Species

Triple ionised parent ions can be observed for benzene and deuterated benzene. $C_6H_6^{3+}$ and $C_6H_5D^{3+}$ can be seen in the left hand side insets of figures 6c and 6d respectively at the given laser intensities. The visible nitrogen contaminant at m/z = 28 which sometimes, along with water, proved very difficult to eliminate, should be ignored. These peaks did not materially affect the results.

For deuterated benzene, the triple ion is unambiguous at m/z = 26.3 (79/3). Using this fact and looking at the ionic yields for benzene at m/z = 26 (peak intensity ~ 0.0256) and deuterated benzene at m/z = 26.3 (peak intensity ~ 0.017) one can conclude that the benzene peak is predominantly $C_6H_6^{3+}$ (~ 65 %) with lesser contribution from $C_2H_2^+$. One can also observe the single ion at m/z =26 for deuterated benzene and expect a similar single component for benzene.

Laser Intensity Dependences

It may be possible to further confirm the appearance of multiples by plotting the intensities of the main mass peaks as a function of the laser intensity. Figure 6e shown on the next page, illustrates an intensity dependence for benzene and deuterated benzene.

Single, double and triple parent ions are shown as well as a few typical single fragments from the mass spectra. The graphs are consistently normalised for quantitative comparisons. The ion curves are multiplied by various numbers in order to separate them out for ease of viewing, although their general intensity order as seen in the plots is correct. Such multiplication was done prior to drawing the figure. To get the actual normalised yield simply divide by the appropriate number.

It appears that multiple ion peaks have a greater gradient and therefore a stronger laser intensity dependence than single peaks. Similar effects have been observed for double parent ions in benzaldehyde (chapter 4 - figure 4g) and benzene, toluene and naphthalene (chapter 5 - figure 5e) at lower laser intensities. The single charged ions seem to follow the slope of the parent ion. The different dependences may be taken as tentative evidence for multiple ion production. In terms of sequential ionisation, one would expect a double charged state to appear as the single charged state tends towards saturation, and likewise a triple charged state to appear when the double begins to volume saturate [Ledingham *et al*, 1998b]. Certainly the figure at least illustrates the initial appearance of the single parent ahead of the double parent which is in turn ahead of the triple parent ion.

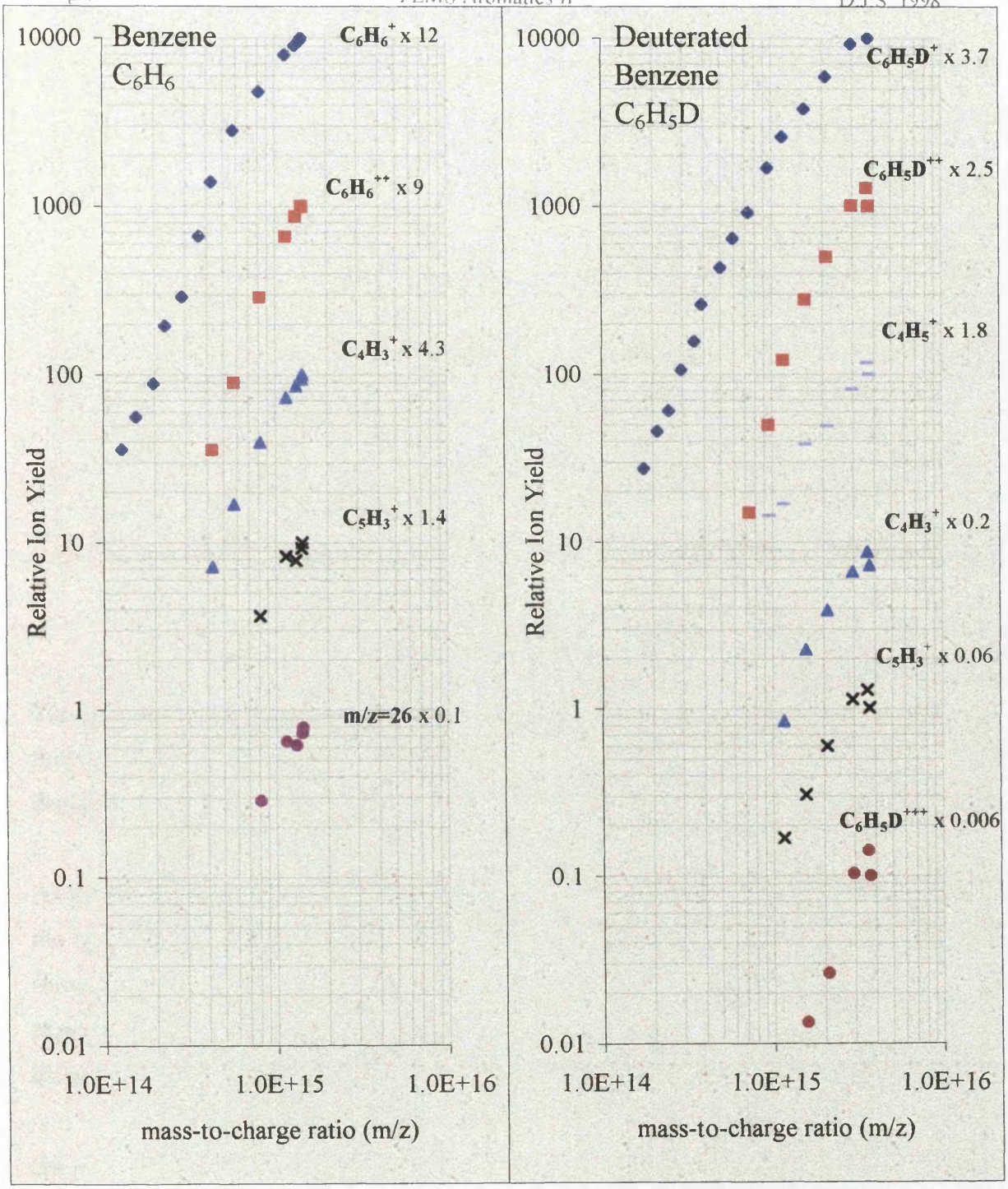

Figure 6e Benzene and Deuterated Benzene Laser Intensity Dependences for Single and Multiply Ionised Masses at 790 nm and 50 fs

Figure 6f confirms the different dependences for the single and multiple fragments. Deuterated benzene is taken as an example.

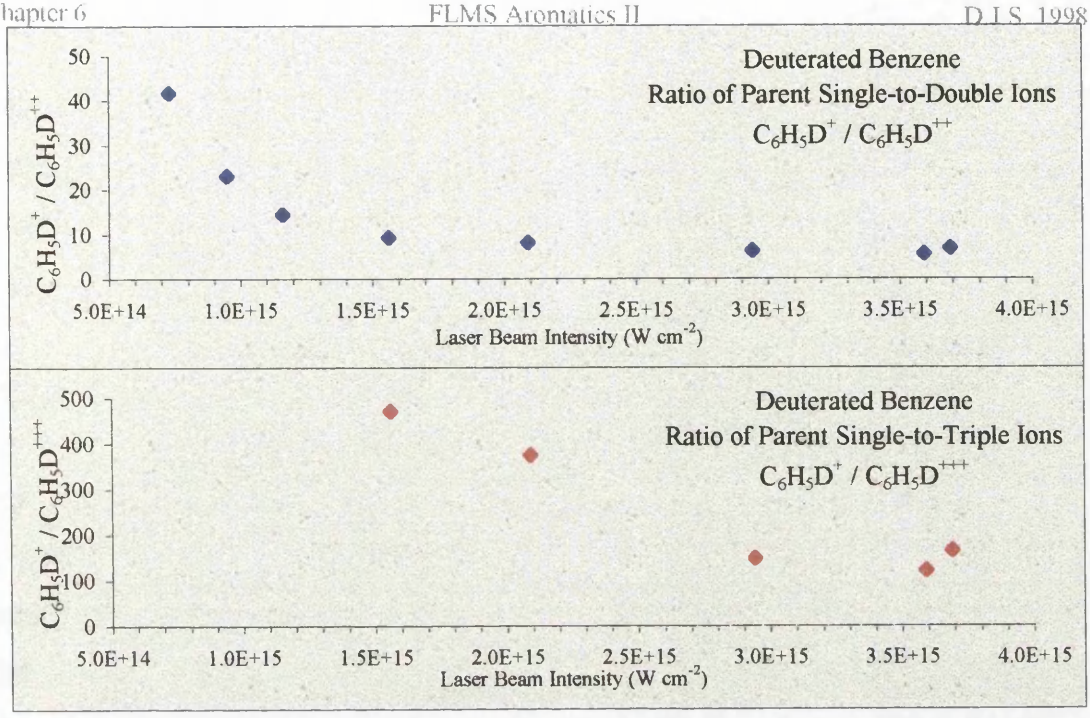

Figure 6f Single-to-Multiple Parent Ratio Dependences at 790 nm and 50 fs

The graph illustrates that the ratios of single to double/triple parent ion peaks are strong functions of laser intensity, particularly in the lower intensity range, after which the dependences levels out. This flattening of the curves mainly represents saturation effects.

As previously stated, the present laser intensity dependences show concurrent features to the corresponding plots in chapters 4 and 5 (figures 4g and 5e respectively). It has been shown that the intensity dependence can be instructive in a number of ways of analysing experimental results. Similar conclusions can be drawn presently compared to the discussions based on the figures in the previous chapters mentioned above.

An important point to note concerns the intensity at which the onset of saturation occurs – the point at which the rate of change ion yield curves slows as the laser intensity increases. Comparing the data of chapters 4, 5 and 6, it is evident that saturation of the aromatic species is not singly a function of laser intensity. Chapters 4 and 5 portray this effect beginning around 10^{14} W cm^{-2} while presently saturation begins at approximately 10^{15} W cm^{-2}. Clearly other factors influence the process. This is due to different experimental conditions. Examples may be slightly different beam spot focal positions

with respect to the sample species and varying beam profiles including differing wing dynamics. Additionally, the appearance of double charged components occurred at a threshold of ~ 2 × 10^{14} W cm^{-2}, whereas in chapter 5, the threshold intensity was approximately ≤ 10^{14} W cm^{-2}, although this difference is small.

§6.2.3 Ionisation Mechanisms and Pathways for Single and Multiple Ion Production

UV resonant laser irradiation of benzene and related aromatics in the nanosecond regime at laser intensities from approximately 10^{7} – 10^{10} W cm^{-2} has been pioneered by the group lead by Schlag and Boesl [Boesl, 1991 and references therein; Dietz *et al*, 1982]. The relevant background has been discussed in the introduction to the previous chapter. The experimental results for such medium mass molecules have indicated that soft ionisation is possible by strictly controlling the laser parameters, particularly intensity, otherwise significant dissociation occurs. After absorption of about four UV photons the C_4, C_3, C_2, fragment ion groups were formed. These ions absorbed further photons in a ladder-switching regime until finally C^+ was formed. At the higher laser intensities, the smaller fragments were produced in great quantities and the parent ion was not visible or very small. The results indicated that the excitation did not proceed up the ionisation ladder of the neutral molecule and no multiply charged ions were detected.

The present results at laser intensities up to the order of 10^{15} W cm^{-2} indicate that all of these ionic fragmentation routes can largely be bypassed, neutral molecules and fragments can be ionised and ionising molecular states with typical lifetimes of 100 fs can be populated [Boesl *et al*, 1980]. Since the parent peak is still the strongest peak at the laser intensities used in the current experiment, the ladder-switching fragmentation pathways reported for the nanosecond regime are no longer taking place to any significant degree.

Further evidence exists in support of this. The appearance potentials for double ionised benzene, toluene and naphthalene are 26 eV, 24.5 eV and 22.8 eV respectively [Dorman *et al*, 1960] and 26 eV for C^+ [Zandee *et al*, 1979]. The fact that the yield of double

ionised parents is significantly greater than the carbon ions in the relevant mass spectra for the three molecules in this and the previous chapter, suggests that nanosecond routes are being bypassed by the femtosecond irradiation. A dominant ladder-climbing mechanism is at work with small dissociation appearing via the parent continuum. This result is expected when using the technique of FLMS as shown in chapters 4 and 5, and is one of the main themes of the present study.

The idea that single ionisation of atoms/molecules under short pulsed intense laser irradiation occurs at the beginning of the pulse ahead of multiple ionisation, has been supported by Cornaggia *et al* [1995] and Lambropolous [1985]. This explanation appears to be concordant with the present results, that is a fast sequential process occurring.

The first ionisation level of the aromatic molecule is reached early on in the pulse profile, that is in the lower intensity wings of the beam. A small amount of fragmentation takes place from the parent species as it successively climbs through the first, second and third ionisation levels as the pulse evolves. When these multiply charged ion states are reached, they may produce further double charged entities by shedding neutral hydrogen atoms. Considering benzene for example, this may occur in the following way:

$$C_6H_6^{2+} \rightarrow C_6H_5^{2+} + H$$

$$\rightarrow C_6H_4^{2+} + 2H$$

$$\rightarrow C_6H_3^{2+} + 3H$$

$$\rightarrow C_6H_2^{2+} + 4H$$

$$\rightarrow C_6H^{2+} + 5H$$

$$\rightarrow C_6^{2+} + 6H$$

A similar dissociation process of the triple charged parent state could also occur.

The question of multiphoton versus tunnelling ionisation was discussed in the introduction. Presently, Keldysh values for the molecules benzene and toluene are found to be between 0.1 and 0.2. This is well into the tunnelling regime.

Coulomb explosions in the region of inter-nuclear distances were also discussed which described the presence of multiply charged atoms and small molecules during intense laser irradiation. In the current case, although C^{2+} is seen which can be construed as evidence of coulomb explosions, it is a very small feature. The multiply charged ions observed must have lifetimes at least as long as the flight times in the TOF (~ tens of μs) and any dissociation, particularly the shedding of hydrogen atoms, seems to be a rather gentle process similar to ordinary photo-dissociation. It appears to be somewhat similar to bond-softening [Bucksbaum et al, 1990] rather than coulomb explosions in the present laser intensity region for the molecules studied.

§6.3 Conclusions

FLMS has been applied to the molecules benzene, deuterated benzene and toluene at a wavelength of 790 nm, pulse widths around 50 fs and laser intensities up to 3×10^{15} W cm^{-2}. This, and other techniques, has allowed analysis to be performed on multiply charged parent species and a surrounding envelope of multiple components, aided by limited molecular fragmentation in the IR wavelength range.

The essential features of the FLMS mass spectra have been investigated and found to be similar to characteristics reported in chapters 4 and 5. FLMS goes a long way to controlling chemical dynamics. Nanosecond associated pathways have been largely bypassed by the femtosecond irradiation. Dominant parent ions have been observed with minimal associated fragmentation. This included single and double ionisation for toluene and single, double and triple ionisation for benzene and its deuterated counterpart. Exclusive parent ions were achieved around 10^{14} W cm^{-2}. Envelopes of multiply ionised peaks around the parent multiply charged ions were a consistent feature in the mass spectra, particularly in the double ionisation region. Deuterated benzene assisted the

identification of ion peaks in the benzene spectra with the appearance of unambiguous deuterated parent multiples $C_6H_5D^{2+}$ and $C_6H_5D^{3+}$ at m/z ratios where single fragment ions could not exist. This allowed semi-quantitative analysis on the intensities of coincident species. Triple ionisation had not previously been observed for benzene in the lower intensity range of chapter 6 (~ 10^{14} W cm^{-2}).

More quantitative peak labelling could be performed using a system which yielded higher resolution ion peaks, such that the deuterated peaks and equivalent non-deuterated peaks are separated i.e ßH$_2$ and ßD whose masses are different but not identified as so in the current mass spectra. One possibility is replacing the linear TOF with a magnetic sector mass spectrometer.

It has been suggested that the mechanism of ionisation is predominantly sequential in that the pulse width profile significantly influences the process. The evolution of the pulse from its lower intensity wings to peak intensity at its midpoint is important. Multiphoton ionisation may initially occur, giving way to a tunnelling process as the intensity increases. To avoid saturation by the multiphoton process, a sharp rise in the pulse intensity profile is advantageous. It is thought that this is achieved presently. Also, the lowest values of the Keldysh parameter have been found to be around 0.1 - 0.2, well within the tunnelling or OTBI regime. One can therefore conclude that tunnelling has a contribution to the ionisation process.

Field ionisation at critical inter-nuclear distances followed by coulomb explosions may be less important in explaining the results for laser irradiation of medium mass molecules compared to small molecules at the laser intensities investigated within. Primary evidence for this comes from only a weak presence of multiply charged atoms in the mass spectra. It is evident that further theoretical study has to be performed together with concise experimental application.

Finally, it is worth noting that in terms of analysis, the results of chapters 5 and 6 show that it can best be performed in lower intensity regions, specifically around the region just

less than 10^{14} W cm^{-2} for general detection. Specifically, one may aim at analysis in which exclusive parent ions are formed. This is possible using intensities in the lower regions of the ranges studied in chapters 5 and presently. It is, however, not just a function of intensity. Other parameters have a role. The goals of the experiment are reflected by the choice of laser parameters. For example, multiple ionisation requires a high laser intensity, perhaps higher than the optimum analytical intensity.

Increasing the intensity further beyond the present value of 3×10^{15} W cm^{-2} would allow an investigation into whether quadruple charged ions could be detected for benzene and naphthalene, and at least triple charged ions for toluene. Increasing the intensity further still may enter the situation into a relativistic regime in which the external electric field becomes much larger than that which the electron senses from the nucleus. Protopapas *et al* [1997] reported that this may occur in the region of 10^{18} W cm^{-2}.

Very recently, an experiment has been performed by the author for toluene at a laser intensity of 3×10^{16} W cm^{-2}, details of which can be found on the next page in appendix 1. The implications of the findings are considered.

Appendix 1

This appendage reports on a very recent investigation of toluene under the same conditions as detailed in this chapter except that the beam intensity has been raised to 3×10^{16} W cm^{-2} representing an order of magnitude increase. The corresponding mass spectrum is shown in figure 6g with expanded insets at local areas of interest.

A triple ionised parent ion, $C_7H_8^{3+}$ (m/z = 30.6 [92/3]) is not conclusively discernible above the background noise, as the left hand side inset of figure 6g demonstrates. Clearly, the pathway leading to the production of a significant stable triple ionised parent is difficult to access, even at such high laser intensities. This result certainly requires further treatment and is in contrast to the other aromatic molecules considered thus far, namely benzene and deuterated benzene with a triple present around 10^{15} W cm^{-2} and 10^{14} W cm^{-2} for naphthalene. Further triples have been observed for a number of other polyatomic molecules by the Glasgow group, and are included in the next chapter.

The double ionised features discussed in figure 6b for toluene are concurrent with the present features in figure 6g.

However, a notable difference in going from the spectrum recorded at 10^{15} to 10^{16} W cm^{-2} is the increased production of C^+ and the appearance of several atomic multiples, particularly of carbon. Figure 6h shows the lower mass regions of toluene's spectra for 3×10^{16} W cm^{-2} and 3×10^{15} W cm^{-2} respectively. The difference in the spectra is significant. Several multiply ionised components of carbon are clearly visible for the higher order intensity. It is feasible that at these higher intensities, coulomb explosions may be taking place, a phenomenon which was thought not to occur for medium mass molecules in the laser intensity regions considered in chapter 5 and the main section of chapter 6.

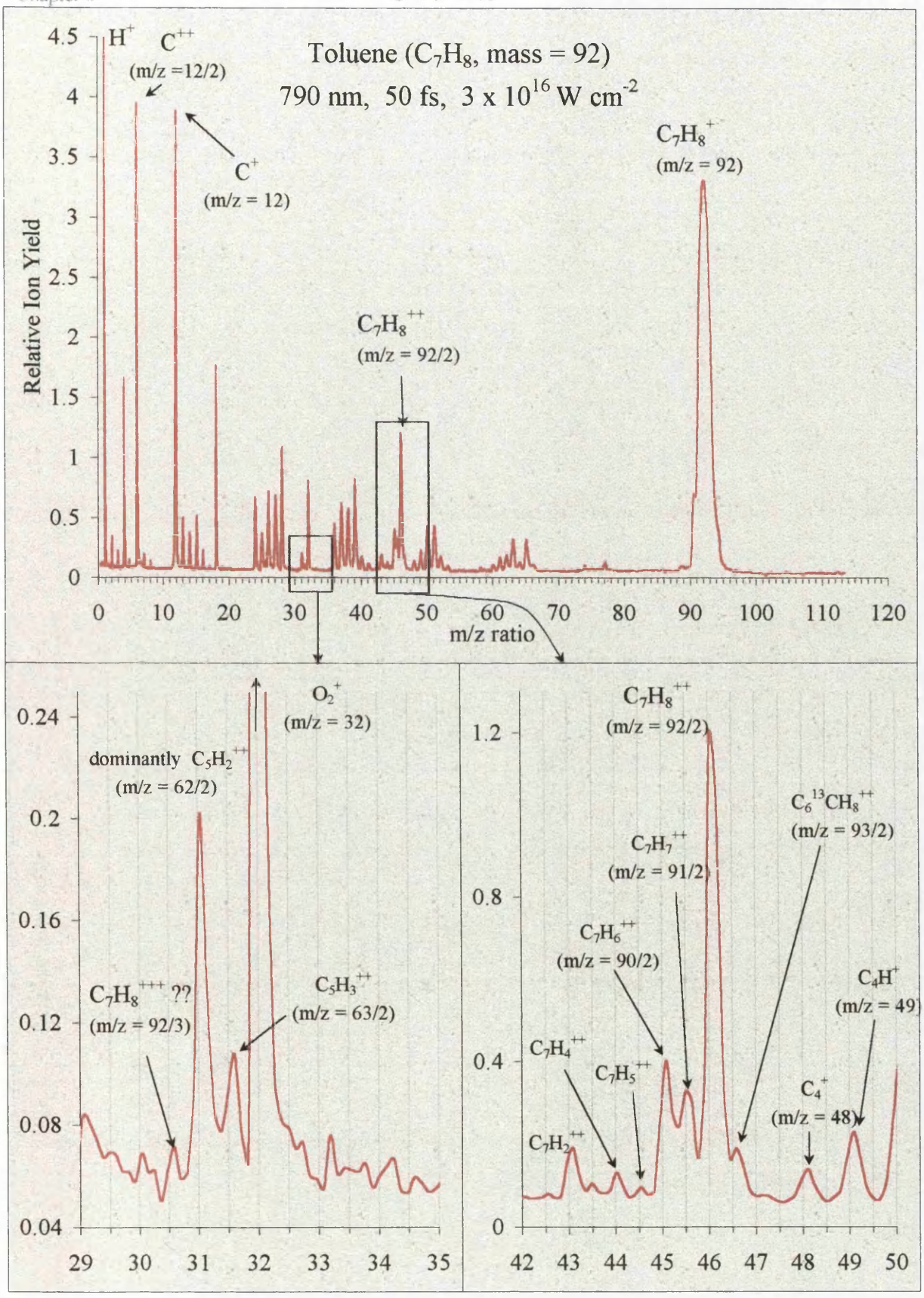

Figure 6g A Higher Intensity Toluene Mass Spectrum with insets at multiply ionised regions

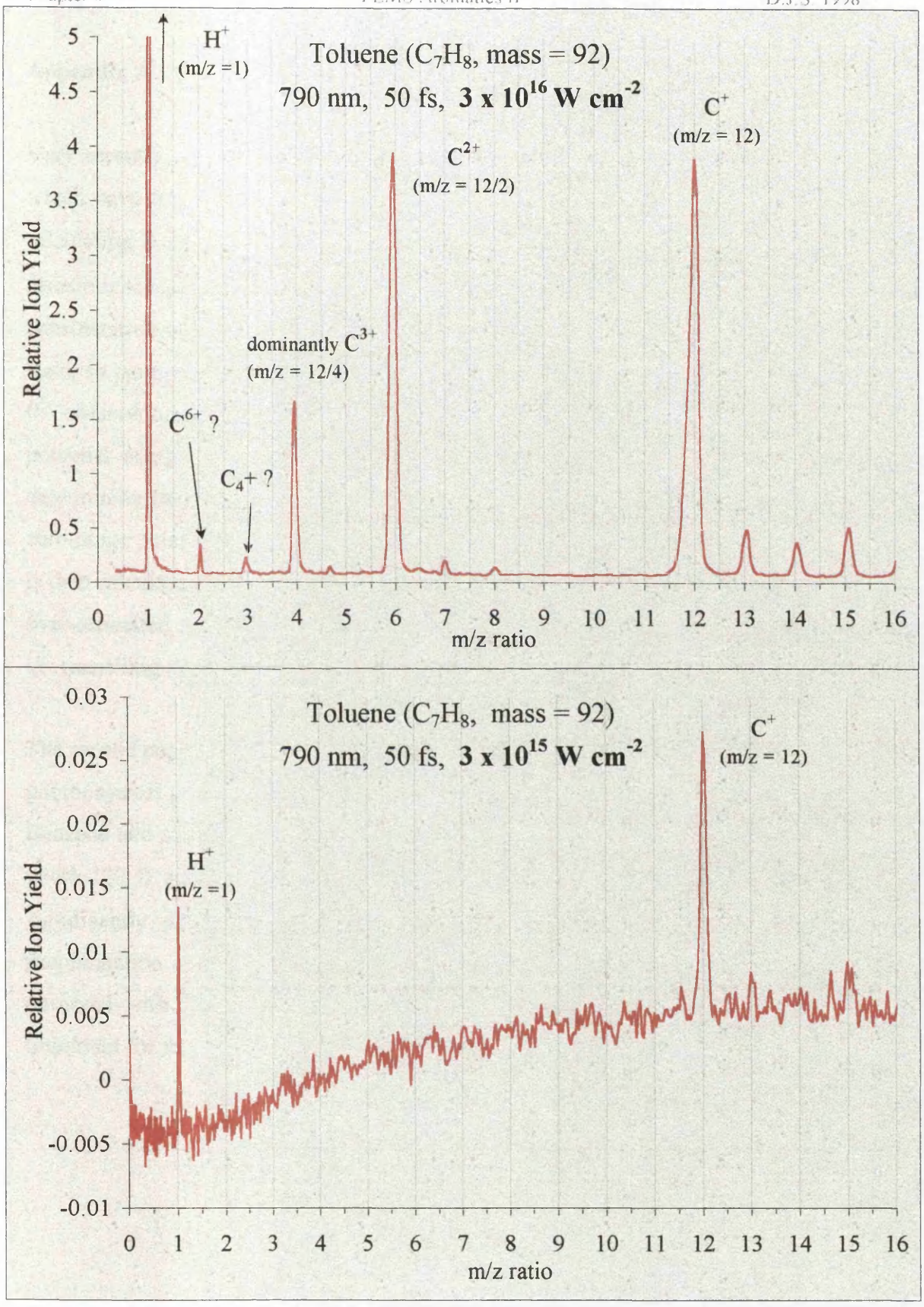

Figure 6h High Intensity Mass Spectra Sections: Multiple Ionised Carbon Comparison for Different Laser Intensities

Appendix 2

Very recently, two papers have been published by DeWitt and Levis [1998a, 1998b] which have important implications for this thesis. The first publication speculates on calculating Keldysh parameters (γ) for atoms, diatomic and polyatomic molecules, and discusses several corrections that can be made for γ values in molecules. This includes a consideration of the rather simplistic zero-range potential which was used in deriving the Keldysh parameter and focuses primarily on corrections to the width of the barrier that the electron tunnels through. In reality, and particularly for molecules, the electrostatic potential energy surfaces are complex. DeWitt considers a method for numerically determining the "tunnel length" that the electron traverses which includes replacing the zero-range potential with coulomb or *ab initio* potential surfaces. The Keldysh parameter is then calculated as described in chapter 2, section 2.4. The zero-range based γ may be over-estimated for molecules, which has implications for the values reported in this thesis i.e. tunnelling may be occurring at lower laser intensities than reported within.

The second paper considers the role of electronic and nuclear structure in determining the photophysical processes that occur when a molecule interacts with an intense laser pulse. Benzene and some other C_6 hydrocarbons are investigated using 780 nm laser pulses of width 170 fs and maximum intensity 3.8×10^{13} W cm^{-2}. The subject molecules have significantly different bonding structures. Depending on the bonding types, the fragmentation may be altered. And an exponential increase in the dissociation rate is observed with increasing numbers of atoms in the molecules. Such altercations are important for future studies.

CHAPTER 7

AN EXTENSION OF FLMS BEYOND AROMATIC MOLECULES

§7.0 Introduction 140

§7.1 Results and Conclusions 140

§7.0 Introduction

This short chapter extends FLMS beyond application to aromatic molecules in an attempt to render FLMS as a broader experimental technique. In particular new results are presented for carbon disulphide (CS_2) and 1,3-butadiene (C_4H_6). The experimental method highlighted in the previous chapters and reported in detail in chapter 3 is employed presently.

1,3-butadiene was examined before the laser refurbishment, whereas CS_2 was investigated post-refurbishment. This is an important point to note because it may affect saturation phenomenon and the intensity appearance thresholds for double charged ion activity.

§7.1 Results and Conclusions

Figures 7a and 7b show mass spectra in detail for carbon disulphide and 1,3-butadiene recorded using IR FLMS, with any double and triple ionised species expanded in the insets. Similar figures for the aromatic molecules benzene, deuterated benzene, benzaldehyde, toluene and naphthalene have been shown in previous chapters.

Techniques employed to label the multiple ions in the spectra are analogous to that described formerly. This included comparing the isotopic ratios of ^{13}C to ^{12}C from single to double charged ions. For example, consider CS_2 ($\equiv {}^{12}C^{32}S_2$). $^{13}CS_2$ should be present in ~ 1 % abundance for a molecule with one carbon atom. Additionally there exists a $C^{33}SS$ isotope at the same m/z value - within the resolution limits of the mass spectrum - also present in ~ 1 % abundance. The ratio of the peak at m/z = 77 (combination of $^{13}CS^+$ and $C^{33}SS^+$) to the peak at m/z = 76 (CS_2^+) should therefore be around 2 %. This is found to be approximately the case. This ratio remains constant at half m/z values (m/z = 38.5 and 38), indicative of dominant double ionisation activity and thus allowing peak identification. A similar argument applies with the consistent single-to-double ion ratios of CS_2^+ / $C^{34}SS^+$ and CS_2^{++} / $C^{34}SS^{++}$.

It is worth noting however, that the identification of peaks in a molecule such as CS_2 i.e. non-hydrocarbon, is simpler because the lack of a hydrogen atom limits various ion permutations and therefore largely minimises ambiguities of coincident species.

CS_2^{++} appeared at an approximate laser intensity of $\geq 10^{14}$ W cm^{-2}, which is in concert with results reported thus far using the post-refurbished laser system. Additionally, an unambiguous triple CS_2 ion is visible.

Turning the attention to 1,3-butadiene (figure 7b), the $^{13}C/^{12}C$ single parent ratio ($C_3{}^{13}CH_6^+$ / $C_4H_6^+$) is 4 – 5 % which is expected for a molecule containing 4 carbon atoms. The ratio of m/z = 27.5 to m/z = 27 is just less than 4 %. The reason for the slight decrease in value is due to a small coincident presence of $C_2H_3^+$ at m/z = 27 where the double ionised C_4H_6 dominates. This slightly increases the peak size.

The double charged parent peak became visible around 10^{14} W cm^{-2}. This is consistent with other findings reported for molecules investigated using the pre-refurbished laser system. A triple ionised parent ($C_4H_6^{3+}$) may be present but it is difficult say unambiguously due to H_2O contamination at the same m/z ratio within the resolution limits of the spectrum.

For both molecules, the general features of the mass spectra are consistent with findings reported in chapters 4 - 6 for the molecules benzaldehyde, benzene, deuterated benzene, toluene and naphthalene. Such features include a dominant parent ion, minimal fragmentation and secondary dominance by the double ionised parent with surrounding double ionised satellite peaks. The conclusion chapter further discusses the generality of FLMS.

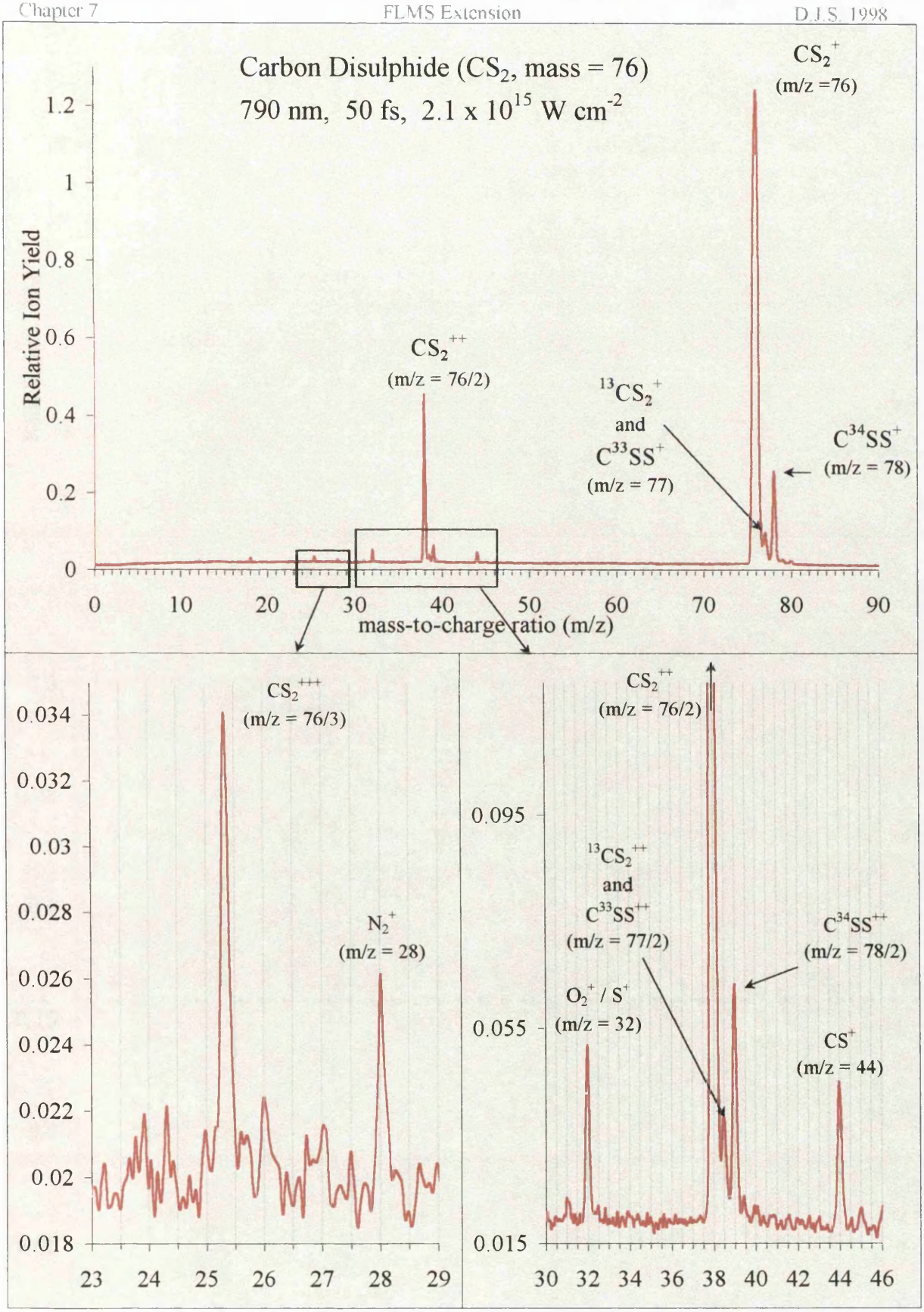

Figure 7a Carbon Disulphide Mass Spectrum with insets of multiply ionised regions

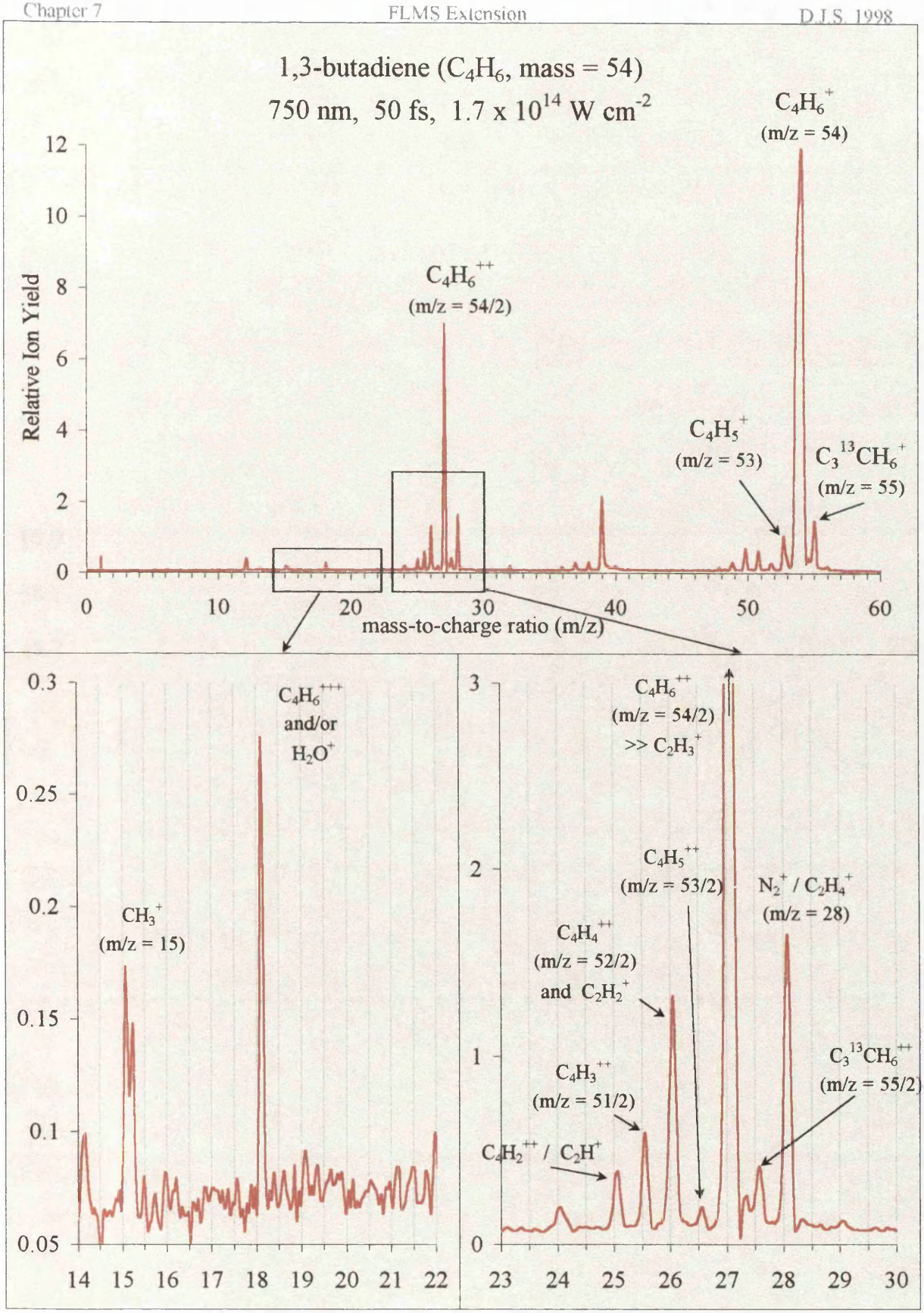

Figure 7b 1,3-butadiene Mass Spectrum with insets of multiply ionised regions

CHAPTER 8

CHARACTERISTIC BEHAVIOUR OF POLYATOMIC MOLECULES IN INTENSE LASER BEAMS - CONCLUSIONS AND FUTURE WORK

§8.0	**Introduction**	145
§8.1	**Principal Conclusions**	146
§8.2	**Future Work**	151

§8.0 Introduction

The potential of femtosecond laser mass spectrometry (FLMS) in both theoretical and experimental science has been shown to be considerable. FLMS has developed in recent years in conjunction with the introduction of reliable short pulse, intense lasers coupled to time-of-flight mass spectrometry (TOF). It can facilitate investigations into molecular detection and dynamics, specifically in the exploration of ionisation and/or dissociation pathways, and their transitional state lifetimes, and the associated mechanisms of such. FLMS combines real-time analysis with trace-sensitivity.

The present study has employed and advanced this elegant experimental procedure in the analysis of a series of polyatomic molecules centred around the aromatic prototype benzene. Where relevant, results have been contrasted to previous nanosecond studies by other authors. The FLMS laser parameters employed were pulse widths of ~ 50 fs - 2.5 ps, wavelengths of 375, 750 and 790 nm at beam intensities from ~ 10^{12} - 10^{16} W cm^{-2}.

The cyclic-aromatic group of molecules have been chosen for study for a number of reasons. Firstly, it has not only been an evolutionary step in going from nanosecond to femtosecond pulse width lasers, but also in the movement from atoms to small to medium mass molecules. The aromatics have also justifiably been the subject of considerable study due to their general industrial and commercial importance. Their significance centres on environmental pollution considerations which has been one of the main motivations for the present work.

Results have also been extended from aromatic cyclic hydrocarbons to other polyatomic molecules which are non hydrocarbon and/or non-cyclic in their structural nature. Concomitant characteristics have been found in the molecular dynamics of all species studied, effectively rendering FLMS as a general technique. Analytical detective research, that is the identification of substances, and the physical spin-offs of FLMS have formed the main part of this thesis. This has centred on FLMS in the infrared wavelength region. Figure 8a located at the end of this chapter, shows mass spectra for the various

polyatomic molecules studied in this thesis irradiated under similar conditions using short intense lasers in the IR wavelength region. It illustrates very effectively the generality of FLMS as discussed later. Note that the atom Xenon is included in the figure for comparative purposes. The specific conditions of pulse width, wavelength and beam intensity are shown alongside the spectra. The stated intensity is indicative of the highest beam flux at which the particular molecule has been studied at the time of writing. Reference should generally be made to figure 8a when reading this chapter.

In general, the contaminants of hydrogen (m/z = 1), water (m/z = 18) and nitrogen (m/z = 28) were difficult to eliminate. However, they caused minimal confusion and can be ignored.

§8.1 Principal Conclusions

The principal conclusions of the research reported in this thesis are as follows. Note that detailed conclusions for particular molecules are located at the ends of chapters 4 - 7.

In terms of a laser based trace-sensitive analytical technique, FLMS may often replace its nanosecond forerunner, resonance enhanced multiphoton ionisation (REMPI). This has been for a number of reasons.

FLMS efficiently produces predominant parent ions with minimal associated fragmentation. The short pulse widths (femtoseconds) coupled to high beam intensities ($> 10^{12}$ W cm^{-2}) has allowed rapid up-pumping through pre-dissociative states such that molecular ionisation levels are reached. Any small fragmentation is thought to occur via the parent ion continuum in an ionisation-dissociation model (ID). In this sense, one can picture the process as ladder-climbing followed by above threshold ladder-switching. The fast pulses are thought to bypass pre-dissociative states which have longer lifetimes. Also, the associated high beam intensities aid the molecular excitation with a very large influx of photons within a very short period of time, leading to saturation in the

interaction region which maximises the sensitivity of FLMS (unity ionisation probability) and can lead to calibration without the use of standards.

This is in contrast to nanosecond studies in which small mass fragments often dominate the mass spectra at the expense of parent ions which is indicative of FLMS largely bypassing nanosecond pathways. However, soft ionisation has been seen to be possible using nanosecond lasers with aromatic molecules but only by strictly controlling the laser beam characteristics of wavelength and intensity in the resonant processes.

In terms of FLMS, the laser parameters have also been shown to be able to control the chemical dynamics, but to a less critical and more capable degree than in the nanosecond case. One of the main reasons for this is because, in contrast to nanosecond studies, FLMS does not tune in to any particular resonant transitions. Once the femtosecond range is reached, the intensity is seen to influence whether or not fragmentation appears. Higher intensities produce greater fragmentation. A degree of wavelength influence has also been revealed. For comparable intensities, an infrared wavelength yields considerably less fragmentation than with ultraviolet. However, dominant parent ions always remain which has considerable analytical implications with respect to FLMS. It is important to note that changes of the pulse width within the ultra-fast region did not materially affect the results. So the conclusion follows that intensity and wavelength variation are the more important control parameters once the short pulse width region has been entered.

It has also been illustrated, and hinted above, that FLMS has the potential to perform sensitive uniform molecular detection, that is, quantitative analysis without the use of standards. FLMS can be thought of as non-resonant in that the associated broad bandwidths do not allow tuning to individual excitation resonant steps. For benzene, toluene and naphthalene, a wavelength independence has been found on parent ionic yields at $\sim 7 \times 10^{13}$ W cm^{-2}. Moreover, the said yields have been found to be concurrent when comparing the different molecules. Universal chemical detection may be a possibility, the implications of which are substantial. One possibility is in the uniform

and therefore quantitative detection of a multi-component substance - the various peaks corresponding to the species present would be visible as a series of clean spikes at correct m/z ratios and intensities in the mass spectrum making for unambiguous identification.

Again such findings contrast nanosecond results which have been seen to be analytically non-uniform for different species due to the individual resonant nature of the process. De-tuning of the laser wavelength can be done in an attempt to correct this but results in decreasing ion yields while the differing ionisation potentials cause a non-uniform probability in detection.

A physical spin-off of the FLMS study has been the general appearance of multiply ionised molecules at IR wavelengths. This new phenomenon has been observed for a considerable range of small to medium mass polyatomic molecules including benzaldehyde (C_7H_6O), benzene (C_6H_6), deuterated benzene (C_6H_5D), toluene (C_7H_8), naphthalene ($C_{10}H_8$), 1,3-butadiene (C_4H_6), carbon disulphide (CS_2), carbon dioxide (CO_2) and methyl iodide (CH_3I). This is less obvious in the UV wavelength region where γ is larger for similar laser intensities.

The appearance of double ionised parent ions occurs at an approximate threshold intensity of 10^{14} W cm^{-2}, although such appearance values are not just functions of laser intensity and may be dependent on other experimental parameters - for example, laser wavelength, pulse width, pulse shape profile and several experimental variants such as beam spot position, size and TOF extraction and detection conditions. However, the results have suggested that double charged ions were produced just below the above threshold when using the pre-refurbished system, while post-refurbished results yielded double charged ions appearing above the same laser intensity threshold.

Variant experimental conditions may also explain the differing laser intensity onsets of saturation for the same molecules in chapters 5 and 6.

In addition to 2^+ ions, triple ionised parents have been found in the majority of the above molecules for higher laser intensities than the above. However no clear intensity threshold has been established for their appearance and not all the molecules have been probed with equally high beam fluxes. The maximum conditions for the said molecules are indicated in the insets of figure 8a. Toluene is the definite exception to triple ion production with no discernible $C_7H_8^{3+}$ peak even at intensities up to $\sim 3 \times 10^{16}$ W cm^{-2}. 1,3-butadiene and benzaldehyde are possible exceptions, but these molecules have not yet been studied in the intensity range above 2×10^{14} W cm^{-2} where triple ions are more likely to occur.

This interesting new result of negligible dissociation and multiple molecular ionisation using IR FLMS with intensities up to $\sim 10^{15}$ W cm^{-2} makes for mass spectra concomitant to atomic spectra with the double ionised peak being the second most dominant ion present. Figure 8a illustrates this with Xenon included as a reference. High ionisation and minimal dissociation in polyatomic molecules implies a considerable degree of stability. This has theoretical permutations in terms of fundamental studies as well as the practical possibility of producing highly coherent radiation.

Additionally, in the local region of the double parent ions, envelopes of double ionised satellite peaks have been identified. Such peaks are interesting in their own right and are a very strong fingerprint of IR FLMS, but have also been used to confirm the presence of dominant double charged parent species. In fact, many innovative methods have been employed to substantiate, or otherwise, the appearance of double and triple charged species to such a degree that one can be absolutely sure that what is being observed in the infrared mass spectra are dominant quantities of multiply ionised components. A particularly effective method involved examing the molecule's deuterated counterpart to reveal unambiguous double charged ions.

From such studies, one can conclude the optimum parameters in which to probe polyatomic molecules. Obviously, the choice of experimental conditions will reflect the aims and objectives of the investigation. For fundamental structural studies, high

intensity UV FLMS should be used to produce significant fragmentation. For analytical investigations optimum detection can be achieved using IR FLMS. Intensities of 10^{14} W cm^{-2} are the most suitable. A balance must be met between exclusive parent production and insufficient abundances of the ion signatures. For example, a little multiple ionisation and/or dissociation with a very dominant parent may be more useful to the analyst than exclusive parent ions present in lesser amounts. Multiple parent ionisation is best studied in the upper regions of the laser intensities used, that is up to ~ 10^{15} W cm^{-2}. The multiple ion production is not compromised by the slight increase in fragmentation. However, intensities higher than this, as shown for toluene in appendix 1 of chapter 6 (~ 10^{16} W cm^{-2}) may lead to coulomb explosions causing multiply charged atoms from the molecules and more fragmented spectra, which is not ideal for analysis. A useful upper limit for analytical FLMS may be ~ 10^{15} W cm^{-2}.

Finally, the mechanism(s) of ionisation have been considered. It is thought that multiphoton ionisation largely explains the results for intensities less than ~ 10^{14} W cm^{-2}, after which tunnelling ionisation contributes to the ionic yields as the physics of the situation becomes more and more non-perturbative. The fact that multiple ionisation is prevalent only at IR wavelengths may simply reflect that the Keldysh values were lower for IR than UV indicative of a tunnelling mechanism at work in the IR.

Up to ~ 10^{15} W cm^{-2}, coulomb explosions are not thought to explain the results for the medium mass molecules irradiated in this thesis using IR FLMS, although for approximately 10^{16} W cm^{-2} and above this may well be the case (a possible exception to this may be CS_2 in which multiply charged atoms - evidence of explosions - of C and S have been observed but with low intensity). Rather, a more gentle, sequential ionisation process is thought to occur such as ionisation matching the evolution of the laser pulse profile in a fast, but non-vertical, stripping of valence electrons as well as hydrogen shredding. Coulomb explosions are associated with transient multiply charged parent species [Codling *et al*, 1994]. For the molecules studied presently, the 2^+ and 3^+ species are stable entities with lifetimes at least as long as the flight times in the TOF (tens of μs).

§8.2 Future Work

It is important to extend the present observations to a wider range of polyatomic molecules in a bid to further generalise the technique of FLMS. Particularly, this is worthwhile for trace-universal chemical detection of such substances as, for example, explosives, drugs, environmental pollutants, radio-nuclides and semi-conductors. Expanding the generality to multi-component samples is of considerable importance, particularly in analytical studies. Practical benefits in this area could be enormous.

There is also a requirement to be more consistent in the recording of the experimental results such that more quantitative statements can be made with regard to threshold intensities etc. This is, and has proved to be difficult, mainly due to an extensive overhaul of the laser system between chapters 5 and 6, and the general fact that keeping experimental variants constant is itself very tricky. Nevertheless, more precise experimental and theoretical studies are required.

It would be advantageous to further increase the laser intensity using the power-amp mentioned in the experimental chapter coupled with superior beam focusing. This would facilitate investigations into multiple ionisation and associated mechanisms. This has in fact been done since the writing of this thesis with new beam intensities peaking around 10^{16} W cm^{-2} at 790 nm and 50 fs. Molecules examined have included toluene (see appendix 1, chapter 6) benzaldehyde and carbon disulphide. Towards 10^{16} W cm^{-2} the molecules are showing signs of coulomb explosions. An intensity threshold may be established for such events which would also represent an upper limit for successful analysis.

Postscript

Although precise quantitative analysis has not been performed in the present study, FLMS has been shown to have considerable potential for such. Considering the laser focal spot dimensions and pressure inside the TOF can allow an estimation of the number

of molecules available for ionisation during each laser pulse shot. Such an estimation may be around 10^4 molecules, all of which are ionised using FLMS operating at a saturating beam intensity. It is evident that more precise calculations and experimental measurement/control could lead to an accurate analytical outcome.

Additionally, and recently, gas mixtures have been examined using IR FLMS, yielding similar detection probabilities for the different species present in the sample. This represents another significant step towards uniform quantitative analysis.

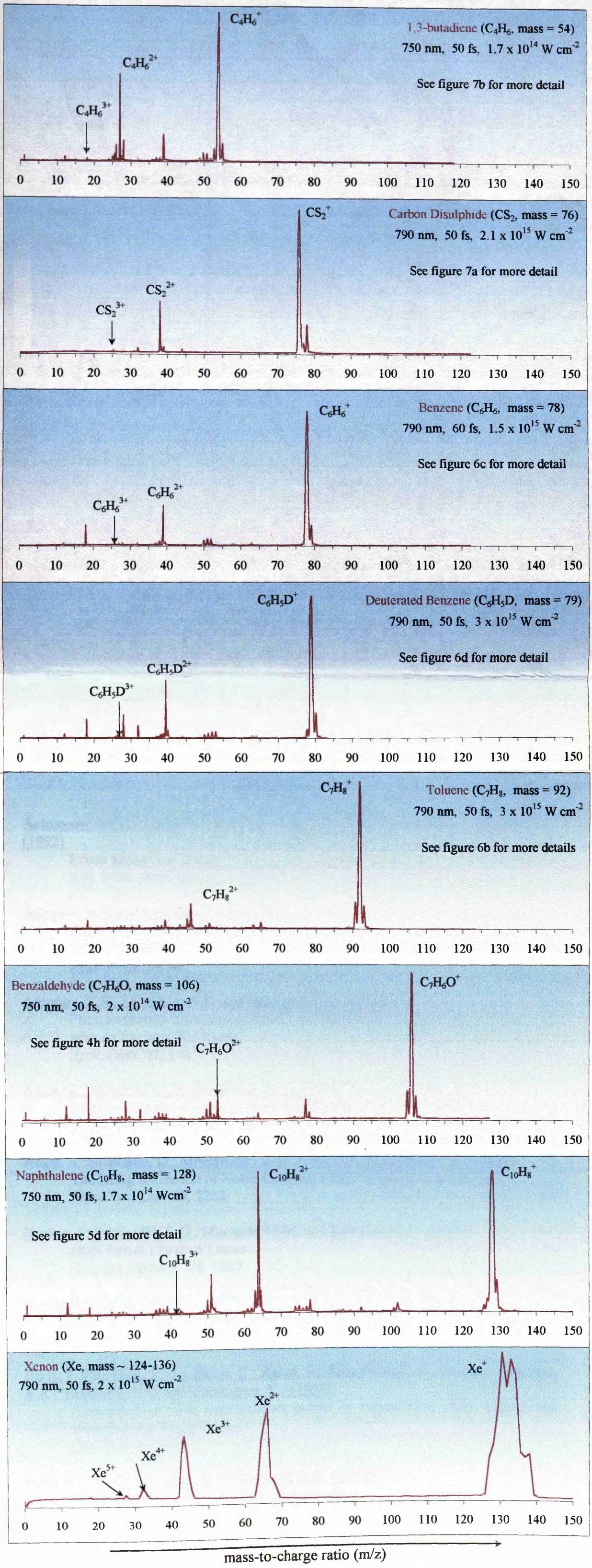

Figure 8a Multi-Molecular Mass Spectra for various polyatomic molecules recorded using infrared FLMS: Ion Yield vs mass-to-charge ratio (m/z)

REFERENCES

Ammosov, M.V.; Delone, N.B.; Ivanov, M.Y.; Bondar, I.I. and Masalov, A.V. (1992).
Cross Sections of Direct Multiphoton Ionization of Atoms.
Adv. in At. and Opt. Phys. **29**, 33.

Antonov, V.S. and Letokhov, V.S. (1981).
Laser Multiphoton and Multistep Photoionization of Molecules and Mass Spectrometry.
Appl. Phys. **24**, 89.

Antonov, V.S.; Letokhov, V.S. and Shibanov, A.N. (1980).
Photoionization Mass-Spectrometry of Benzene and Benzaldehyde Molecules with an Excimer KrF Laser.
Appl. Phys. **22**, 293.

Augst, S.; Meyerhofer, D.; Strickland, D. and Chin, S.L. (1991).
Laser ionization of noble gases by Coulomb-barrier suppression.
J. Opt. Soc. Am. B **8**, 858.

Augst, S.;Strickland, D.; Meyerhofer, D.D.; Chin, S.L. and Eberly, J.H. (1989).
Tunneling Ionization of Noble Gases in a High-Intensity Laser Field.
Phys. Rev. Lett. **63**, 2212.

Backus, S; Durfee III, C.G.; Murnane, M.M. and Kapteyn, H.C. (1998).
High Power Ultrafast Lasers.
Rev. Sci. Instrum. **69**, 1207.

Barnwell, C.N. (1983).
Fundamentals of Molecular Spectroscopy, 3rd Edition.
McGraw-Hill UK Ltd. Maidenhead, England.

Barty, C.P.J.; Guo, T.; Le Blanc, C.; Raksi, F.; Rose-Petruck, C.; Squier, J.; Wilson, K.R.; Yakovlev, V.V. and Yamakawa, K. (1996).
Generation of 18-fs multiterawatt pulses by regenerative pulse shaping and chirped-pulse amplification.
Opt. Lett. **21**, 668.

Barty, C.P.J.; Gordon III, C.L. and Lemoff, B.E. (1994).
Multiterawatt 30-fs Ti;sapphire laser system.
Opt. Lett. **19**, 1442.

Bekov, G.I. and Letokhov, V.S. (1983).
Laser Atomic Photoionization Spectral Analysis of Element Traces.
Appl. Phys. B **30**, 161.

Berger, M.; Goldblatt, I.L. and Steel, C. (1973).
Photochemistry of Benzaldehyde.
J. Am. Chem. Soc. **95**, 1717.

Bethune, D.S. (1981).
Dye cell design for high-power low-divergence excimer-pumped dye lasers.
Appl. Opt. **20**, 1897.

Boesl, U.; Zimmermann, R.; Weickhardt, C.; Lenoir, D.; Schramm, K.W.; Kettrup, A. and Schlag, E.W. (1994).
Resonance-Enhanced Multi-Photon Ionization: A Species-Selective Ion Source for Analytical Time-of-Flight Mass Spectroscopy.
Chemosphere **29**, 1429.

Boesl, U (1991).
Multiphoton Excitation and Mass-Selective Ion Detection for Neutral and Ion Spectroscopy.
J. Phys. Chem. **95**, 2949.

Boesl, U.; Neusser, H.J. and Schlag, E.W. (1980).
Visible and UV multiphoton ionization and fragmentation of polyatomic molecules.
J. Chem. Phys. **72**, 4327.

Brabec, T.; Ivanov, M. and Corkum, P. (1996).
Coulomb focussing in intense field atomic processes.
Phys. Rev. A **54**, R2511.

Bucksbaum, P.H.; Zavriyev, A.; Muller, H.G. and Schumacher, D.W. (1990).
Softening of the H_2^+ Molecular Bond in Intense Laser Fields.
Phys. Rev. Lett. **64**, 1883.

Chin, S.L.; Decker, J.E.; Walsh, T.D.G.; Liang, Y. and Xu, G. (1993).
Tunnel Ionization of Molecules by an Intense CO_2 Laser.
Laser Physics **3**, 298.

Chin, S.L.; Liang, Y; Decker, J.E.; Ilkov, F.A. and Ammosov, M.V. (1992).
Tunnel ionization of diatomic molecules by an intense CO_2 laser.
J. Phys. B: At. Mol. Opt. Phys. **25**, L249.

Codling, K. and Frasinski, L.J. (1997).
Molecules in Intense Laser Fields: an Experimental Viewpoint.
Structure and Bonding **86**, 2.

Codling, K. and Frasinski, L.J. (1994).
Coulomb explosion of simple molecules in intense laser fields.
Contemp. Phys. **35**, 243.

Codling, K. and Frasinski, L.J. (1993).
Dissociative ionization of small molecules in intense laser fields.
J. Phys. B: At. Mol. Opt. Phys. **26**, 783.

Constant, E.; Staplefeldt, H. and Corkum, P.B. (1996).
Observation of Enhanced Ionization of Molecular Ions in Intense Laser Fields.
Phys. Rev. Lett. **76**, 4140.

Cornaggia, C.; Salin, F. and Le Blanc, C. (1996).
Changes in the SO_2 geometry during the laser-induced multiple ionization and fragmentation.
J. Phys. B: At. Mol. Opt. Phys. **29**, L749.

Cornaggia, C.; Schmidt, M. and Normand, D. (1995).
Laser-induced nuclear motions in the Coulomd explosion of $C_2H_2^+$ ions.
Phys. Rev. A **51**, 1431.

Cornaggia, C.; Schmidt, M. and Normand, D. (1994).
Coulomb explosion of CO_2 in an intense femtosecond laser field.
J. Phys. B: At. Mol. Opt. Phys. **27**, L123.

Cornaggia, C.; Lavancier, J.; Normand, D.; Morellec, J. and Agostini, P. (1991).
Multielectron dissociative ionization of diatomic molecules in an intense femtosecond laser field.
Phys. Rev. A **44**, 4499.

Cornaggia, C.; Lavancier, J.; Normand, D.; Morellec, J. and Liu, H.X. (1990).
Intensity dependence of the multielectron dissociative ionization of N_2 at 305 and 610 nm.
Phys. Rev. A **42**, 5464.

Davis, C.C. (1996).
Lasers and Electro-Optics, Fundamentals and Engineering.
Cambridge University Press, Trumpington St, Cambridge CB2 1RP.

Decorpo, J.J.; Hudgens, J.W.; Lin, M.C.; Saalfield, F.; Seaver, M.E. and Wyatt, J.R. (1980).
Characterization of Multiphoton Ionization Mass Spectrometry.
Adv. Mass Spectrom. **8A**, 133.

De Hoffman, E. (1996).
Mass Spectrometry Principles and Applications.
Wiley and Sons, UK.

DeWitt, M.J. and Levis, R.J. (1998a).
Calculating the Keldysh adiabaticity parameter for atomic, diatomic and polyatomic molecules.
J. Chem. Phys. **108**, 7739.

DeWitt, M.J. and Levis, R.J. (1998b).
The role of electron delocalization in the ionization of C_6 hyrocarbons using intense 780 nm laser pulses of femtosecond duration.
J. Chem. Phys. **108**, 7045.

DeWitt, M.J.; Peters, D.W. and Levis, R.J. (1997).
Photoionization/dissociation of alkyl substituted benzene molecules using intense near-infrared radiation.
Chem. Phys. **218**, 211.

DeWitt, M.J. and Levis, R.J. (1995).
Near-infrared femtosecond photoionization/dissociation of cyclic aromtaic hydrocarbons.
J. Chem. Phys. **102**, 8760.

Dietrich, P.; Ivanov, M.Yu.; Ilkov, F.A. and Corkum, P.B. (1996).
Two-Electron Dissociative Ionization of H_2 and D_2 in Infrared Laser Fields.
Phys. Rev. Lett. **77**, 4150.

Dietrich, P. and Corkum, P.B. (1992).
Ionization and dissociation of diatomic molecules in intense infrared laser fields.
J. Chem. Phys. **97**, 3187.

Dietz, W.; Neusser, H.J.; Boesl, U.; Schlag, E.W. and Lin, S.H. (1982).
A Model for Multiphoton Ionisation Mass Spectroscopy with Application to Benzene.
Chem. Phys. **66**, 105.

Dorman, F.H. and Morrison, J.D. (1960).
Double and Triple Ionization in Molecules Induced by Electron Impact.
J. Chem. Phys. **35**, 575.

Fassett, J.D. and Travis, J.C. (1988).
Spectrochem Acta **43B**, 1407.

Fassett, J.D.; Moore, L.J.; Travis, J.C. and DeVoe, J.R. (1985).
Laser Resonance Ionization Mass Spectrometry.
Science **230**, 262.

Fork, R.L.; Shank, C.V. and Yen, R.T. (1982).
Amplification of 70-fs optical pulses to gigawatt powers.
Appl. Phys. Lett. **41**, 223.

Frasinski, L.J.; Codling, K. and Hatherly, P. (1987).
Femtosecond Dynamics of Multielectron Dissociative Ionization by Use of Picosecond Laser.
Phys. Rev. Lett. **58**, 2424.

Freeman, R.R. and Bucksbaum, P.H. (1991).
Investigations of above-threshold ionization using subpicosecond laser pulses.
J. Phys. B: At. Mol. Opt. Phys. **24**, 325.

Fujimoto, J.G.; Weiner, A.M. and Ippen, E.P. (1984).
Generation and measurement of optical pulses as short as 16 fs.
Appl. Phys. Lett. **44**, 832.

Gedanken, A.; Robin, M.B. and Keubler, N.A. (1982).
Nonlinear Photochemistry in Organic, Inorganic, and Organometallic Systems.
J. Phys. Chem. **86**, 4096.

Gibson, G.; Luk, T.S. and Rhodes, C.K. (1990).
Tunneling ionization in the multiphoton regime.
Phys. Rev. A **41**, 5049.

Giles, A.J.; Posthumus, J.H.; Thompson, M.R.; Frasinski, L.J.; Codling, K.; Langley A.J.; Shaikh, W. and Taday, P.F. (1995).
Interferomic Shaping of Femtosecond Laser Pulses.
Jn. Opt. Comm. **118**, 537.

Giusti-Suzor, A.; Mies, F.H.; DiMauro, L.F.; Charron, E. and Yang, B. (1995).
Dynamics of H_2^+ in intense laser fields.
J. Phys. B: At. Mol. Opt. Phys. **28**, 309.

Graham, P.; Ledingham, K.W.D.; Singhal, R.P.; Smith, D.J.; Wang, S.; McCanny, T.; Kilic, H.S.; Langley, A.J.; Taday, P.F. and Kosmidis, C. (1998).
Dissociative Ionization and Angular Distributions of CS_2 and its Ions.
To be published in *Proceedings of the 9th International Symposium on Resonance Ionisation Spectroscopy (RIS) 1998.*
UMIST, Manchester.

Grun, C.; Weickhardt, C. and Grotemeyer, J. (1996).
Multiphoton Ionization Mass-Spectrometry of metal organic compounds avoiding ultrafast neutral dissociation channels by femtosecond laser activation.
European Mass Spectrom. **2**, 197.

Hatherly, P.A.; Stankiewicz, M.; Codling, K.; Frasinski, L.J. and Cross, G.M. (1994).
The multielectron dissociative ionization of molecular iodine in intense laser fields.
J. Phys. B: At. Mol. Opt. Phys. **27**, 2993.

He, C.; Basler, J.N. and Becker, C.H. (1997a).
Uniform elemental analysis of materials by sputtering and photoionization mass spectrometry.
Nature **385**, 797.

He, C. and Becker, C.H. (1997b).
Absolute nonresonant multiphoton ionization cross section of NO at 532 nm.
Phys. Rev. A **55**, 1300.

He, C. and Becker, C.H. (1996).
Surface analysis by laser ionization.
Curr. Opinion in Sol. State. and Mat. Sci. **1**, 493.

Hirata, Y. and Lim, E.C. (1980).
Nonradiative electronic relaxation of gas aromatic carbonyl compounds: Benzaldehyde.
J. Chem. Phys. **72**, 5505.

Hurst, G.S. and Payne, M.G. (1988).
Elemental analysis using resonance ionization spectroscopy.
Spectrochem Acta **43B**, 715.

Hurst, G.S.; Payne, M.G.; Kramer, S.D. and Young, J.P. (1979).
Resonance ionization spectroscopy and one-atom detection.
Rev. Mod. Phys. **51**, 767.

Hutchinson, M.H.R. (1989).
Terawatt lasers.
Contemp. Phys. **30**, 355.

Ilkov, F.A.;Decker, J.E. and Chin, S.L. (1992).
Ionization of atoms in the tunnelling regime with experimental evidence using Hg atoms.
J. Phys. B: At. Mol. Opt. Phys. **25**, 4005.

Johnson, P.M. (1980).
Molecular Multiphoton Ionization Spectroscopy.
Acc. Chem. Res. **13**, 20.

Johnson, P.M. (1976a).
The multiphoton ionization spectrum of benzene.
J. Chem. Phys. **64**, 4143.

Johnson, P.M. (1976b).
The multiphoton ionization spectrum of trans-1,3-butadiene.
J. Chem Phys. **64**, 4638.

Johnson, P.M.; Berman, M.R. and Zekhaim, D. (1975).
Nonresonant Multiphoton Ionization Spectrsocopy: The Four Photon Ionization Spectrum of Nitric Oxide.
J. Chem. Phys. **62**, 2500.

Keldysh, L.V. (1965).
Ionization in the Field of a Strong Electromagnetic Wave.
Sov. Phys. JETP **20**, 1307.

Kilic, H.S.; Ledingham, K.W.D.; Kosmidis, C.; McCanny, T.; Singhal, R.P.; Wang, S.L.; Smith, D.J.; Langley, A.J. and Shaikh, W. (1997).
Multiphoton Ionization and Dissociation of Nitromethane Using Femtosecond Laser Pulses at 375 and 750 nm.
J. Phys. Chem. A. **101**, 817.

Kmetec, J.D.; Macklin, J.J. and Young, J.F. (1991).
0.5-TW, 1125 fs Ti:sapphire laser.
Opt. Lett. **16**, 1001.

Knight, P. (1989).
Quantum Optics, The New Physics.
Cambridge University Press, Cambridge, UK.

Knox, W.H. (1988).
Femtosecond Optical Pulse Amplification.
IEEE J. Quantum Electron. **24**, 388.

Kosmidis, C.; Ledingham, K.W.D.; Kilic, H.S.; McCanny, T., Singhal, R.P.; Langley, A.J .and Shaikh, W. (1997).
On the Fragmentation of Nitrobenzene and Nitrotoluenes Induced by a Femtosecond Laser at 375 nm.
J. Phys. Chem. A **101**, 2264.

Kyrala, G.A. (1993).
Ultra-High Irradiance Lasers and Their Interactions.
Comments At. Mol. Phys. **28**, 325.

Lambropoulos, P. (1985).
Mechanisms for Multiple Ionization by Strong Pulsed Lasers.
Phys. Rev. Lett. **55**, 2141.

Langley, A.J.; Noad, W.J.; Ross, I.N. and Shaikh, W. (1994).
High-brightness femtosecond laser using titanium-sapphire technology and amplification in dyes.
Appl. Opt. **33**, 3875.

Langley, A.J.; Noad, W.J.; Ross, I.N. and Shaikh, W. (1993).
Single-pulse autocorrelator and spectrometer system for the measurement of subpicosecond laser pulses.
Rutherford Appleton Laboratory (RAL) Annual Report.

Lavancier, J.; Normand, D.; Cornaggia, C.; Morellec, J. and Liu, H.X. (1991).
Laser-intensity dependence of the multielectron ionization of CO at 305 and 610 nm.
Phys. Rev. A **43**, 1461.

Lecroy Corporation.
700 Chestnut Ridge Road
Chestnut Ridge, New York NY 10977-6499.

Ledingham, K.W.D.; Singhal, R.P.; Smith, D.J.; McCanny, T.; Graham, P.; Kilic, H.S.; Peng, W.X.; Wang, S.; Langley, A.J. and Taday, P.F. (1998a).
The Behaviour of Polyatomic Molecules in Intense Infrared Laser Beams.
J. Phys. Chem. A **102**, 3002.

Ledingham, K.W.D.; Smith, D.J.; Singhal, R.P.; Kilic, H.S.; McCanny, T.; Graham, P.; Langley, A.J. and Taday, P.F. (1998b).
Multiply Charged Ionisation from Aromatic Molecules Following Irradiation in Intense Laser Fields.
To be published.

Ledingham, K.W.D. and Singhal, R.P. (1997).
High Intensity Mass Spectrometry - A Review.
Int. J. Mass Spec. Ion. Processes **163**, 149.

Ledingham, K.W.D.; Singhal, R.P.; Kilic, H.S.; McCanny, T.; Smith, D.J.; Peng, W.X.; Kosmidis, C.; Langley, A.J. and Taday, P.F. (1996/7).
Femtosecond Laser Mass Spectrometry as an Ultra-Sensitive Analytical Technique.
Rutherford Appleton Laboratory Annual Report, 154 (1996 - 1997).

Ledingham, K.W.D.; Singhal, R.P.; Kilic, H.S.; McCanny, T.; Smith, D.J.; Wang, S.; Kosmidis, C.; Langley, A.J. and Shaikh, W. (1995/6).
The Potential of Femtosecond Laser Mass Spectrometry.
Rutherford Appleton Laboratory Annual Report, 165 (1995 - 1996).

Ledingham, K.W.D.; Kilic, H.S.; Kosmidis, C.; Deas, R.M.; Marshall, A.; McCanny, T.; Singhal, R.P.; Langley, A.J. and Shaikh, W. (1995a).
A Comparison of Femtosecond and Nanosecond Multiphoton Ionization and Dissociation for Some Nitro-molecules.
Rapid Commun. Mass Spectrom. **9**, 1522.

Ledingham, K.W.D.; Kosmidis, C.; Georgiou, S.; Couris, S. and Singhal R.P. (1995b).
A comparison of the femto-, pico- and nano-second multiphoton ionization and dissociation processes of NO_2 at 248 and 496 nm.
Chem. Phys. Lett. **247**, 555.

Ledingham, K.W.D. (1995c).
Multiphoton Ionization and Laser Mass Spectrometry.
An Introduction to Laser Spectroscopy (ed. D.L. Andrews) Plenum Press Spring St New York 10013.

Ledingham, K.W.D. and Singhal, R.P. (1992).
Laser Mass Spectrometry.
Applied Laser Spectroscopy, 365, Andrews, D.L. (Ed.) V.C.H. Publishers Inc.

Ledingham, K.W.D. (1987).
Making Light of Counting Atoms.
Scope Winter 1987.

Letokhov, V.S. (1988).
Detecting individual atoms and molecules with lasers.
Scientific American Sept, 44.

Letokhov, V.S. (1987).
Laser Photoionisation Spectroscopy.
Academic Press Inc. Orlando, Florida, 32887.

Letokhov, V.S. (1986).
Laser Analytical Spectrochemistry.
Adam Hilger Bristol and Boston.

Levis, R.J. and DeWitt, M.J. (1996).
Photoionization of Polyatomic Molecules Using Intense, Near-Infrared Radiation of Femtosecond Duration.
Resonance Ionization Spectroscopy Ed. N. Winograd AIP Conf. Ser. **388,** 45.

L'Huiller, A. and Mainfray, G. (1984).
Multiphoton Ionization Versus Dissociation of Diatomic Molecules Irradiated by an Intense 40 ps Laser Pulse.
Chem. Phys. Lett. **103**, 447.

L'Huiller, A.; Lompre, L.A.; Mainfray, G. and Manus, C. (1983).
Multiply charged ions induced by multiphoton absorption processes in rare-gas atoms at 1.064 μm.
J. Phys. B: At. Mol. Opt. Phys. **16**, 1363.

Liang, Y.; Augst, S.; Chin, S.L.; Beaudoin, Y. and Chaker, M. (1994).
High harmonic generation in atomic and diatomic molecular gases using intense picosecond laser pulses - a comparison.
J. Phys. B: At. Mol. Opt. Phys. **27**, 5119.

Lompre, L.A.; Mainfray, G.; Manus, C.; Repoux, S. and Thebault, J. (1976).
Multiphoton Ionization of Rare Gases at Very High Intensity (10^{15} W/cm^2) by a 30-psec Laser Pulse at 1.06μm.
Phys. Rev. Lett. **36**, 949.

Long, S.R.; Meek, J.T.; Harrington, P.J. and Reilly, J.P. (1983).
Benzaldehyde photochemistry studied with laser ionization mass and photoelectron spectroscopy.
J. Chem. Phys. **78**, 3341.

Lubman, D.M. (1988a).
Analytical multiphoton ionization mass spectrometry. Part I. Theory and instrumentation.
Mass Spectrom. Rev. 7, 535.

Lubman, D.M. (1988b).
Analytical multiphoton ionization mass spectrometry. Part II. Applications.
Mass Spectrom. Rev. 7, 559.

Lubman, D.M. (1987).
Optically Selective Molecular Mass Spectrometry.
Anal. Chem. **59**, 31A.

Main, P.; Strickland, D.; Bado, P.; Pessot, M. and Mourou, G. (1988).
Generation of Ultrahigh Peak Power Pulses by Chirped Pulse Amplification.
IEEE J. Quantum Electron. **24**, 398.

Mainfray, G. and Manus, C. (1991).
Multiphoton Ionization of Atoms.
Reports on Prog. Phys. **54**, 1333.

Marshall, A.; Clark, A.; Jennings, R.; Ledingham, K.W.D. and Singhal, R.P. (1992).
Wavelength-Dependent Laser-Induced Fragmentation of Nitrobenzene.
Int. J. Mass Spectrom. Ion Processes **112**, 273.

Mataloni, P.; Santosuosso, M. and De Martini, F. (1991).
High Gain Amplification of Femtosecond Pulses with Low Amplified Spontaneous Emission in a Multipass Dye Cell.
Appl. Phys. **52**, 273.

McMurry, J. (1984).
Organic Chemistry.
Brooks/Cole Publishing Company, Monterey, California.

Neusser, H.J.; Boesl, U.; Weinkauf, R. and Schlag, E.W. (1984).
High-Resolution Laser Mass Spectrometry.
Int. J. Mass Spec. and Ion Processes **30**, 147.

Niu, S.; Zhang, W. and Chait, B.T. (1998).
Direct Comparison of Infrared and Ultraviolet Wavelength Matrix-Assisted Laser Desorption/Ionization Mass Spectrometry of Proteins.
J. Am. Soc. for Mass Spectrom. **9**, 1044.

Normand, D.; Dobosz, S.; Lezius, M.; D'Oliveira, P. and Schmidt, M. (1996).
Interaction dynamics of molecules in strong laser fields.
I.O.P. Conf. Ser. **154**, 287.

Normand, D.; Cornaggia, C.; Lavancier, J.; Morellec, J. and Liu, H.X. (1991).
Multielectron dissociative ionization of O_2 in an intense picosecond laser field.
Phys. Rev. A **44**, 475.

Perry, M.D. and Mourou, G. (1994).
Terawatt to Petawatt Subpicosecond Lasers.
Science **264**, 917.

Petty, G.; Tai, C. and Dalby, F.W. (1975).
Nonlinear resonant photoionization in molecular iodine.
Phys. Rev. Lett. **34**, 1207.

Posthumus, J.H.; Codling, K.; Frasinski, L.J. and Thompson, M.R. (1997a).
The Field-Ionization, Coulomb Explosion of Diatomic Molecules in Intense Laser Fields.
Laser Physics **7**, 813.

Posthumus, J.H.; Thompson, M.R.; Frasinski, L.J. and Codling, K. (1997b).
Molecular dissociative ionisation using a classical over-the-barrier approach.
I.O.P. Conf. Ser. **154**, 298.

Posthumus, J.H.; Giles, A.J.; Thompson, M.R.; Shaikh, W.; Langley, A.J.; Frasinski, L.J. and Codling, K. (1996).
The dissociation dynamics of diatomic molecules in intense laser fields.
J. Phys. B: At. Mol. Opt. Phys. **29**, L525.

Protopapas, M; Keitel, C.H. and Knight, P.L. (1997).
Atomic physics with super-high intensity lasers.
Rep. Prog. Phys. **60**, 389.

Purnell, J.; Snyder, E.M.; Wei, S. and Castleman Jr, A.W. (1994).
Ultrafast laser-induced Coulomb explosion of clusters with high charge states.
Chem. Phys. Lett. **229**, 333.

Ravindra Kumar, G.; Safvan, C.P.; Rajgara, F.A. and Mathur, D. (1994a).
Dissociative ionization of molecules by intense laser fields at 532 nm and 10^{12} - 10^{14} W cm^{-2}.
J. Phys. B: At. Mol. Opt. Phys. **27**, 2981.

Ravindra Kumar, G.; Safvan, C.P.; Rajgara, F.A. and Mathur, D. (1994b).
Intense laser field ionisation of CS_2 at 532 nm. Does dissociation precede ionisation?
Chem. Phys. Lett. **217**, 626.

Rolland, C. and Corkum, P.B. (1986).
Amplification of 70 fs Pulses in a High Repetition Rate Dye Laser Amplifier.
Opt. Commun. **59**, 64.

Rudd, J.V.; Korn, G.; Kane, S.; Squier, J. and Mourou, G. (1993).
Chirped-pulse amplification of 55-fs pulses at a 1-kHz repetition rate in a Ti:Al_2O_3 regenerative amplifier.
Opt. Lett. **18**, 2044.

Safvan, C.P.; Bhardwaj, V.R.; Ravindra Kumar, G.; Mathur, D. and Rajgara, F.A. (1996).
Single and multiple ionization of CS_2 in intense laser fields: wavelength dependence and energetics.
J. Phys. B: At. Mol. Opt. Phys. **29**, 3135.

Salin, F.; Georges, P.; Roger, G. and Brun, A. (1987).
Single-shot measurement of a 52-fs pulse.
Appl. Opt. **26**, 4528.

Sanderson, J.H.; Thomas, R.V.; Bryan, W.A.; Newell, W.R.; Taday, P.F. and Langley, A.J. (1997).
Multielectron-dissociative-ionization of SF_6 by intense femtosecond laser pulses.
J. Phys. B: At. Mol. Opt. Phys. **30**, 4499.

Schlag, E.W. and Neusser, H.J. (1983).
Multiphoton Mass Spectrometry.
Acc. of Chem. Res. **16**, 355.

Schutze, M.; Trappe, C.; Tabellion, M.; Lupke, G. and Kurz, H. (1996).
An all-optical mass spectrometric system based on picosecond-laser pulses.
Surface and Interface Anal. **24**, 399.

Schutze, M.; Trappe, C.; Tabellion, M. and Kurz, H. (1995).
Surface analysis using ultrashort laser pulses and time-of-flight mass spectrometry.
Fresenius J. Anal. Chem. **353**, 575.

Sears, F.W.; Zemanski, M.W. and Young, H.D. (1987).
University Physics, seventh edition.
Addison-Wesley, Wokingham, England.

Seaver, M.E.; Hudgens, J.W. and Decorpo, J.J. (1980).
ArF Excimer Laser Multiphoton-Ionization Mass Spectrometry of Organic Molecules.
Int. J. Mass Spectrom. Ion. Phys. **34**, 159.

Seideman, T.; Ivanov, M.Yu. and Corkum, P.B. (1995).
Role of Electron Localization in Intense-Field Molecular Ionization.
Phys. Rev. Lett. **75**, 2819.

Shank, C.V.; Fork, R.L.; Yen, R. and Stolen, R.H. (1982).
Compression of femtosecond optical pulses.
Appl. Phys. Lett. **40**, 761.

Silva, C.R .and Reilly, J.P. (1996).
Theoretical Calculations on Excited Electronic States of Benzaldehyde and Observation of the S2-S0 Jet-Cooled Spectrum.
J. Phys. Chem. **100**, 17111.

Singhal, R.P.; Kilic, H.S.; Ledingham, K.W.D.; McCanny, T.; Peng, W.X.; Smith, D.J.; Kosmidis, C.; Langley, A.J. and Taday, P.F. (1998)
Comment on "On the ionisation and dissociation of NO_2 by short intense laser pulses."
Accepted for publication in *Chem. Phys. Lett.*

Singhal, R.P.; Kilic, H.S.; Ledingham, K.W.D.; Kosmidis, C.; McCanny, T.; Langley, A.J. and Shaikh, W. (1996).
Multiphoton Ionisation and Dissociation of NO_2 by 50 fs laser pulses.
Chem. Phys. Lett. **253**, 81.

Singhal, R.P. (1995).
Nonlinear Optics.
An Introduction to Laser Spectroscopy (ed. D.L. Andrews) Plenum Press Spring St New York 10013.

Singhal, R.P.; Land, A.P.; Ledingham, K.W.D. and Towrie, M. (1989).
Population Rate Equations Modelling of a Resonant Ionisation Process.
J. Anal. Atom. Spectrom. **4**, 599.

Singhal, R.P. and Ledingham, K.W.D. (1987).
How to count atoms.
New Scientist **26**, 52.

Smith, D.J.; Ledingham, K.W.D.; Kilic, H.S.; Singhal, R.P.; McCanny, T.; Peng, W.X.; Langley, A.J. and Taday, P.F. (1998a).
Ionization and Dissociation of Benzaldehyde using Short Intense Laser Pulses.
J. Phys. Chem. A **102**, 2519.

Smith, D.J.; Ledingham, K.W.D.; Singhal, R.P.; Kilic, H.S.; McCanny, T.; Langley, A.J.; Taday, P.F. and Kosmidis, C. (1998b).
Time-of-flight Mass Spectrometry of Aromatic Molecules Subjected to High Intensity Laser Beams.
Rapid Commun. Mass Spectrom. **12**, 813.

Smith, D.J.; Ledingham, K.W.D.; Singhal, R.P.; McCanny, T.; Graham, P.; Langley, A.J.; Taday, P.F. and Kosmidis, C. (1998c).
Environmental Applications of Femtosecond Laser Mass Spectrometry.
To be published.

Sogard, M.R. (1988).
Nonresonant Multiphoton Ionization Yields from Gaussian Laser Beams.
J. Opt. Soc. Am. B Opt. Phys. **5**, 1890.

Spence, D.E.; Kean, P.N. and Sibbett, W. (1991).
60-fsec pulse generation from a self-mode-locked Ti:sapphire laser.
Opt. Lett. **16**, 42.

Strickland, D. and Mourou, G. (1985).
Compression of Amplified Chirped Optical Pulses.
Opt. Commun. **56**, 219.

Svelto, Orazio (1989).
Principles of Lasers.
Plenum Press, Spring St, New York

Taday, P.F.; Mohammed, I.; Langley, A.J. and Ross, I.N. (1998).
To be published.

Taday, P. (1997).
Private communication.

Talebpour, A; Larochelle, S. and Chin, S.L. (1998).
Suppressed tunnelling ionization of the D_2 molecule in an intense Ti:sapphire laser pulse.
J. Phys. B: At. Mol. Opt. Phys. **31**, L49.

Talebpour, A.; Chien, C-Y.; Liang, Y.; Larochelle, S. and Chin, S.L. (1997a).
Non-sequential ionization of Xe and Kr in an intense femtosecond Ti-sapphire laser pulse.
J. Phys. B: At. Mol. Opt. Phys. **30**, 1721.

Talebpour, A.; Larochelle, S. and Chin, S.L. (1997b).
Non-sequential and sequential double ionization of NO in an intense femtosecond Ti-sapphire laser pulse.
J. Phys. B: At. Mol. Opt. Phys. **30**, L245.

Talebpour, A.; Larochelle, S. and Chin, S.L. (1997c).
Dissociative ionization of NO in an intense field: a route towards enhanced ionization.
J. Phys. B: At. Mol. Opt. Phys. **30**, 1927.

Thorn EMI Limited.
35 Seward Street
London
EC1V 3PA.

Trappe, C.; Schutze, M.; Raff, M.; Hannot, R. and Kurz, H. (1993).
Use of ultrashort laser pulses for desorption from semiconductor surfaces and nonresonant post-ionization of sub-monolayers.
Fresenius J. Anal. Chem. **346**, 368.

Vijayalakshmi, K.; Safvan, C.P.; Ravindra Kumar, G. and Mathur, D. (1997).
On the ionisation and dissociation of NO_2 by short intense laser pulses.
Chem. Phys. Lett. **270**, 37.

Walsh, T.D.G.; Ilkov, F.A.; Decker, J.E. and Chin, S.L. (1994).
The tunnel ionization of atoms, diatomic and triatomic molecules using intense 10.6 μm radiation.
J. Phys. B:At. Mol. Opt. Phys. **27**, 3767.

Walsh, T.D.G.; Decker, J.E. and Chin, S.L. (1993).
Tunnel ionization of simple molecules by an intense CO_2 laser.
J. Phys. B:At. Mol. Opt. Phys. **26**, L85.

Weast, R.C. (1972).
CRC Handbook of Chemistry and Physics, 53rd Edition.
CRC Press - a division of the Chemical Rubber Co.

Weickhardt, C.; Grun, C.; Heinicke, R.; Meffert, A. and Grotemeyer, J. (1997).
The Application of Resonant Multiphoton Ionization by Sub-picosecond Laser Pulses for Analytical Laser Mass Spectrometry.
Rapid Comm. Mass Spectrom. **11**, 745.

Weinkauf, R.; Aicher, P.; Wesley, G.; Grotemeyer, J. and Schlag, E.W. (1994).
Femtosecond versus Nanosecond Multiphoton Ionization and Dissociation of Large Molecules.
J. Phys. Chem. **98**, 8381.

Wiley, W.C. and McLaren, I.H. (1955).
Time-of-Flight Mass Spectrometer with Improved Resolution.
Rev. Sci. Instrum. **26**, 1150.

Willey, K.F.; Brummel, C.L. and Winograd, N. (1997).
Photoionization mechanisms for $Cr(CO)_6$ using high intensity laser pulses in the near-IR.
Chem. Phys. Lett. **267**, 359.

Yang, J.J.; Gobeli, D.A. and El-Sayed, M.A. (1985).
Change in the Mechanism of Laser Multiphoton Ionization-Dissociation in Benzaldehyde by Changing the Laser Pulse Width.
J. Phys. Chem. **89**, 3426.

Yang, J.J.; Gobeli, D.A.; Pandolfi, R.S. and El-Sayed, M.A. (1983).
Wavelength Dependence of the Multiphoton Ionization-Fragmentation Mass Spectrometric Pattern of Benzaldehyde.
J. Phys. Chem. **87**, 2255.

Yariv, A. (1997).
Optical Electronics in Modern Communications.
Oxford University Press, Oxford, England.

Zandee, L. and Bernstein, R.B. (1979).
Resonance-enhanced multiphoton ionization and fragmentation of molecular beams: NO, I_2, benzene and butadiene.
J. Chem. Phys. **71**, 135.

Zare, R.N. (1984).
Laser Chemical Analysis.
Science **226**, 298.

Zhou, J.; Taft, G.; Huang, C.; Murnane, M.M. and Kapteyn, H.C. (1994).
Pulse Evolution in a broad-band Ti:sapphire laser.
Opt. Lett. **19**, 1149.